# A 2-D MODEL STUDY OF THE INFLUENCE OF THE SURFACE ON MESOCALE CONVECTION DURING THE INDIAN MONSOON

by

Roger A. Pielke, P.I.
NSF Grant # ATM-8915265

Department of Atmospheric Science
Colorado State University
Fort Collins, Colorado

Colorado State University

Department of Atmospheric Science

Paper No. 485

# A 2-D MODEL STUDY OF THE INFLUENCE OF THE SURFACE ON MESOSCALE CONVECTION DURING THE INDIAN MONSOON

Zejin Xian

Department of Atmospheric Science
Colorado State University
Fort Collins, Colorado
Summer, 1991

Atmospheric Science Paper No. 485

## ABSTRACT

## A 2-D MODEL STUDY OF THE INFLUENCE OF THE SURFACE ON MESOSCALE CONVECTION DURING THE INDIAN MONSOON

A two-dimensional Colorado State University Regional Atmospheric Modeling System model is used to simulate a summer monsoon cloud cluster and its associated mesoscale convective system observed over the Bay of Bengal on 3-8 July 1979. Summer Monsoon Experiment (SMONEX) data is applied to initialize the model. A modification of the Kuo convective parameterization and microphysical process are employed in the simulations.

The simulated monsoon cloud cluster forms over the ocean and propagates westward to the land with the upper tropospheric easterly flow. Mesoscale convection appears over the land when the monsoon cloud cluster approaches the coast. The landfalling cloud cluster brings rainfall inland. The maximum 24 hour precipitation appears in the region of 200-300 km west of the coastline.

Sensitivity simulations are performed for a variety of land characteristics and water surface temperatures. The major conclusions of these tests are:

1. Wetter soil is more conducive for the formation of mesoscale convective systems because it supplies more moist static energy to them. Therefore, more precipitation is intercepted on the wetter ground surface.

2. Rough land promotes more mesoscale convection and produces stronger upward motion in the landfalling cloud cluster than smooth land. However, the simulated precipitation does not have an apparent increase when the land roughness is enlarged.

3. The simulated cloud cluster does not have any apparent difference over the ocean, which has either high or low surface temperature before it moves onshore. However, when the cloud cluster formed over higher sea surface temperature (SST) moves inland, significant rainfall and mesoscale convection occur over the land. In contrast, the intensities of the precipitation and upward motion in the lower SST case are weak.

4. For the simulated monsoon cloud cluster formed in low SST and soil moisture environment conditions, the system decays quickly after it moves inland a few hours later. The rainfall is concentrated in a narrow range between 100 to 300 km west of the coast.

Zejin Xian
Department of Atmospheric Science
Colorado State University
Fort Collins, Colorado 80523
Summer, 1991

ACKNOWLEDGEMENTS

I would first like to thank my advisor, Dr. Roger A. Pielke, for his support and guidance during this study. His helpful suggestions and ideas on many of the modelled mesoscale convection related aspects of this work are greatly appreciated. I would also like to thank my other committee members, Dr. Robert L. Grossman, Dr. Richard H. Johnson, and Dr. Paul W. Mielke for useful discussions and comments which improved the text. Dr. Grossman's thorough review of my study and Professor Johnson's suggestions on summer monsoon research are especially appreciated.

Drs. Craig Tremback and Bob Walko are thanked for answering many model-related questions. Dr. Mel Nicholls provided initial help in modelling cloud problems. Mr. Xubin Zeng and Dr. Mike Weissbluth are thanked for several helpful discussions concerning this work.

This study was supported by the National Science Foundation (NSF) under Grant #ATM-8915265. The computing was done on the CRAY X-MP and Y-MP at the National Center for Atmospheric Research (NCAR) and the Stardent super workstation at the Department of Atmospheric Science, Colorado State University.

Dallas McDonald in acknowledged for her professional preparation of the paper.

TABLE OF CONTENTS

# LIST OF FIGURES

LIST OF TABLES

# Chapter 1

# INTRODUCTION

## 1.1 The General Behavior of Monsoon Depressions Over the Bay of Bengal

Summer monsoon depressions are common and important meteorological phenomena over the Indian monsoon area during the summer. There are a number of features associated with the summer monsoon (Johnson and Houze, 1987): (1) an onset vortex over the Arabian Sea, (2) deep convection and heavy rainfall along the southern edge of the Tibetan Plateau, (3) terrain convection associated with the Western Ghats, (4) Bay of Bengal depressions, and (5) mid-tropospheric cyclones over the northeastern Arabian Sea and northern Bay of Bengal.

Figure 1.1 gives the low-level circulation and significant convection features in the summer monsoon regions. Throughout the monsoon period, a variety of very significant cyclonic disturbances develop over the Bay of Bengal. The statistics (ICSU/WMO, 1976) show that about two monsoon depressions per month form over the Bay of Bengal, and move westward or northwestward inland and bring large amounts of precipitation over the eastern Indian continent.

In 1979, the Summer Monsoon Experiment (SMONEX) was carried out in the Bay of Bengal (ICSU/WMO, 1976; Fein and Kiettner, 1980). This experiment was designed to study the southwesterly monsoon in the vicinity of the Indian subcontinent. It is known that the typical scale of depressions in this region is around 500 km in the formative stage. Although the depressions form in the northern part of the Bay of Bengal, they do not reach hurricane intensity because they stay over the ocean only a short time period and the large vertical wind shear over the troposphere inhibits a local accumulation of the latent heat released in the disturbance.

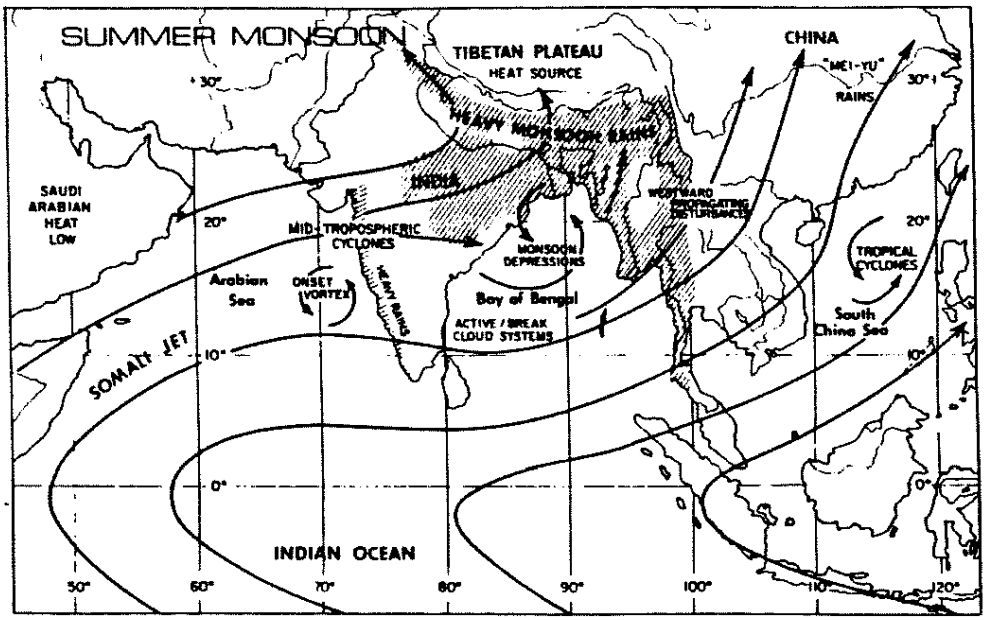


Figure 1.1: The low level flow of summer monsoon (adopted from Johnson and Houze, 1987).

During SMONEX, a specific depression which formed over the Bay of Bengal was investigated in detail. The observational data and analysis results for this depression obtained by Nitta (1980), Nitta and Masnda (1981), and Sanders (1984), showed that the flow associated with the depression formed a closed vortex at low- and mid-levels on July 3, 1979. The depression formed over the Bay of Bengal at 19°N and 90°E and moved westward with a speed of ~222 km day$^{-1}$. The maximum vorticity of the developed depression reached $1.5 \times 10^{-4}$ s$^{-1}$ around the center. The zonal mean wind was westerly above 600 hPa. There existed large northward momentum fluxes around 600 hPa. The analysis of divergence indicated that the maximum convergence appeared around 700 hPa on July 7 with a value of $-3 \times 10^{-5}$ s$^{-1}$. Upper-level divergence existed around 200 hPa and was near $2 \times 10^{-5}$ s$^{-1}$.

Sanders (1984) found that the rain from the Bay of Bengal depression was generated in numerous convection towers. The rain was distributed with the storm-scale ascent area and had a mesoscale precipitation feature.

Houze and Churchill (1987) analyzed the mesoscale precipitation features associated with the Bay of Bengal depression. They found that the precipitation occurred in a mesoscale rain area of 100-300 km in the horizontal dimension and each of them contained intense convective cells. Each mesoscale precipitation feature was characterized by a widespread cloud shield base at about the 400 hPa level. The rain falling from the cloud deck was partly convective and partly stratiform. Some of the convective towers were very intense and overshot the top of the cloud shield. The convective region consisted of an arc-shaped, southward moving line of intense convective rain oriented generally east-west and followed to the north by a wide region of stratiform clouds and precipitation. The orientation and structure of the arc lines may relate to the strong easterly monsoonal shear in this region. The large mesoscale precipitation features tended to be elongated from the west-east to the northwest-southeast.

On the coast, substantial precipitation occurred after 0300 GMT on the 6th and ended by 0300 GMT on the 8th as the depression center passed inland (Sanders, 1984). After the system moved into the Indian peninsula, a substantial vertical separation was

produced as the 850 hPa center moved northwestward and the 500 hPa center westward with a speed of 5 m $s^{-1}$.

## 1.2 The Structure of the Monsoon Depression Over the Bay of Bengal

The structure of the Bay of Bengal depression based on observations has been investigated by many researchers, e.g., Koteswaram and George (1958), Krishnamurti et al. (1975), and others. Their studies are mainly concerned with the structure of the depression as it moved inland over central India.

A typical depression had a warm core in the lower troposphere during its developing stage over the ocean. After it fully developed, the depression developed a cold core structure in the lower troposphere and a warm core in the upper troposphere (Krishnamurti, 1975; Godbole, 1977). The warm area in the depression was also an area with a relative humidity higher than 90%. Therefore, a large mass of clouds associated with the depression formed when the depression moved westward toward the Indian coast.

Warner (1984) summarized the core structure of the depression on 7 July 1979 as sloped toward the southwest with height, with buoyant cloudy ascent within the cold air to the south and west of the axis, and warm subsidence of clear air to the northwest of the axis. The convergence near the cloud base reached values of nearly $-2 \times 10^{-4}$ $s^{-1}$ in areas of $\sim$300 $km^2$ to the south and west of the center with divergence and subsidence of a similar magnitude to the northeast of the center. Warner and Grumm (1984) further found that the area covered by the updrafts was 0.5% in cumulus. The cloudy ascent was sustained upward through the 700 hPa level only in a mesoscale line of cumulus clouds. This line lasted 3 hours and propagated faster than the low-level wind. Mid-level stratus (700-200 hPa) and cumulus dominated the total cloud coverage. The cloud mapping showed that the cumulus generally penetrated to above 9 km. A dense high overcast based around 7.5 km had embedded cumulus. However, the total cloud was dominated by mid-level thin fragmentary stratus and cumulus debris. Warner and Grumm further confirmed that the ascent in the lower troposphere was concentrated in mesoscale features of cumulus clouds covering nearly 1% of the inner area of the depression.

## 1.3 The Mechanisms Driving the Monsoon Depression

The mechanisms that drive the depression during its lifetime need to be described. Krishnamurti et al. (1976) concluded that the depression was driven by cumulus convection although the disturbance might originate from barotropic or baroclinic instability of the mean flow. Webster (1983) estimated that the maximum value of the vertical distribution of convective heating was about 5 K $day^{-1}$ over the Bay of Bengal area during the summer. The latent heat released by the cumulus convection yields an increase of the temperature within the clouds. These increased temperatures then drive a stable ascent of the saturated air to produce stable latent heating where there is a cold air core and low air pressure.

Sanders (1984) found that the thermal stratification near the depression over the Bay of Bengal above 850 hPa is approximately moist-adiabatic. The wind analyses showed that the basic zonal currents, westerly in the lower troposphere and easterly in the middle levels, were weakened as the depression formed. The convective heating released from a number of convective towers and the large scale wind shear were the major mechanisms supporting the depression. Houze (1989) suggested a typical cloud system structure as in Fig. 1.2. He emphasized the microphysical and kinematic aspects of the precipitation processes in the convection and stratiform regions.

## 1.4 Landscape Effects on the Local Convection

There are a number of research works that study the effects of mountains (Grossman and Durran, 1984) and offshore flow forced by the terrain (Dudhia, 1989) on monsoon convection. However, there is little work concerning the influence of landscape characteristics on monsoon convection.

Physick (1980) showed the relative contributions of sensible and latent heat fluxes on the inland penetration rate of sea breezes. Large values of sensible heat provided more direct heating to the atmosphere, thereby resulting in a large horizontal pressure gradient and more rapid inland propagation of the sea breeze. The characteristics of landscape, as verified by many researchers in recent years (e.g., McCumber and Pielke, 1981; Garrett,

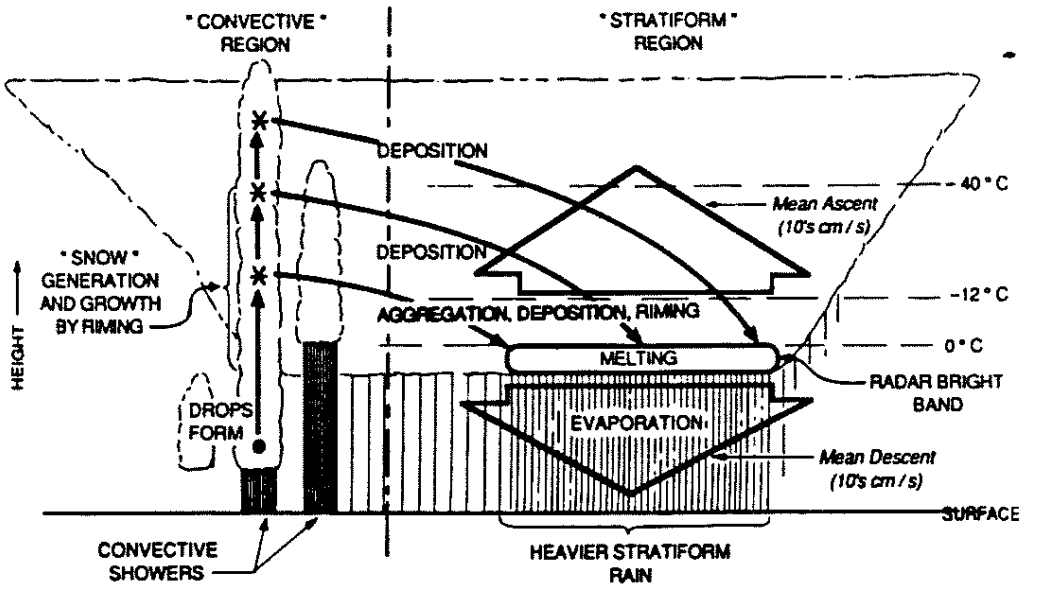


Figure 1.2: Tropic cloud structure (from Houze, 1989).

1982; Anthes, 1984; Pielke, 1984; Segal et al., 1984; Pielke and Segal, 1986; Mahfouf et al., 1987; etc.) are important in influencing the development of the mesoscale system over land through the influence on the magnitude of surface latent and sensible heat fluxes to the atmosphere. These fluxes (i) directly influence energy available for cumulus convection, and (ii) can create mesoscale circulation as strong as a sea breeze (e.g., Segal et al., 1988) when a spatial gradient in landscape type results in large horizontal gradients of sensible heat fluxes.

Generally, on a wet land surface, the increased latent heat fluxes through soil moisture flux and evaporation of intercepted rain will increase the moisture supply to the atmosphere (Ookouchi et al., 1984). Mahfouf et al. (1987) and Lanicci et al. (1987) summarized that the low soil moisture over the Mexican plateau allowed the development of a deep mixed layer, thereby increasing severe storm activity in that area. Yan and Anthes (1988) compared the sea breeze circulation over dry and moist land. For a relative dry surface, they found that the upward motion associated with the sea breeze front generated

a thin moist layer up to about 700 hPa. Away from the front the air in the lower PBL was relatively dry. The cloud did not produce rainfall on the first day. On the second day, the updraft associated with the sea breeze front generated saturation of the moist layer which resulted in deep precipitating clouds. However, when the land surface was wet, the sea breeze was weaker with a cooler, shallower, and more moist planetary boundary layer (PBL). In spite of the weaker circulation, however, the wet land sea breeze produced more precipitation than that of the dry land sea breeze.

The landfall decay process of tropical cyclones and its associated rainfall distribution can be significantly influenced by land surface conditions (Tuleya et al., 1984). Pielke and Zeng (1989) suggested that severe thunderstorms were more likely over irrigated areas than over adjacent dry prairie land since the added water vapor provided greater buoyant energy for the cumulus cloud convection.

Nicholls et al. (1990) found that formation of deep convection associated with the sea breeze over the Florida peninsula was related to soil moisture content. The dry soil simulation generated rapidly developing sea-breezes which moved inland quickly, whereas the wet soil run produced a much more slowly developing sea breeze.

In the Bay of Bengal and Indian coast region, warm and moist tropical air is significant in the evolution of the monsoon depression. Based on observations, Keshavamurty (1971) suggested that the significant association between vorticity at 900 hPa and observed rainfall distribution indicated the important role of Ekman pumping and CISK (conditional instability of the second kind) mechanisms to explain the future growth of the depression over the Indian continent. Webster (1983, 1987) suggested that surface hydrological effects can influence the 10 to 20 days variation of the Indian summer monsoon.

## 1.5 Working Hypothesis of the Study

Based on the previous discussions, the following hypothesis is made. The monsoon depression forms over the Bay of Bengal where the cumulus anvil shears to the west by the strong easterly flow above 400 hPa. The high-level anvil moves inland ahead of the landfalling depression and brings rainfall and reduces the incoming solar radiation

reaching the ground. Therefore the normal sea breeze (Lohar and Chakravarty, 1990) does not occur due to the decrease of the temperature gradient between the land and the sea. The anvil rainfall increases the soil moisture well to the west of the surface depression and makes the environment for the next cluster more conducive to deep convection, since a substantial latent heat source would be present over the land in the form of warm, wet soil. The warm, wet soil would subsequently modify the boundary layer air over it producing higher moisture static energy. Given a favorable mid- and upper tropospheric wind and thermodynamic environment, the next cluster would propagate further inland before weakening occurs. This study will test this hypothesis by using a numerical model to identify relationships between land surface characteristics and inland characteristics of Bay of Bengal mesoscale convective systems which have moved from ocean to land.

Based on the previous discussions, it seems that in order to represent the mesoscale convective system during the summer monsoon season properly, a numerical model for this purpose needs the following characteristics. First, the model should have a realistic convective cloud parameterization to represent mesoscale cloud development associated with convective transport of heat and moisture. Second, there should be a microphysical parameterization that can reproduce the observed ice-dominated stratiform anvil clouds and their associated latent heating. Third, a radiation transfer parameterization should be included in the model to represent the impact of anvil clouds on the infrared and solar radiation heating process as on land. Finally, a realistic soil-atmosphere parameterization is needed to represent the momentum and heat flux transfer from the Earth to the atmosphere. A detailed description of the model is given in Chapter Two.

# Chapter 2

# THE NUMERICAL MODEL USED IN THE STUDY

## 2.1 Basic Equations Used in the Model

The CSU Regional Atmospheric Modeling System (RAMS), in a two-dimensional hydrostatic version, is used. The basic equations from Tremback (1990) are given as

Momentum equations

$$\frac{\partial u}{\partial t} = -u\frac{\partial u}{\partial x} - w\frac{\partial u}{\partial z} - \theta\frac{\partial \pi'}{\partial x} + fv + \frac{\partial}{\partial x}(K_m^h\frac{\partial u}{\partial x}) + \frac{\partial}{\partial z}(K_m^z\frac{\partial u}{\partial z}) \tag{2.1}$$

$$\frac{\partial v}{\partial t} = -u\frac{\partial v}{\partial x} - w\frac{\partial v}{\partial z} - fu + \frac{\partial}{\partial x}(K_m^h\frac{\partial v}{\partial x}) + \frac{\partial}{\partial z}(K_m^z\frac{\partial v}{\partial z}) \tag{2.2}$$

Thermodynamic equation

$$\frac{\partial \theta_{il}}{\partial t} = -u\frac{\partial \theta_{il}}{\partial x} - w\frac{\partial \theta_{il}}{\partial z} + \frac{\partial}{\partial x}(K_h^h\frac{\partial \theta_{il}}{\partial x}) + \frac{\partial}{\partial z}(K_h^z\frac{\partial \theta_{il}}{\partial z}) + (\frac{\partial \theta_{il}}{\partial t})_{con} + (\frac{\partial \theta_{il}}{\partial t})_{res} + (\frac{\partial \theta_{il}}{\partial t})_{rad} \tag{2.3}$$

Moisture and condensation mixing ratio continuity equations ($n = 1, 2, 3$)

$$\frac{\partial r_n}{\partial t} = -u\frac{\partial r_n}{\partial x} - w\frac{\partial r_n}{\partial z} + \frac{\partial}{\partial x}(K_h^h\frac{\partial r_n}{\partial x}) + \frac{\partial}{\partial z}(K_h^z\frac{\partial r_n}{\partial z}) + (\frac{\partial r_n}{\partial t})_{con} + (\frac{\partial r_n}{\partial t})_{res} \tag{2.4}$$

Continuity equation

$$\frac{\partial \rho u}{\partial x} + \frac{\partial \rho w}{\partial z} = 0 \tag{2.5}$$

Hydrostatic equation

$$\frac{\partial \pi}{\partial z} = -\frac{g}{\theta_v} + g(r_t - r_v) \tag{2.6}$$

The symbols in the above equations are defined in the Appendix.

## 2.2 Numerical Methods

The grid structure is identical to the Arakawa-C grid (Mesinger and Arakawa, 1976). The advection operator is the flux form of 2nd-order leapfrog for the horizontal advection and forward for the vertical advection (Tremback et al., 1987). The Coriolis force term is also included in the simulations. The time-split scheme (Tremback et al., 1985) is used for the model time integration.

The horizontal resolution length is 10 km. There are 23 levels with a minimum stretched grid of 250 m resolution near the ground and uniformly 1.0 km grid spacing from 6 km to the top of the model (19 km). The time step is 10 seconds. The model domain covers 1000 km with 500 km of land and 500 km of ocean for all of the simulations.

The lateral boundaries are chosen as Klemp and Wilhelmson (1978). The top boundary condition is similar to Klemp and Durran (1983) except a modified form of Rayleigh friction (Cram, 1990) is used at the top layers.

## 2.3 Physical Parameterizations

A radiation parameterization that includes both solar and infrared radiation (Chen and Cotton, 1983) is used. This scheme includes the effects on radiative transfer of condensation, water vapor, ozone, and carbon dioxide.

The model used a cumulus convective parameterization. Convective parameterization is necessary to express subgrid-scale transport by updrafts and downdrafts of cumulus clouds which vertically redistribute heat, moisture, and momentum within the model and also produce convective rainfall. The convective terms are significant forcing terms in the model. As mentioned previously, summer monsoon depressions in the Bay of Bengal are associated with deep cumulonimbus convection and stratiform as shown by Johnson and Houze (1987), and Houze and Churchill (1987). The convective process in the depression plays a significant effect on the maintenance and development of the depression. The convective parameterization used here is a modification of the Kuo (1974) parameterization described by Molinari et al. (1985). The difference between the environmental potential

temperature and a convective potential temperature profile is used to estimate the convective heating. Convection is activated if the grid column is convectively unstable and there is resolved upward vertical motion at the lifting condensation level (LCL). The source level air for the convection is defined as the highest $\theta_e$ air that is less than 3 km above the ground. The cloud top, however, is defined as the level above which the potential temperature of the moist adiabatic becomes less than the grid temperature.

To deal with "resolved" condensation and precipitation processes, the microphysical parameterizations described by Tripoli and Cotton (1982), and Flatau et al. (1989) are used in the simulations. In the model, the water species of vapor, rain, pristine ice crystals, snow, aggregates, and graupel are considered.

Turbulent diffusion uses a first order eddy viscosity type based on a local exchange coefficient that is a function of deformation and stability. The definitions of the kinetic and thermal eddy coefficients used here are similar to Xian and Pielke (1991).

For the lower boundary condition of the model, the surface layer model from Louis (1979) and soil model parameterizations of Tremback and Kessler (1985) are used. The soil model involves formulating prognostic equations from the surface energy balance for the soil surface temperature and water content by choosing a finite depth soil-atmosphere interface layer. However, the current simulation only considers a bare soil in order to isolate the effects of soil wetness and soil roughness on the mesoscale convective system associated with the monsoon cloud cluster. The sea surface temperature is specified and kept constant throughout the simulations.

## Chapter 3

# THE MODEL SIMULATIONS

As mentioned previously, the goal of this research is to show the effect of land surface characteristics on mesoscale convection as an idealized monsoon depression over the Bay of Bengal moves inland over India. These experiments represent a set of sensitivity simulations and are not designed to model a case study in detail. Therefore, all the simulations are completed with different parameters that represent different environmental conditions. Table 1 presents several basic parameters used in the simulations. In this chapter the control simulation will be discussed.

Table 3.1: Basic Parameters Used in the Simulations

| Experiment | Soil Moisture ($cm^{-3}cm^3$) | SST (K) (sea surface temp.) | Land Roughness (m) | Main Feature |
|---|---|---|---|---|
| CON | 0.6 | 302 | 0.05 | Control experiment |
| SLM | 0.3 | 302 | 0.05 | Dry land |
| SHM | 0.8 | 302 | 0.05 | Wet land |
| SRS | 0.6 | 302 | 0.10 | Rough surface |
| SMS | 0.6 | 302 | 0.01 | Smooth surface |
| SLT | 0.6 | 300 | 0.05 | Cold ocean |
| SHT | 0.6 | 304 | 0.05 | Warm ocean |
| SML | 0.3 | 300 | 0.05 | Dry land and cold ocean |

## 3.1 Observations and Model Initializations

During the Indian summer monsoon season, there are usually about one to three depressions per month which form over the Bay of Bengal area. These depressions are usually associated with mesoscale convective systems over both the ocean and adjacent land. A typical weather condition in which a summer monsoon depression occurred on 3-8 July 1979 over the Bay of Bengal is chosen in the control simulation for the initial

atmospheric background. The reasons for choosing this case are (1) it appeared to be a typical summer monsoon depression which formed over the Bay of Bengal and moved onto the Indian continent; and (2) there were observational studies related to the structure of the depression while it moved across the ocean.

The satellite and radar data and some detailed daily analysis were given by Warner (1984) and Houze and Churchill (1987). Figure 3.1a-b show the satellite photographs from 00Z 7 July 1979 to 00Z 8 July 1979. The depression center associated with an obvious cloud cluster was still over the ocean on 7 July. The evident overshooting cloud towers indicate that the clouds in the depression consisted of stratiform clouds with embedded deep cumulonimbus convection. By 8 July, the depression center had moved inland. Figure 3.2 shows the outline of the cloud shield associated with the depression that developed over the northeast Bay on 3 July 1979 and deepened until 7 July reaching India on the west side of the Bay by 8 July. The deep cloud cells occupied a small fraction of the total cloud area on 7 July. They tended to be concentrated in groups with some obvious tendency for small groups to be arranged in lines oriented east-northeast to west-southwest. The remainder of the cloud pattern had a mid- to high-level stratiform cloud structure.

Warner and Grumm (1984) showed that the anvil base was nearly at 400 hPa with the highest cumulus tops at an altitude of 15.5 km (Warner, 1984). Figure 3.3 depicts the echo pattern of the depression on 7 July 1979. The most intense radar echo is located at the eastern end of the picture. The high reflectivity represents the intense rainfall rate in the intense convective cores. More detailed microphysical observational data (Gamache, 1990) showed that liquid water was almost completely absent in the convective updrafts at the temperatures between $-10$ and $-22°C$. The total particle number concentration in the convective clouds was about 10 times the concentration found in the stratiform clouds. The convective updraft number concentrations averaged 16, 26, and 10 $l^{-1}$ in the upper, middle, and lower stratiform categories, respectively. The area near the convective clouds contained many small particles. These particles seem to be ejected from convective updrafts into the immediate stratiform cloud environment. The middle-stratiform clouds had a greater number of larger particles than the upper-stratiform clouds.

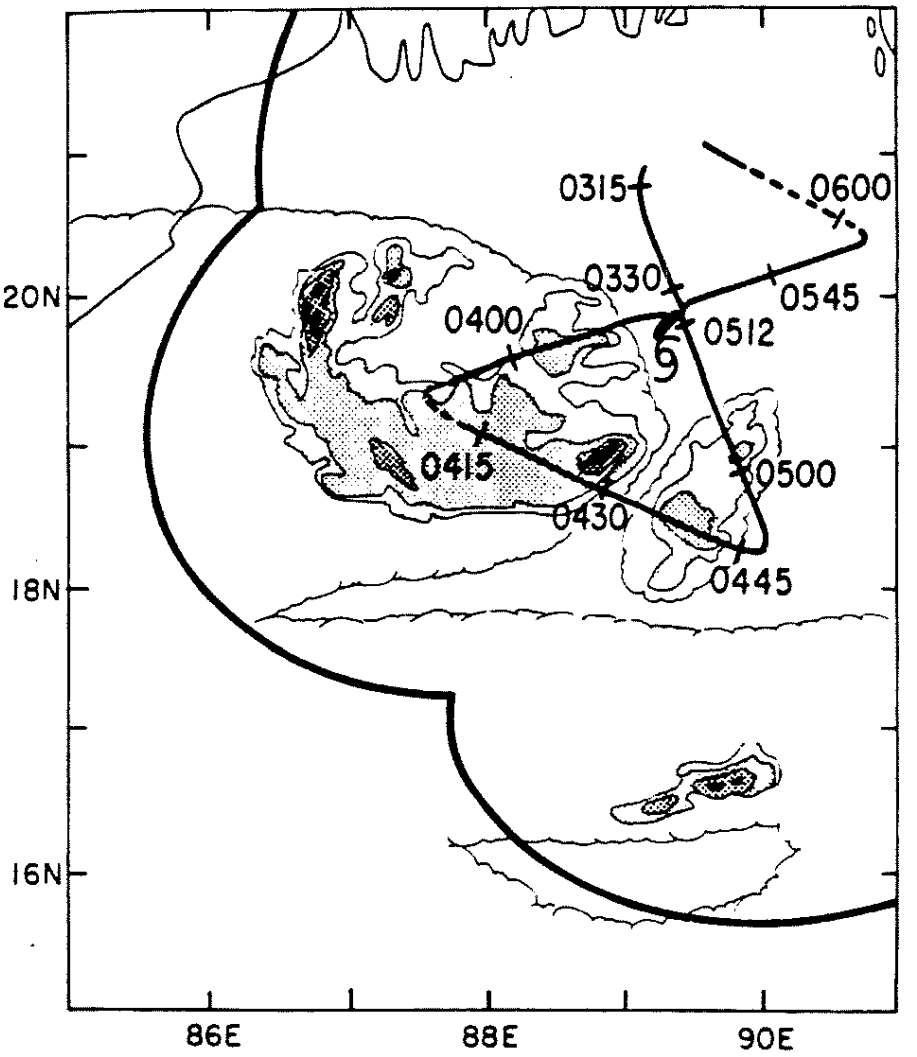


Figure 3.3: Echo pattern of depression (from Houze and Churchill, 1987).

Figure 3.4: 24 hour observed rainfall at 00Z, 8 July 1979 (from Krishnamurti et al. 1983).

Figure 3.4 shows the 24 hour rainfall ending at 00Z 8 July 1979. The landfalling depression brought a large amount of rain to the eastern coast of the Indian subcontinent. It appears that the inland movement of deep convection in the cloud cluster associated with the depression brings moderate rainfall to India's northeast coast (Fein, 1980 and Sanders, 1984).

The sounding used in the model is adopted from SMONEX aircraft dropwindsonde on 7 July 1979 (Warner, 1984) and is taken to be horizontally uniform over the model domain. The wind data, however, is not available from that observation and as discussed later, the wind distribution is an important factor in affecting the genesis and maintenance of the depression.

The large scale analysis of this July monsoon depression over the Bay of Bengal by Nitta (1980) showed that the mean average vertical profile of zonal wind had a weak westerly flow below 700 hPa and easterly flow from 700 hPa to the upper levels of the troposphere. The maximum value of the east-west component around 100 hPa was about 20 m $s^{-1}$. The meridional wind had a weak northerly flow below 300 hPa and southerly flow above 300 hPa. Lee and Gray (1986) discussed the relation between vertical wind

shear and formation of a tropical cloud cluster. They indicated that a strong vertical wind shear would prevent progressive accumulation of warm air in a deep vertical column, which was necessary to lower the surface pressure. By the same argument, the strong vertical wind shear was not favorable for cloud cluster evolution. Non-developing cloud clusters occurred under an environment with a strong vertical zonal wind shear and weak meridional vertical wind shear between 500 and 200 hPa. In the current study, a weaker wind shear conducive for the development of the monsoon depressions has been used to initialize the wind field since model results, consistent with the conclusions of Lee and Gray (1986), indicate that a weak low-level easterly and high-level strong westerly wind is not favorable for the genesis and maintenance of cloud clusters over the ocean. A weak wind shear of upper-level easterly wind and low-level westerly wind, therefore, is chosen in the model simulations. Figure 3.5a-b give the thermodynamic sounding and $u$-component applied in the model initialization.

In order to simulate the initial disturbance that can be used to represent the basic characteristics of the mesoscale convective system in the summer monsoon depression formed over the Bay of Bengal, a "wet and warm perturbation" method is used. Based on the previous discussions, two kinds of thermal structures of the initial perturbation are assumed. One is warm at the upper level and cold at the low level. The another one is the opposite. The maximum and minimum temperature anomalies are 4°C and −2°C, respectively, within 250 km of the center. Figure 3.6a-b are the upward motion fields after two and seven hour model simulations with the low-level cold and upper-level warm initial perturbation. Updrafts are initiated around the disturbance area after one hour of simulation (Fig. 3.6a). The low level of the initial disturbance, however, is controlled by the sinking motion due to the cold air downdraft from the perturbation. There is no convection over the ocean. Ten hours later, the disturbed upward motion system moves near the coast (Fig. 3.6b). Although the clouds include partly convection and partly stratiform types, the precipitation caused by the landfalling cloud cluster is not large. The final 18 hour simulated results indicate that the disturbed system decays completely after it has moved inland 4 hours.

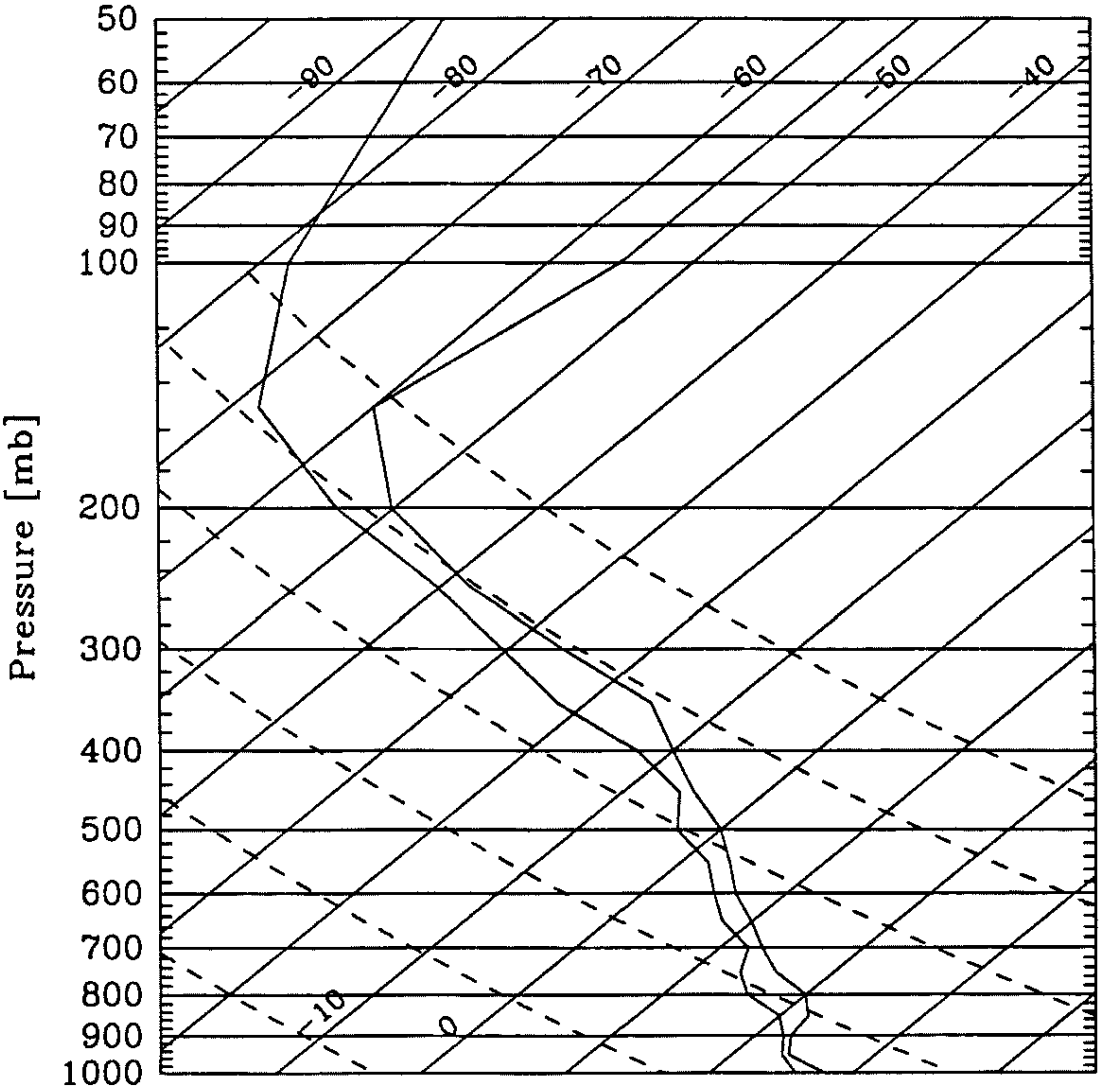


Figure 3.5: (a) Initial sounding of thermal structure.

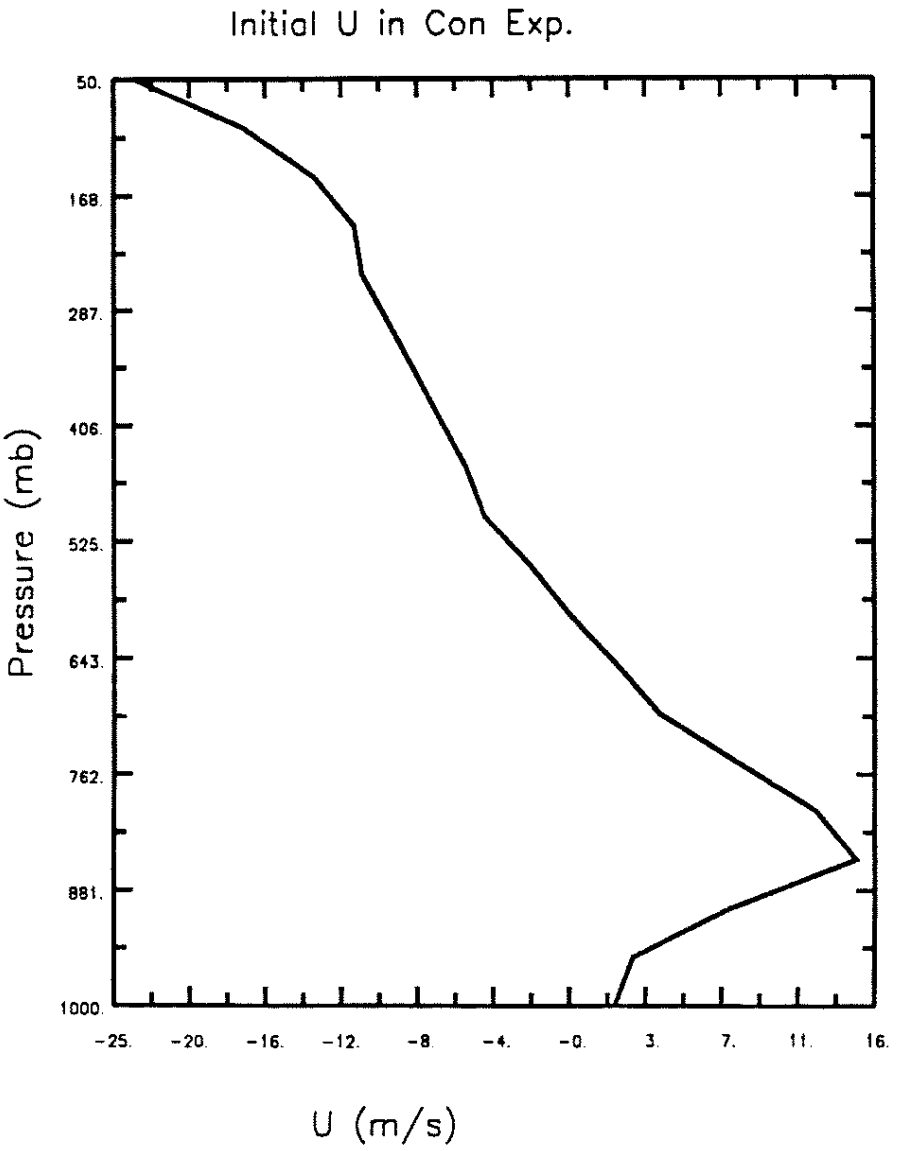


Figure 3.5: (b) East-west wind component.

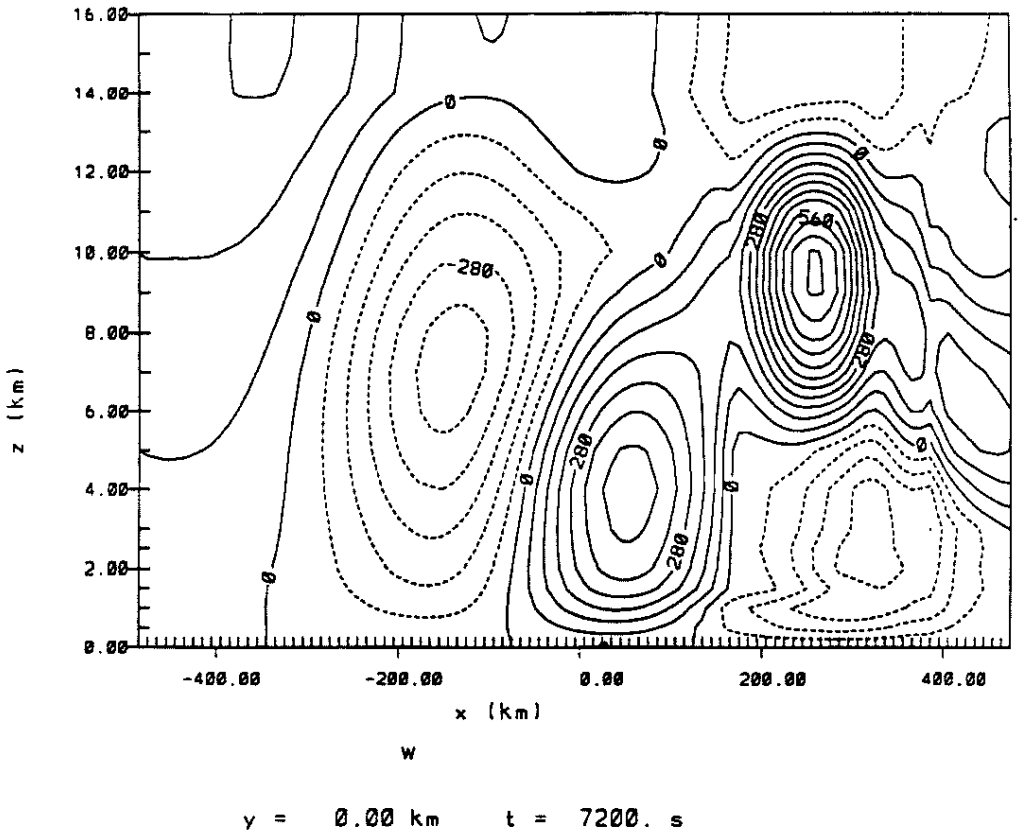


Figure 3.6: (a) Two hour model simulation of vertical velocity $w$ with cold low-level and warm high-level initial perturbation.

However, the low-level warm and upper-level cold initial baroclinic perturbation results in a more persistent feature. The buoyancy force is quite large and strong ascent associated with the heating over the ocean occurs after one hour of model simulation (Fig. 3.7a). A large amount of heating (nearly 110 K $day^{-1}$) is released between the heights of 8 and 13 km. Although this heating is large, it is necessary for the modelled atmosphere to maintain the disturbed cloud cluster. One hour after this heat warms the air, upward motion occurs over the ocean in that region (Fig. 3.7b). The maximum vertical velocity appears between 10 to 12 km above the sea level. The disturbed system, which has a positive relative vorticity of a magnitude of $0.13 \times 10^4$ $s^{-1}$, includes partly convective (central area of the cloud cluster) and partly stratiform (front and rear of the cloud cluster) clouds that can be distinguished both from cloud water content and the updraft motion within the area. The maximum ice content in the cloud cluster is between 8 to 10 km. A portion of the anvil ice is spread westerly by the high-level easterly flow. This appears to represent a mesoscale convective system as well as one can in two dimensions. Therefore, this form of a perturbation disturbance seems more reasonable than the former one and each of the following simulations have used this initial disturbance.

### 3.2 Development Stage

After the initial disturbance is inserted in the model, the simulated cloud cluster develops over the ocean due to the lifting of the low-level air as condensation occurred above the 4 km height. Precipitation does not appear over the ocean until 3 hours of simulation (0700 LST). Rainfall is produced from simulated mesoscale cumulus with a 1.5 g $kg^{-1}$ cloud water mixing ratio and lasts about one hour. The top of the cloud reaches about 12.5 km and the anvil around the cloud top stretches 180 km to the west from the main cloud cluster. The upper-level easterly wind forces the cloud cluster to propagate west. Meanwhile, a large amount of moisture from the evaporation over the ocean forms in front of the cloud cluster while it propagates westerly.

About two hours after sunrise (0800-0900 LST), the latent heat fluxes from the ocean are about nine times larger than those from the inland surface. However, at 1000 LST,

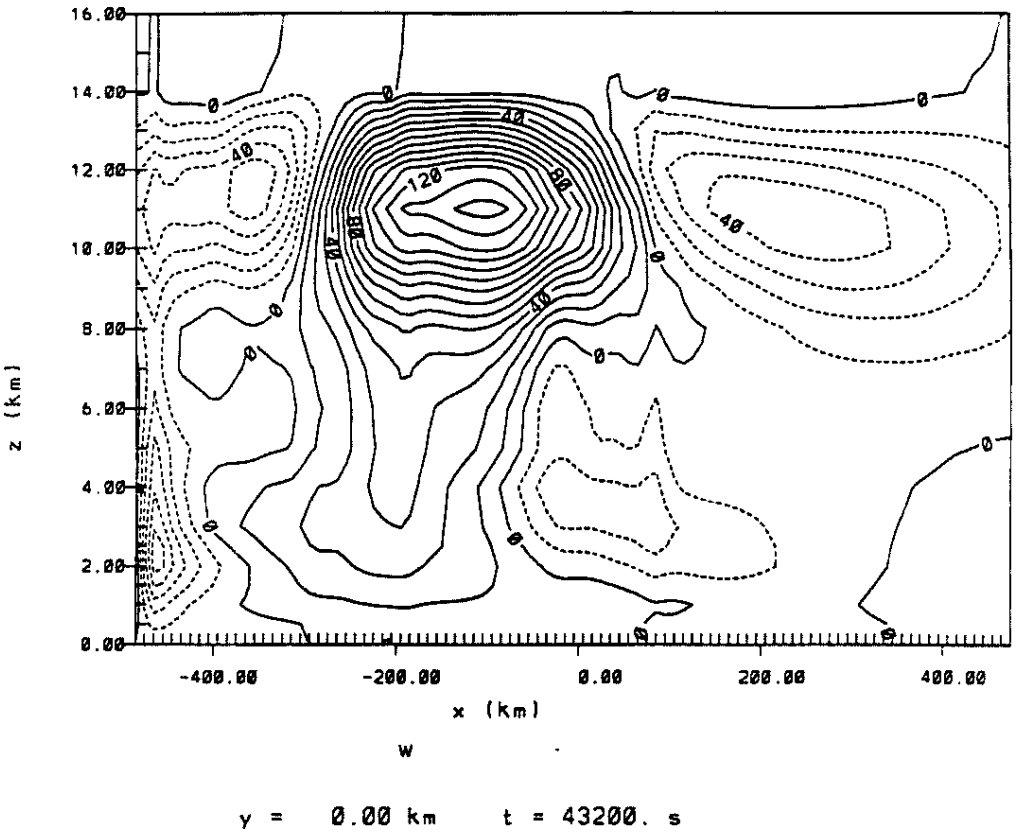


Figure 3.6: (b) Twelve hour model simulation of vertical velocity $w$ with cold low-level and warm high-level initial perturbation.

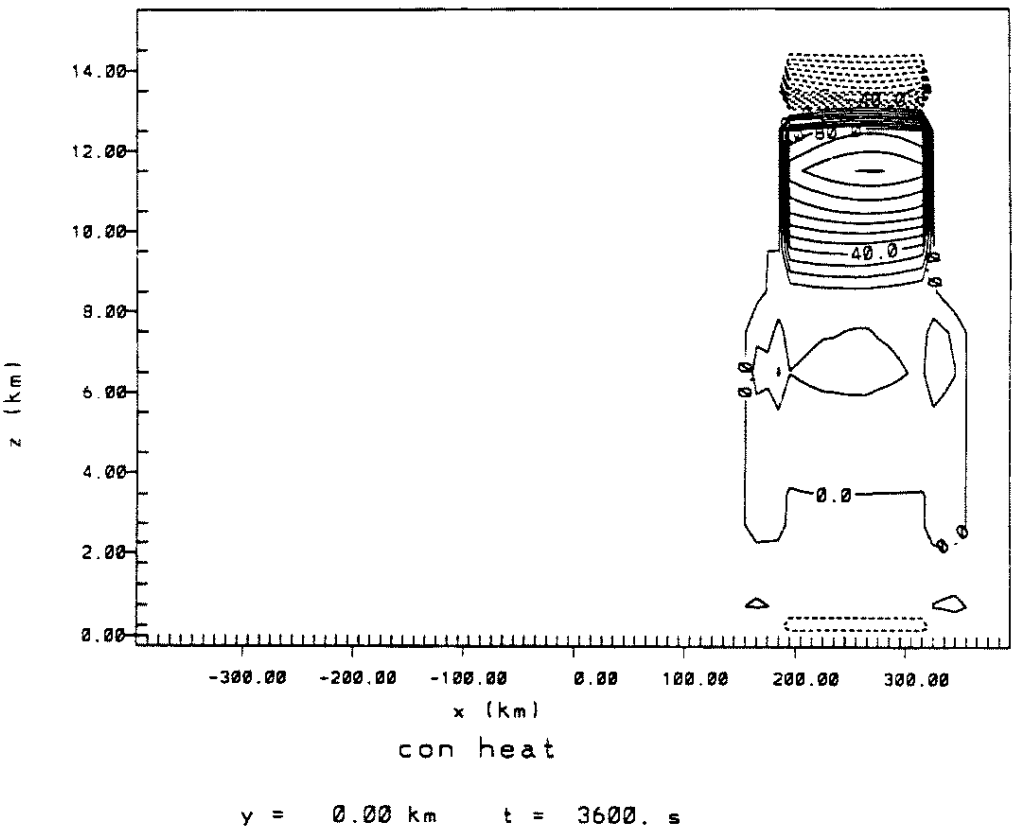


Figure 3.7: (a) Convective heating rate of the control run at 0500 LST.

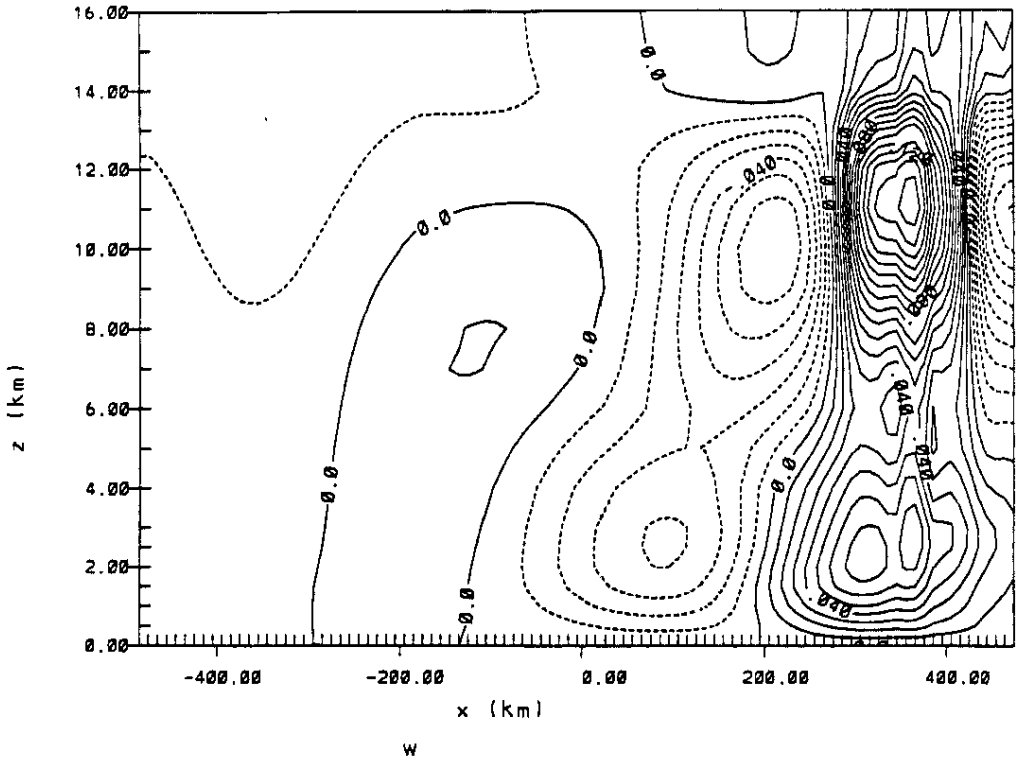


Figure 3.7: (b) Vertical velocity $w$ of the control run at 0600 LST.

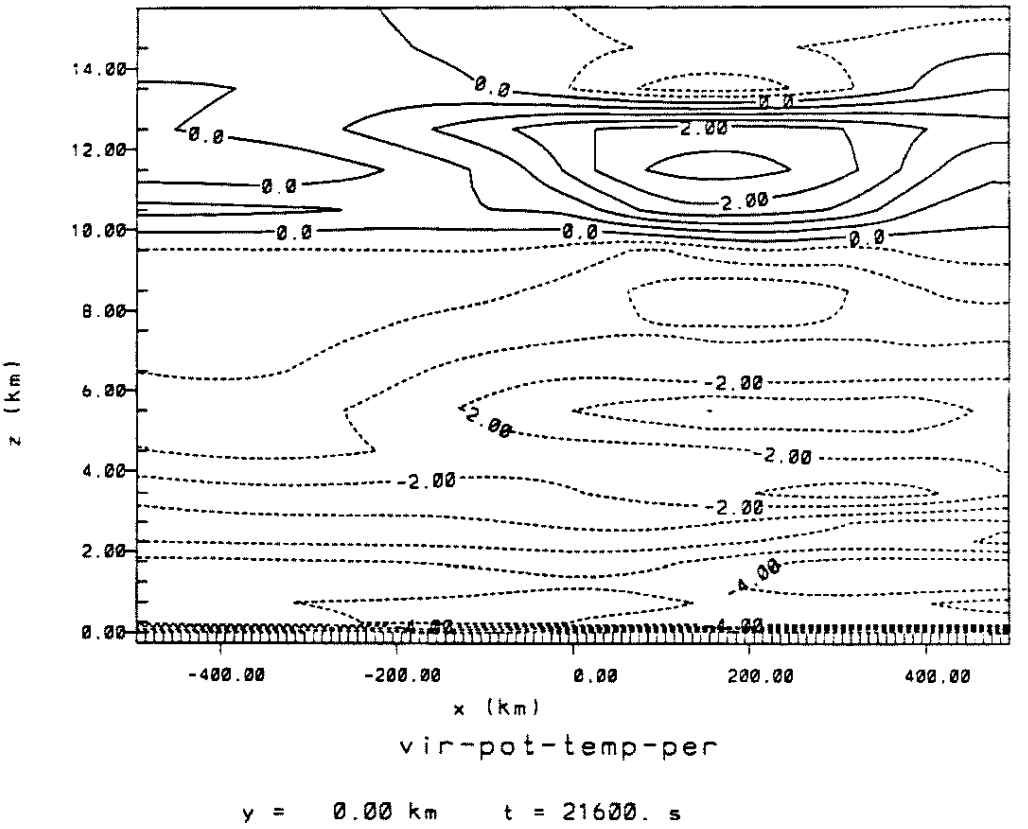


Figure 3.8: (b) Control run at 1000 LST for virtual potential temperature perturbation ($\theta'_v$).

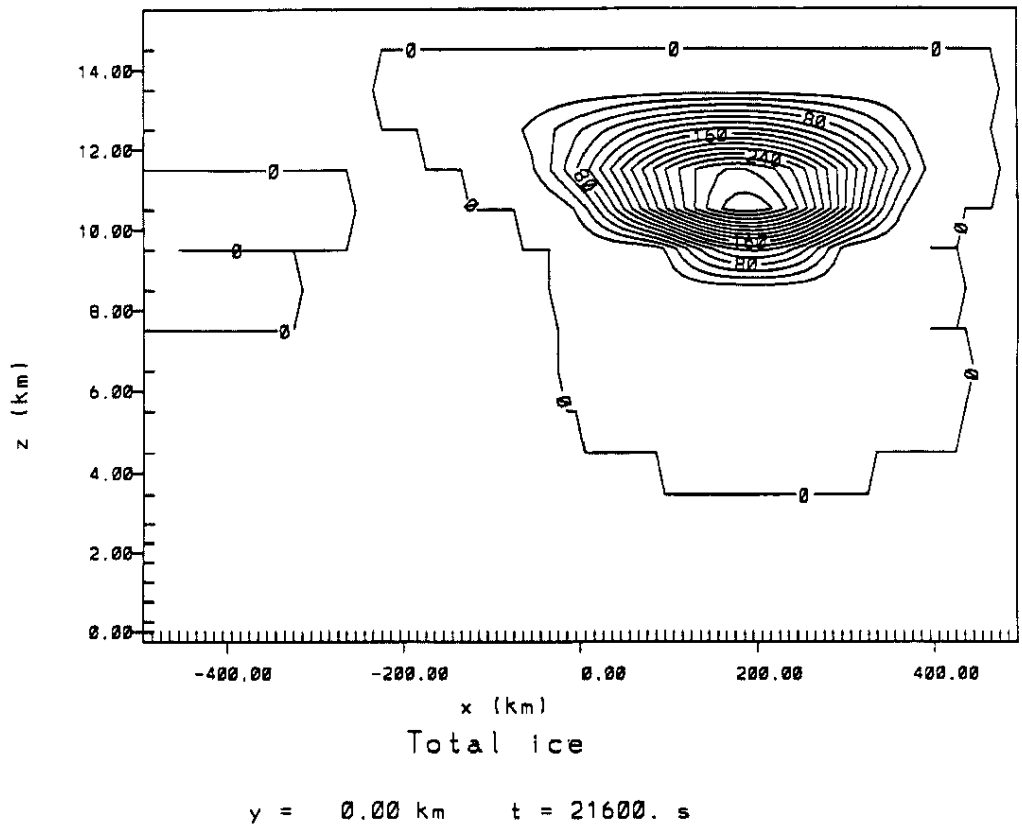


Figure 3.8: (c) Control run at 1000 LST for totla ice mixing ratio.

tens of cm $s^{-1}$ moves near the coast at 1100 LST, the average latent heat fluxes overland increases to almost 600 W $m^{-2}$ (Fig. 3.9) although the sensible heat flux is not that large because of the high soil moisture. In addition, the increase of the boundary layer mixing

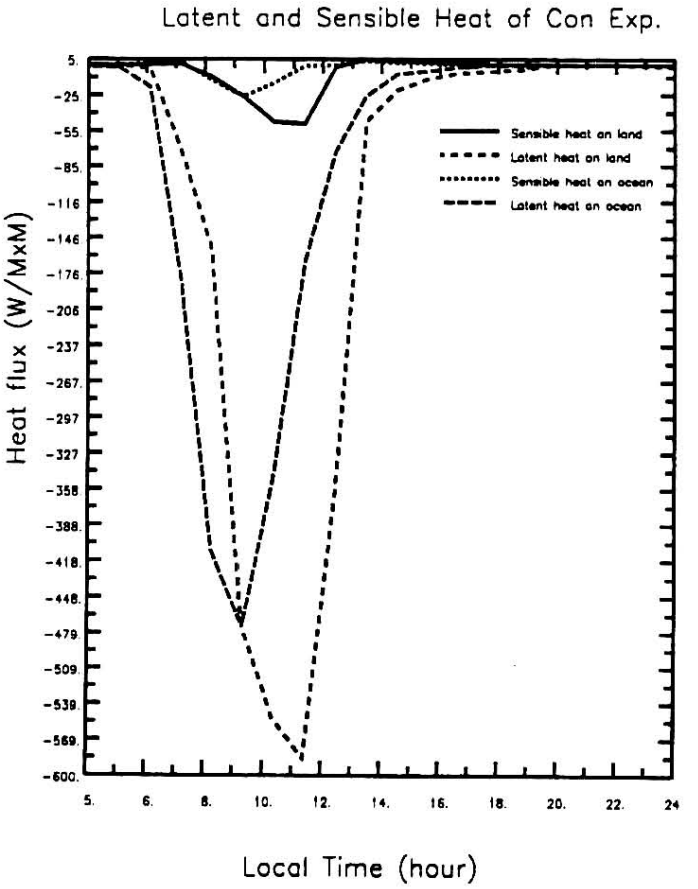


Figure 3.9: Variation of averaged sensible and latent heat flux over land and ocean of the control run against time.

process over land at high sun angle transfers more low-level moist static energy higher into the atmosphere. Furthermore, the warmed air over the land is brought toward the ocean by the low-level westerly flow and the mesoscale convection is promoted over the ocean adjacent to the land.

New convection occurs in the region where warm air from the land converges with the cold flow in front of the cloud cluster. The maximum convective heating rate reaches about 9.5 K $day^{-1}$ at a height of around 10 km. This warmed air due to latent heat released from the convection, initiates the upward motion in front of the old cloud cluster

and more convective motion occurs over the ocean. The new convection which occurred at the leading edge of the cloud cluster modelled here is consistent with the conceptual model in Fig. 1.2 discussed by Houze and Hobbs (1982) and Houze (1989). As mentioned previously, the depression formed in the Bay of Bengal on 7 July 1979, was constituted partly by the mesoscale convective cells. The modelled results are consistent with the observations.

A mesoscale convective system develops over land at 1200 LST due to the increase of incoming solar radiation and greater land surface evaporation. The maximum convective heating rate within the convective system reaches a value of 80 K $day^{-1}$ at 1300 LST. The convective cloud top, indicated by a convective cooling rate of 100 K $day^{-1}$, reaches to about 16 km. The maximum cloud water mixing ratio within the cloud cluster is 1.2 g $kg^{-1}$ at a height of 1.25 km near the coast. The cloud cluster consists of a major stratiform over the ocean and cumulus over both the land and ocean in front of it. Figure 3.10a gives the convective heating rate at 1300 LST.

By about 1300 LST there is a small amount of land precipitation far from the coast that is spread inland by the high-level easterly flow. The vertical velocity field (Fig. 3.10b) shows that there is a weak downdraft to the west of the updraft at the high level. However, most of the rain droplets associated with the downdraft beneath the anvil evaporate before they reach the surface. Therefore, there is only minor precipitation recorded on the ground about 200 km west of the coastline. This anvil rainfall lasts about two hours.

Figure 3.11a-c depicts the vertical velocity, convective heating, and total ice content at 1400 LST. The vertical velocity exhibits two major upward motion centers. One is from the old cloud cluster while it moves inland. Another one, which forms over the land adjacent to the coast, is from local convection due to moist ascending air lifted by the release of sensible and latent heat fluxes to the atmosphere from the heated land surface. The ratio of latent heat fluxes to the sensible heat fluxes over land is about 100–500 during most of the daytime because of high soil moisture loss (maximum 40% from the initial value) from the land. It is apparent that the existence of the local mesoscale convective system promotes the further development of the landfalling cloud cluster.

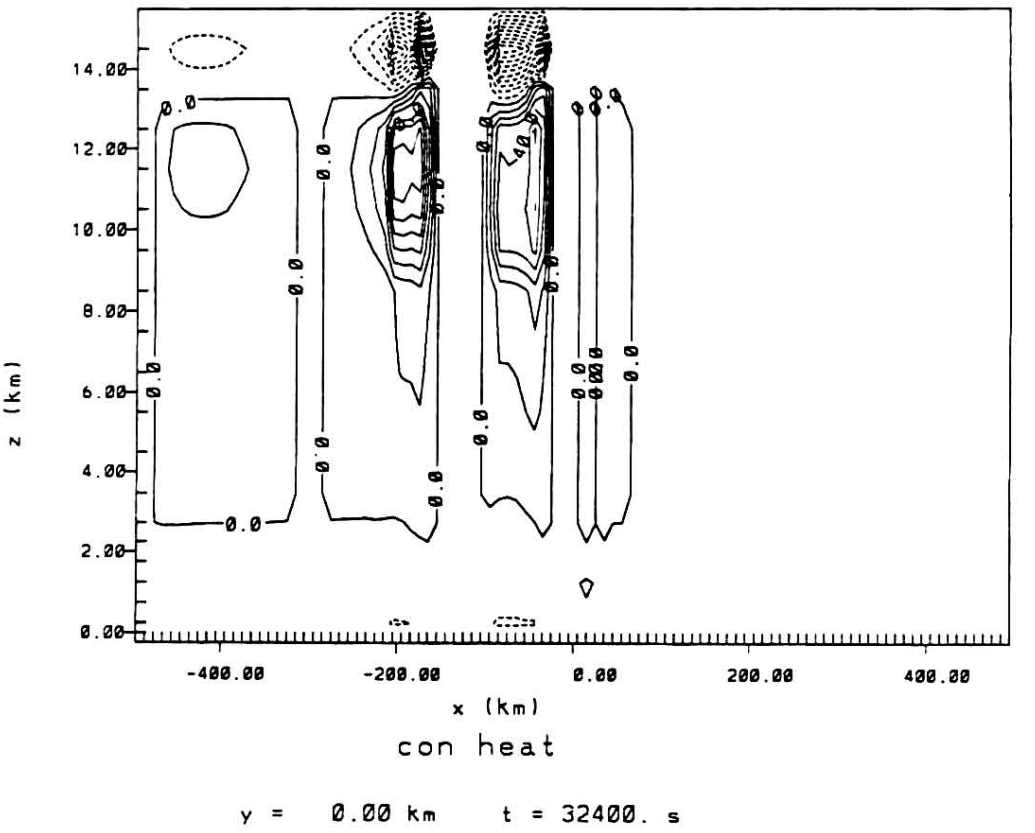


Figure 3.10: (a) Control run at 1300 LST for convective heating rate.

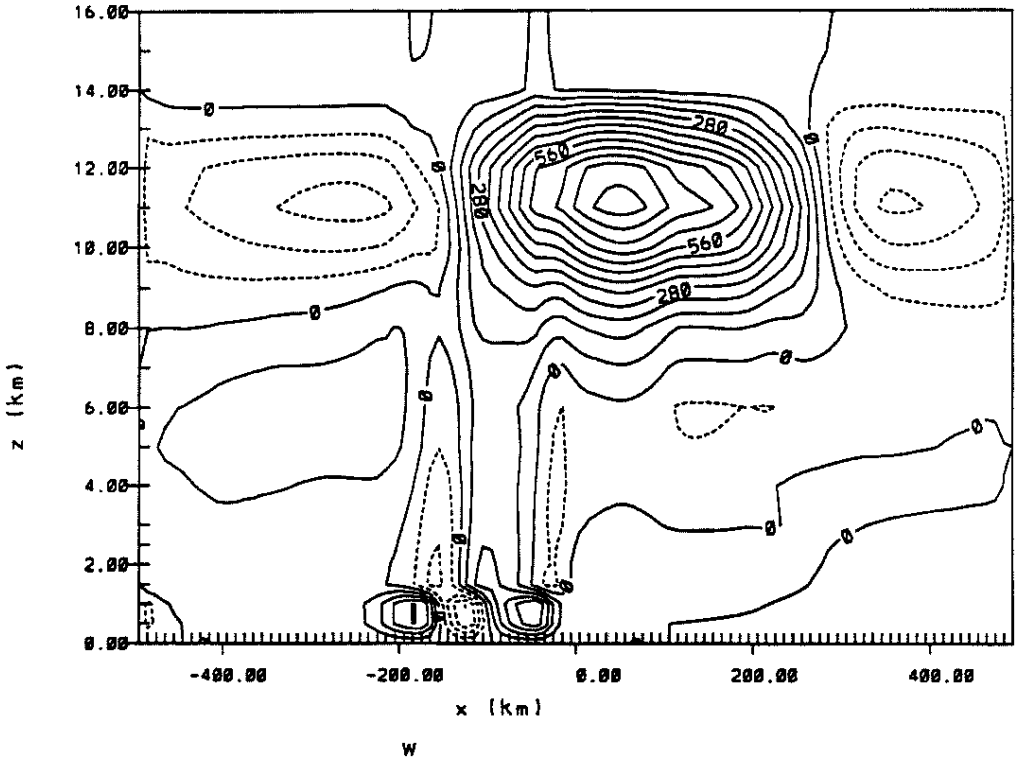


Figure 3.10: (b) Control run at 1300 LST for vertical velocity $w$.

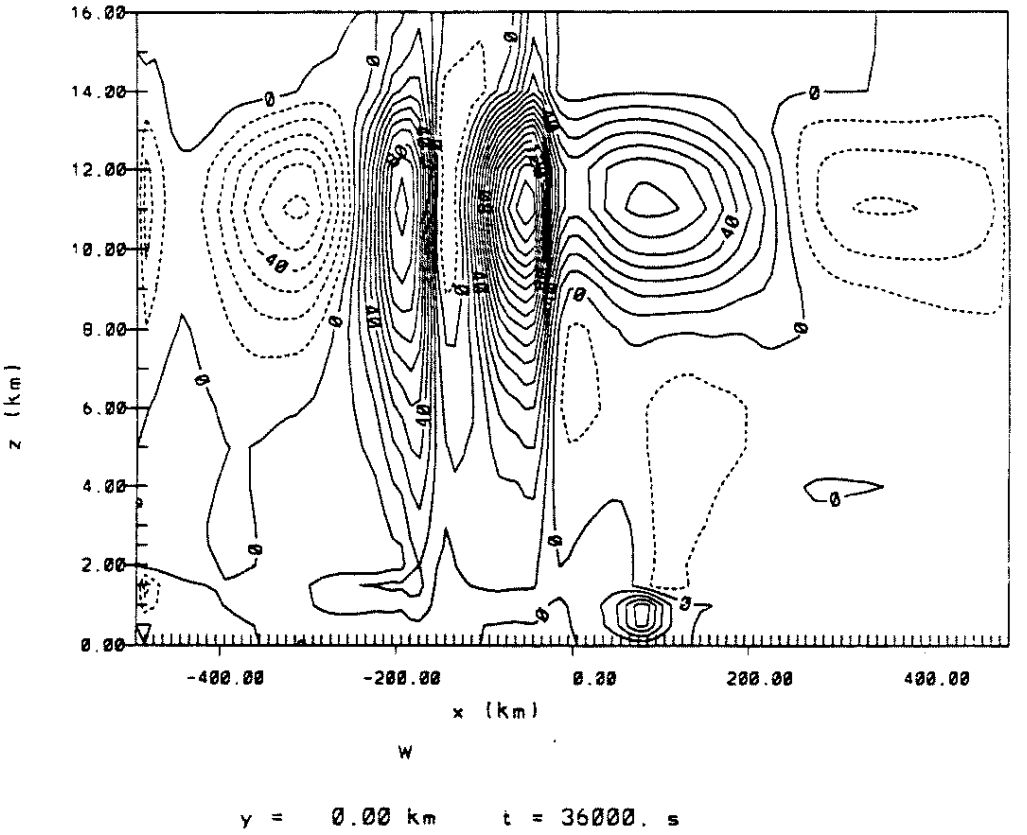


Figure 3.11: (a) Control run at 1400 LST for vertical velocity $w$.

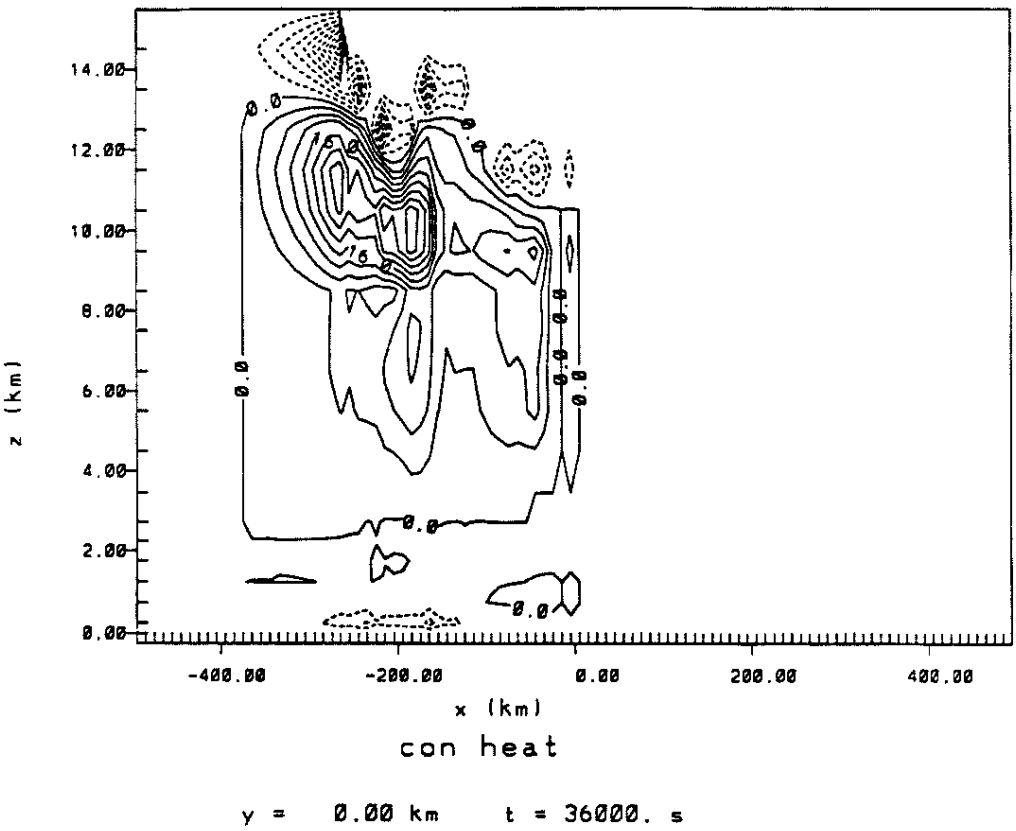


Figure 3.11: (b) Control run at 1400 LST for convective heating rate.

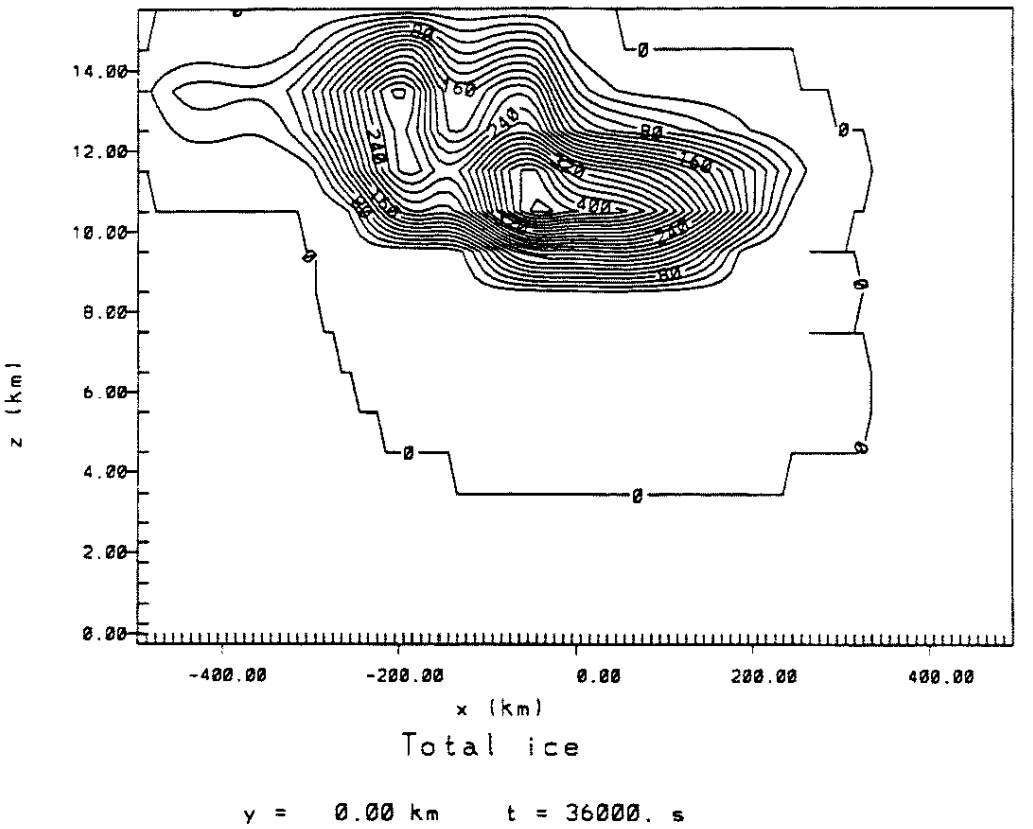


Figure 3.11: (c) Control run at 1400 LST for total ice mixing ratio.

The intensified mesoscale convective system also increases the ice mixing ratio within the cloud cluster with a value of 0.33 g $kg^{-1}$ over the ocean and 0.44 g $kg^{-1}$ over the land. The virtual potential temperature perturbation $\theta'_v$ shows an increase of +6.3 K between 10 to 13 km between the land and water. The upward motion within the convective system transports plentiful amounts of moisture to the high altitudes and increases the water content and thermal instability of the atmosphere. However, the soil moisture content has decreased by about 20% from the initial value adjacent to the coastline, and 40% some hundreds of kilometers from the coastline since the early morning due to the evaporation from the ground surface (Fig. 3.12). However, the soil temperature near the coastline does not vary much due to reduction of the incoming solar radiation by the cloud.

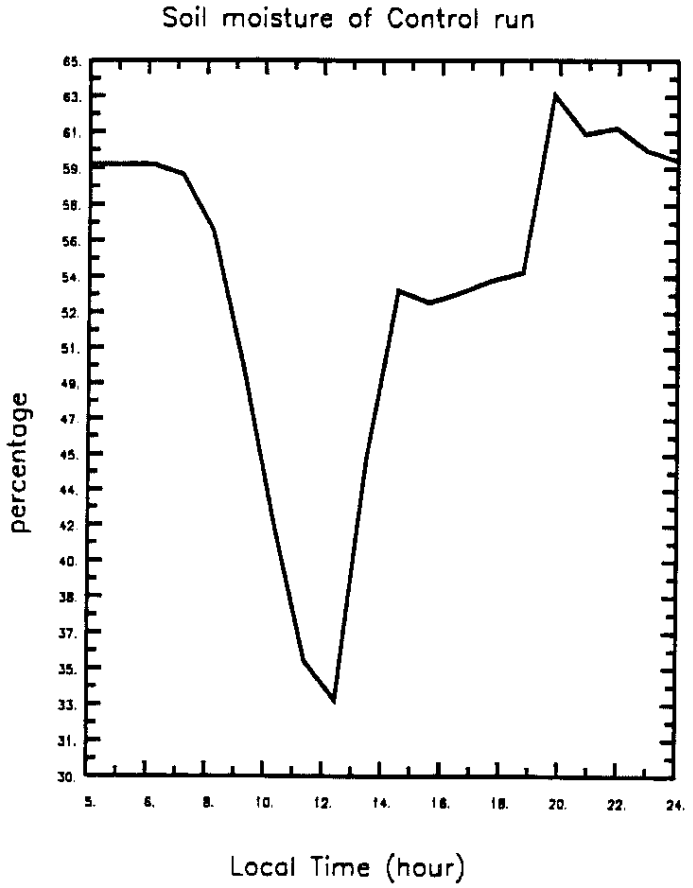


Figure 3.12: The variation of the soil moisture with time of the control run at 100 west of the coastline.

By 1600 LST, an apparent upward motion associated with the landfalling mesoscale cloud cluster forms over the land. The maximum upward motion center is located between

10 to 12 km (Fig. 3.13a). The upper-level easterly wind forms a strong vertical shear in front of the cloud cluster between those levels (Fig. 3.13b). The upward motion is apparent and new mesoscale convection with a maximum heating rate of 14 K $day^{-1}$ at the 8 km height appears at about 250 km west of the coast. However, precipitation occurs over a wide region that includes 100 km over the ocean and 300 km over the land although the magnitudes are small (Fig. 3.14). The large area of rainfall is the result of both stratiform and convective cloud precipitation. For stratiform rainfall, the precipitation particles in the upper portion of the anvil cloud are initially in the form of ice particles which grow as they descend until they melt below the 0°C level and then partially evaporate while falling as rain droplets through unsaturated air below the base of the anvil in the cloud cluster. The stratiform rain associated with the mesoscale downdraft usually fall in the central and rear part of the cloud cluster. The convective showers, however, come from the melting of the ice particles and the super-cooled water droplets at the top and middle portion of the convective towers. The maximum cloud water mixing ratio is 1.2 g $kg^{-1}$ over the land and 1.3 g $kg^{-1}$ over the ocean at this time.

One hour later (1700 LST), the rainfall increases and covers the region between 100 to 400 km west of the coastline. Most of the rainfall at this time comes from the front of the cloud cluster. Figure 3.15 represents the rain mixing ratio at this time. The heavy rainfall at the leading edge of the cloud cluster is similar to the tropic squall line convection cloud clusters demonstrated by Houze (1982) with respect to the low-level outflow and the mesoscale rainfall features. Therefore, the easterly flow in the surface layer increases after the original cloud cluster moves inland. This flow transports moist air in the lower boundary layer from the ocean surface to supply the convective system over the land. Figure 3.16 gives the variation of the west-east component as a function of time at 250 m above the ground and 50 km west of the coastline. The increase of the low-level easterly wind is significant since the cloud cluster has moved inland.

Three hours later (2000 LST), a warm and wet layer with a maximum cloud water mixing ratio of 1.9 g $kg^{-1}$ and a +1.2°C virtual potential temperature perturbation forms around 4-5 km above sea level and extends 200 km over land and 200 km over the ocean,

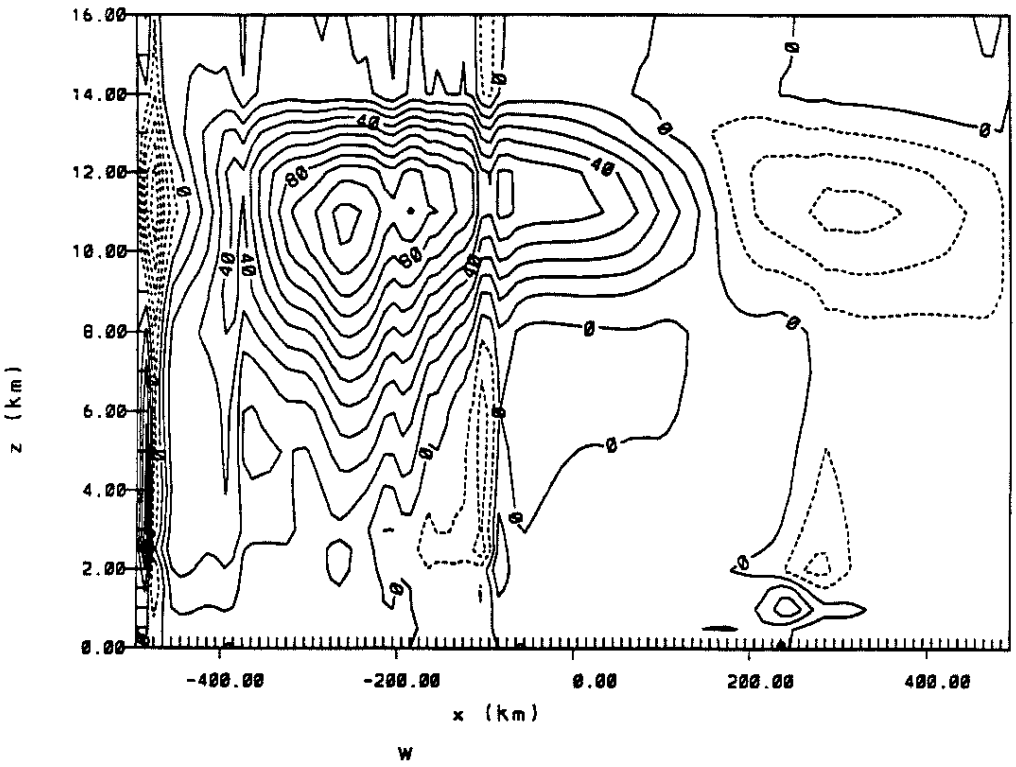


Figure 3.13: (a) Vertical velocity $w$ of the control run at 1600 LST.

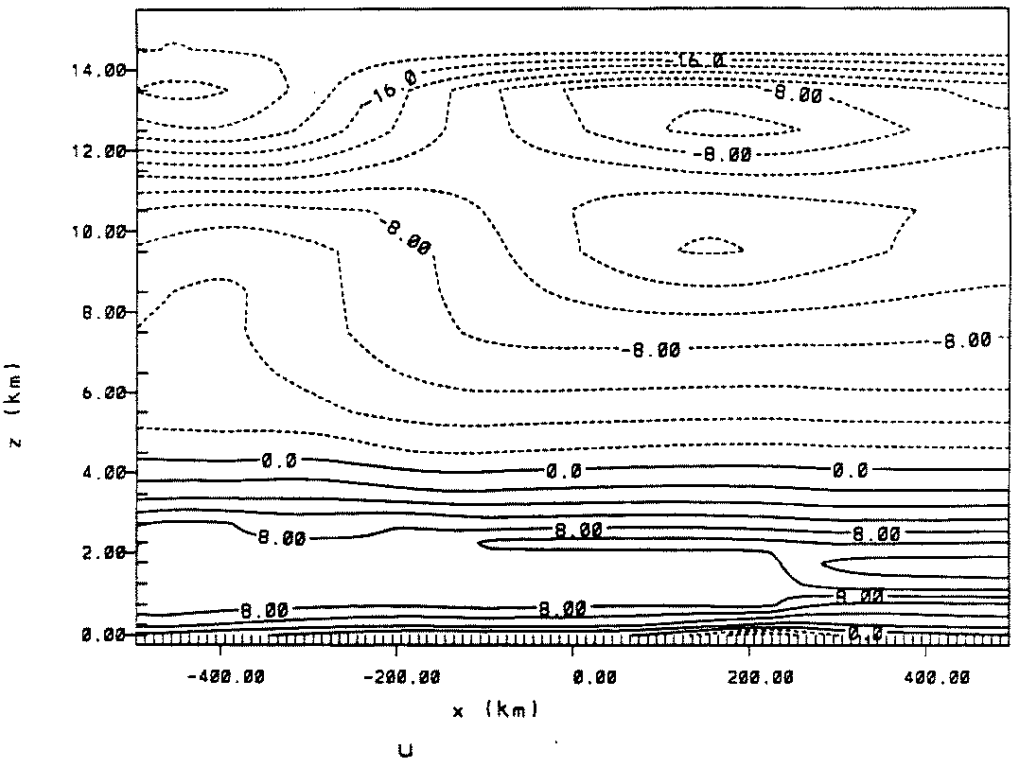


Figure 3.13: (b) West-east wind $u$ of the control run at 1600 LST.

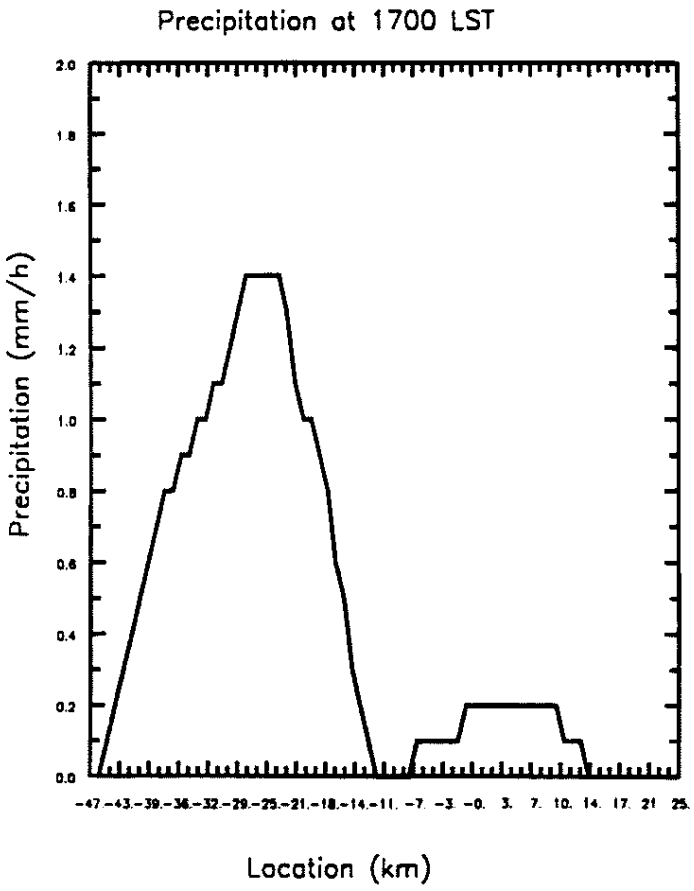


Figure 3.14: Precipitation of the control run at 1700 LST.

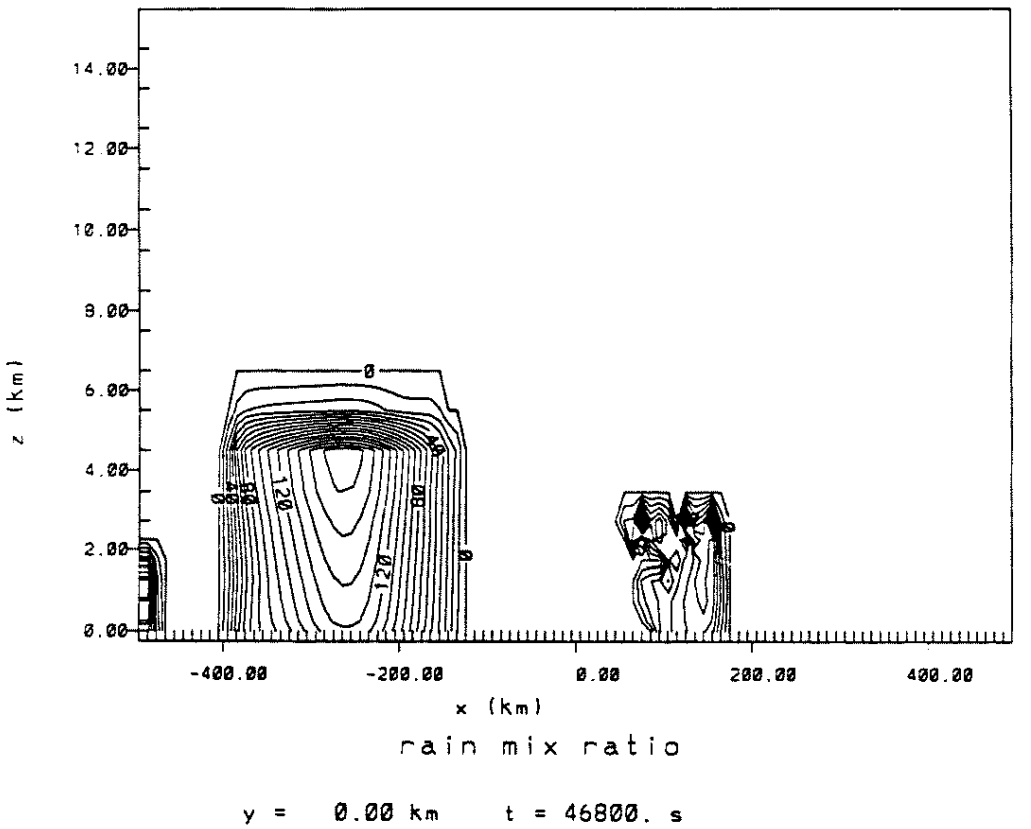


Figure 3.15: Rain mixing ratio of the control run at 1700 LST.

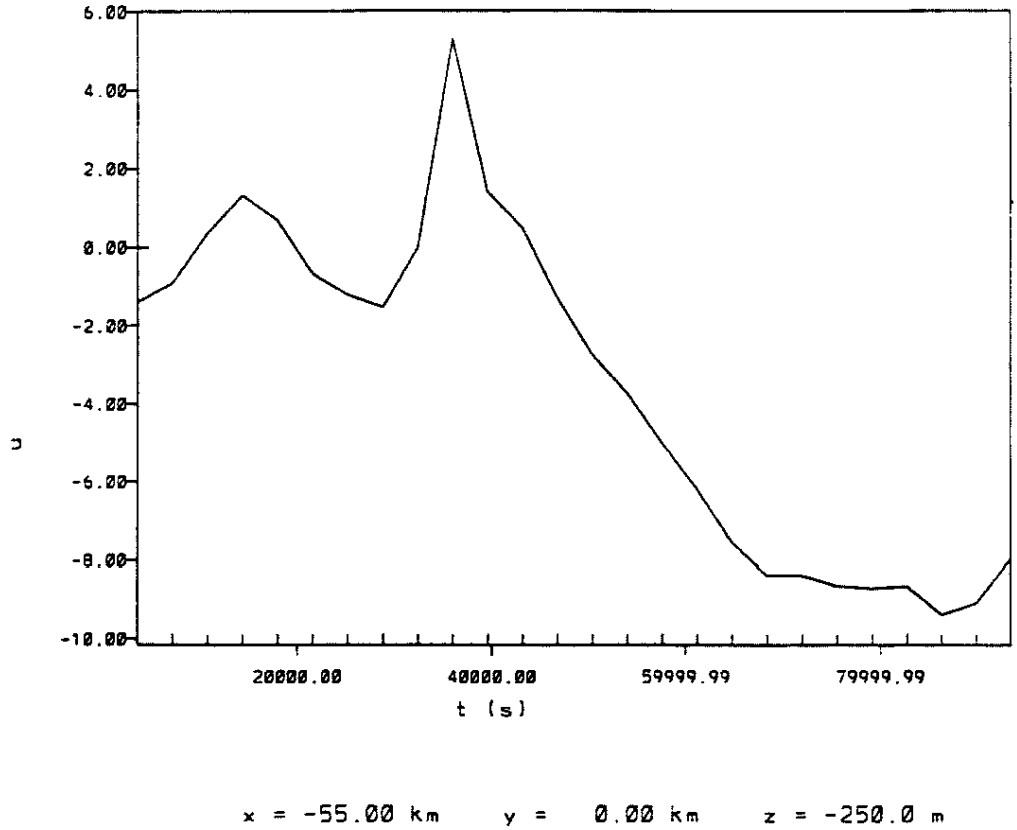


Figure 3.16: Variation of low level west-east wind $u$ of the control run 50 km west of the coast against time.

respectively. This relatively moist and warm thin layer may be caused by latent and infrared radiative heating within the cloud that is associated with the mesoscale ascending motion. A certain amount of precipitation falls at 50 km east and 150 km west of the coastline. Figure 3.17a-b illustrates the $\theta'_v$ and the rain mixing ratio at this time. The pattern of rainfall and corresponding thermal structure (Fig. 3.17c) indicate that most of the rain comes from the stratiform cloud that existed in the rear of the cloud cluster. The new cloud is indicated by a significant "valley" at 4 km level in the $\theta_e$ field over the land and sea near the coast region.

### 3.3 Decayed Stage

By about 2200 LST (18 hours of simulation), the cloud cluster has been weakened considerably in terms of cumulus convection activity and mesoscale precipitation. This occurs because the inland propagation of the cloud cluster moves it into less favorable conditions. The moisture flux over the soil is lower than that over water. The boundary layer turbulent mixing process is reduced in the late evening because the buoyancy term is negligible and the shear production term is the only energy input to the lower atmosphere. Figure 3.18 shows the vertical velocity field at this time. The ascending motion, which is associated with a weak ascent, is apparent although the magnitudes are small. The sinking motion due to nocturnal radiative cooling dominates a wide portion of the domain. The total ice content in the cloud cluster has decreased from 0.72 g $kg^{-1}$ at 2000 LST to 0.63 g $kg^{-1}$ between the heights of 13 to 14 km (Fig. 3.19). This lower ice content indicates that the weak ascending motion and absence of deep cumulus convection cannot transfer significant amounts of low-level moist air to the upper level. Hence, the cloud cluster loses its energy source.

The evolution of the lower level east-west wind component also indicates the land-falling of the cloud cluster. Figure 3.20 represents the variation of the lower level east-west wind with time 100 km west of the coast. The wind varies greatly near 1500 m above the ground. The turbulent mixing process is significant at 1400 LST when the monsoon cloud cluster approaches the coast. However, the onshore flow at the levels below 500 m

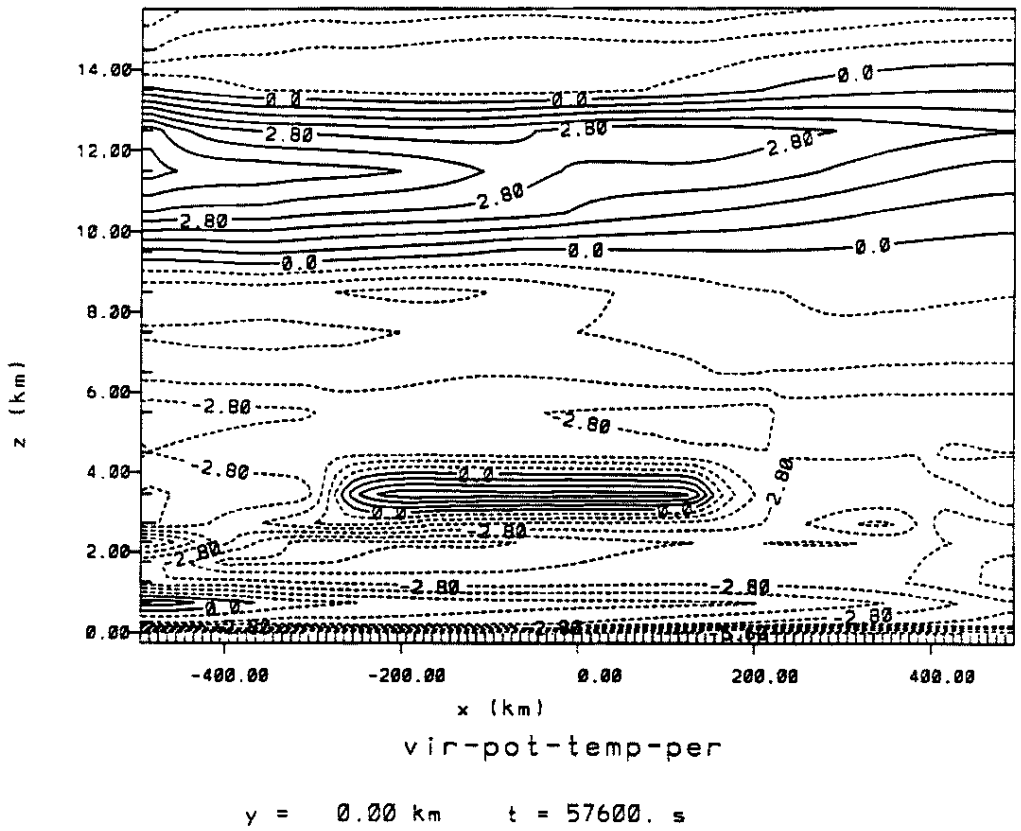


**Figure 3.17: (a) Virtual potential temperature perturbation ($\theta'_v$) at 2000 LST of the control run.**

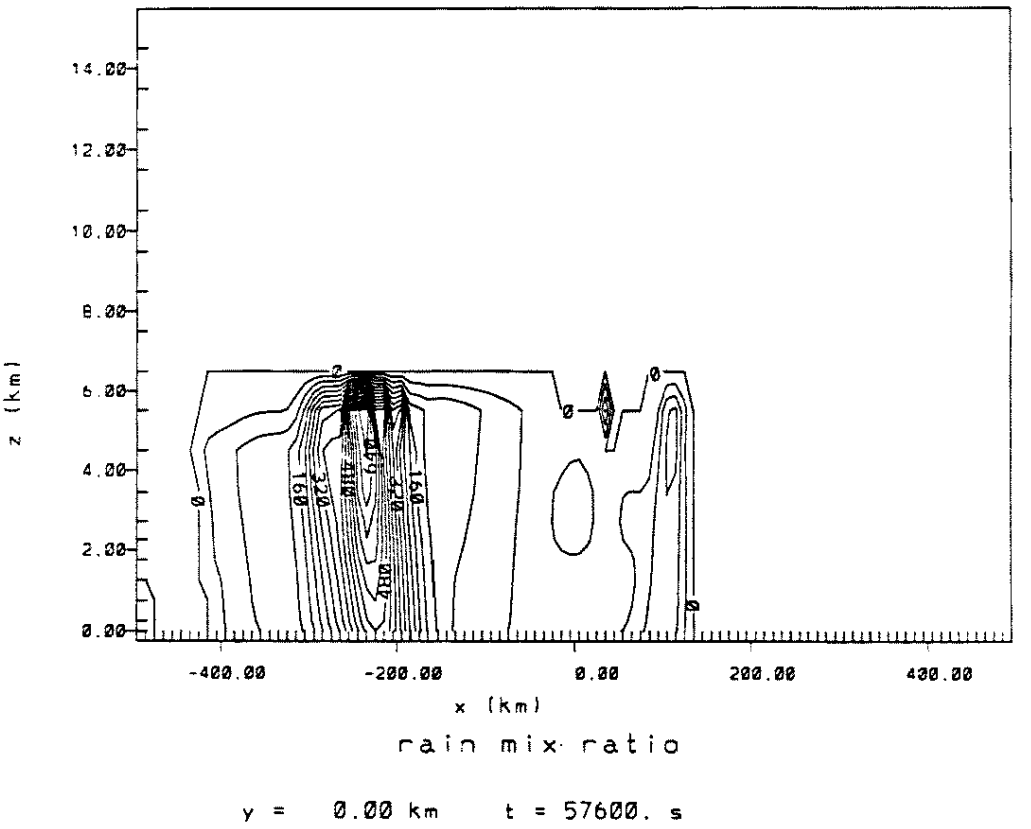


Figure 3.17: (b) Rain mixing ratio at 2000 LST of the control run.

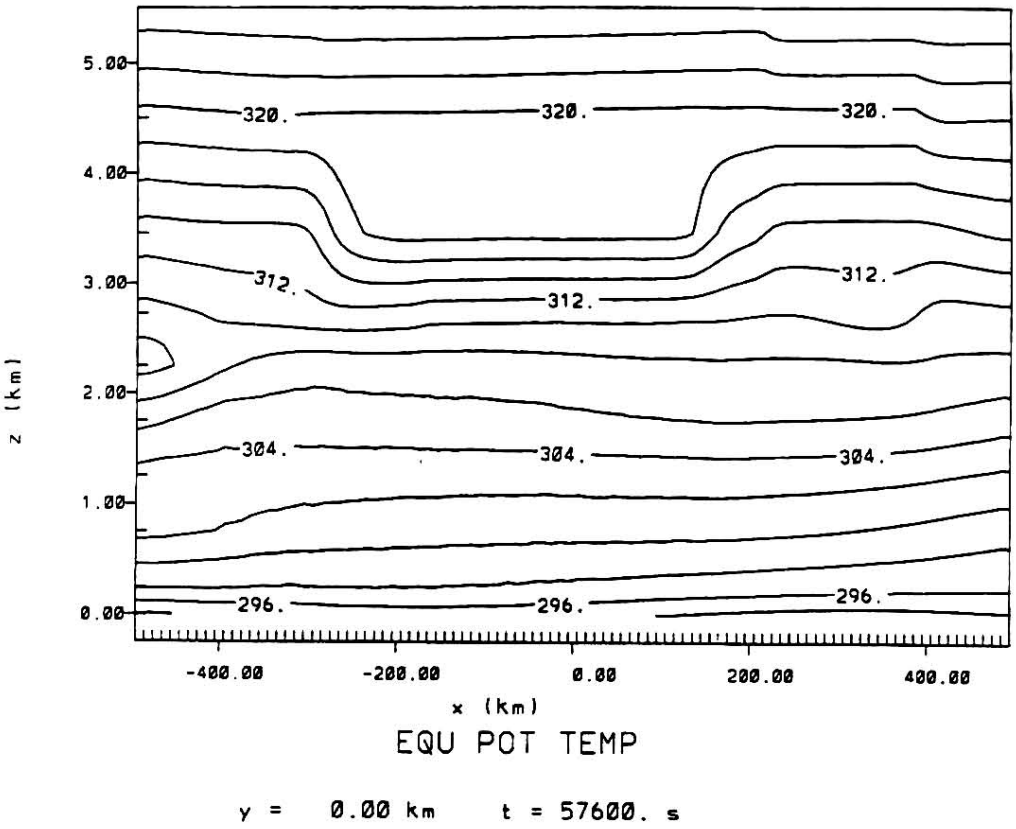


**Figure 3.17: (c) Equivalent potential temperature at 2000 LST of the control run.**

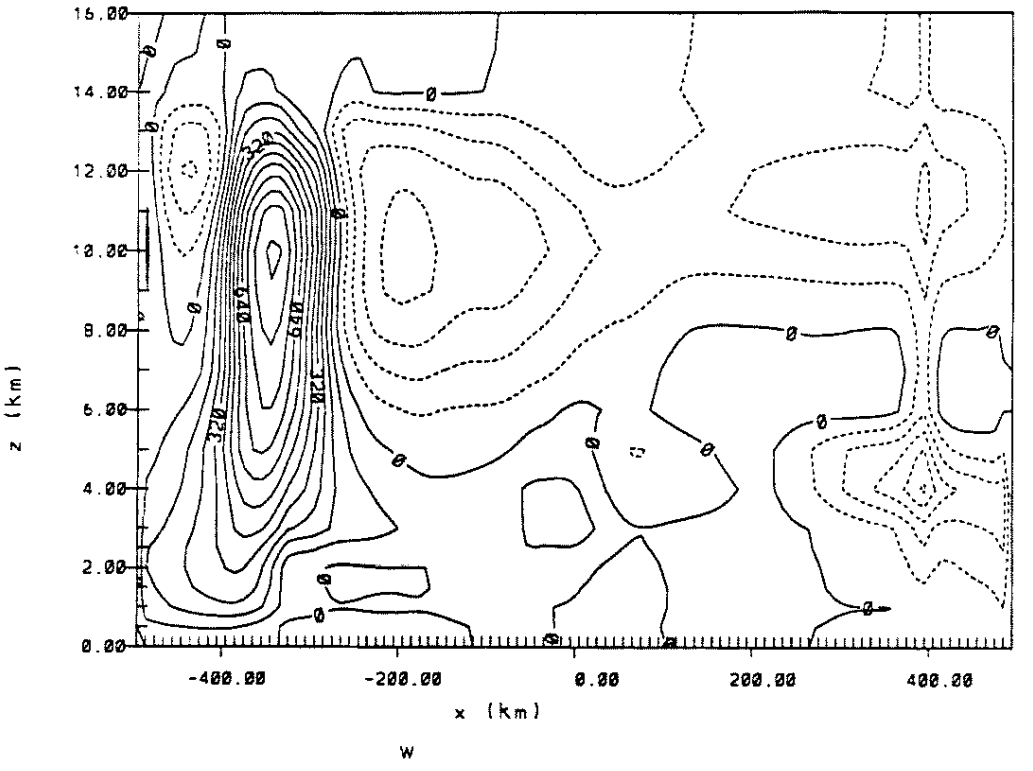


Figure 3.18: Vertical velocity $w$ of the control run at 2200 LST.

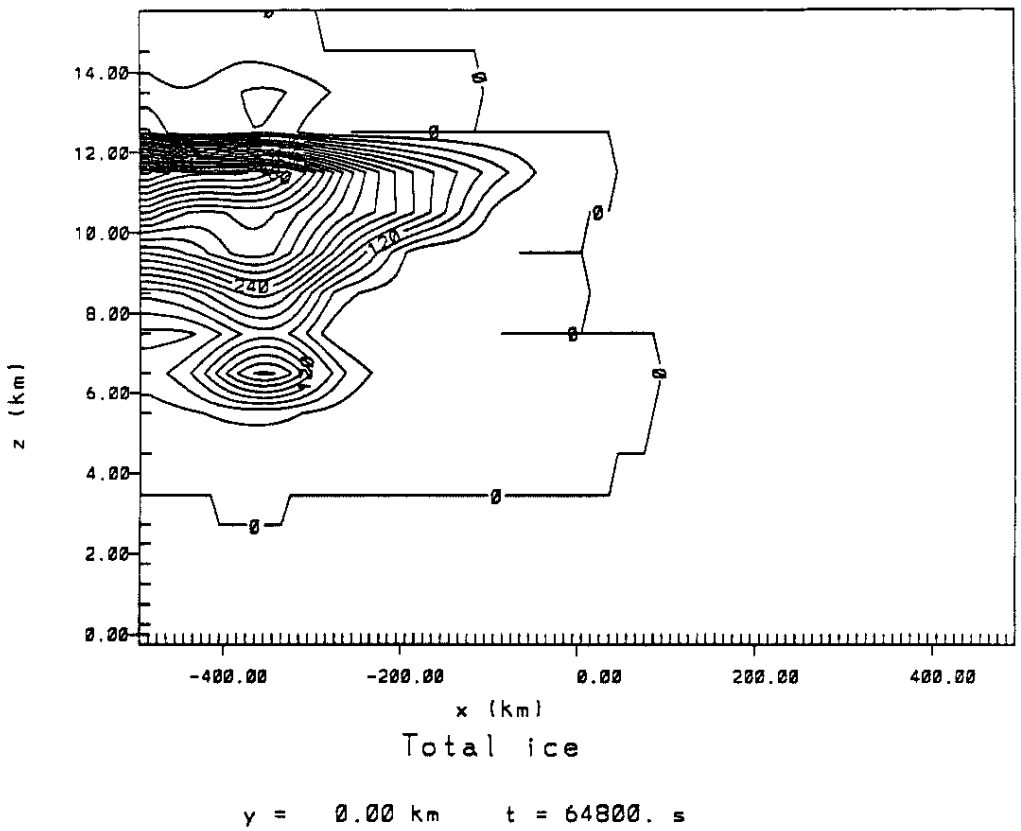


Figure 3.19: Total ice content of the control run at 2200 LST.

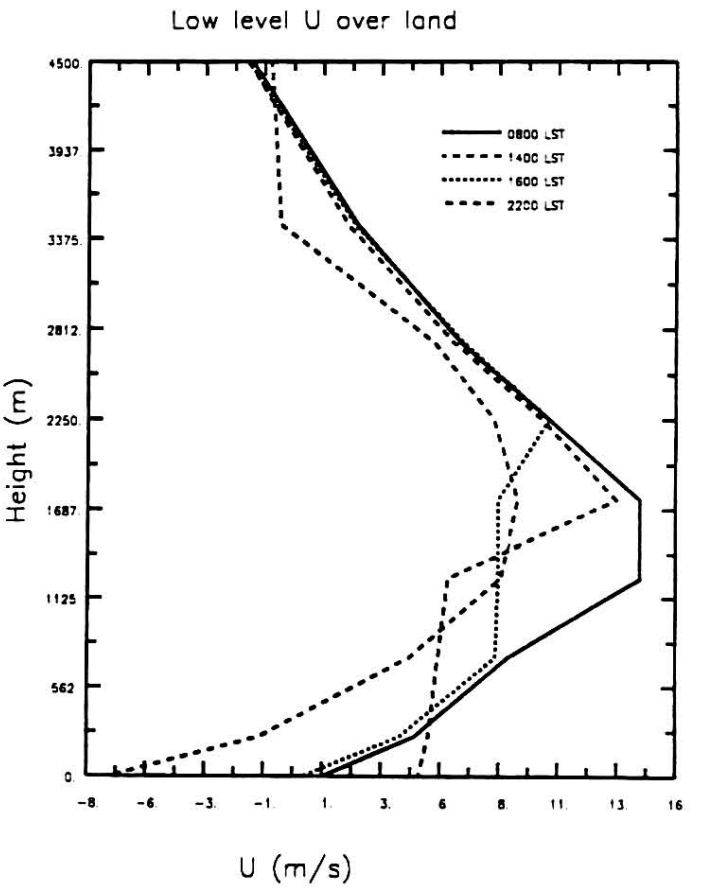


Figure 3.20: The east-west wind of the control run at 0800, 1400, 1600, and 2200 LST.

increases when the boundary layer becomes stable and the landfalling cloud cluster decays. The reason for this is that the higher low-level moisture due to the previous rainfall keeps the air within the boundary layer warmer than the air over the ocean. Therefore, the pressure gradient force drives as a sea-breeze like westerly wind.

As mentioned previously, in the rear part of the cloud cluster the air is moistened by the evaporation of water droplets. A thin and wet moist air layer has formed at a height of about 4 km from late evening until early morning. Figure 3.21 represents the total precipitation over the land. About 80% of the rain fell from the cloud cluster before 2200

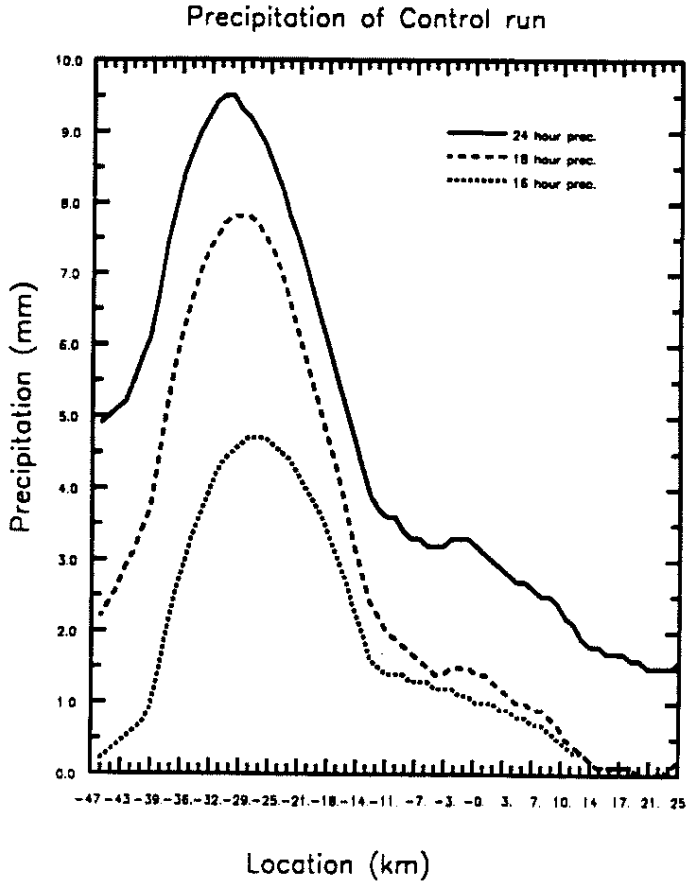


Figure 3.21: Total rainfall of 16, 18, and 20 hour simulation in the control run.

LST. The maximum rainfall was concentrated in the region between 200 to 300 km west of the coastline.

The current model simulation results suggest that rainfall over the east coast of the India subcontinent during the monsoon season is partly from the major cloud cluster in the monsoon depression and partly from the local convective clouds which interact with the landfalling cloud cluster. The distribution of the precipitation is very consistent with the observational data mentioned in Fig. 3.4. Actual observed 24 hour precipitation from 00Z 7 July to 00Z 8 July shows that the maximum rainfall is located from 200 to 300 km northwest of the Indian east coast. The recorded 24 hour precipitation indicates that the maximum value is 96 mm at about 250 km northwest of the coast. However, the magnitude of the stratiform and convective rainfall from the modelled result (11.8 mm) is less than that in the real world (Fig. 3.21). However, the observed maximum is a point value, whereas the simulated rainfall is an area-average. The simulated value is probably also too small because horizontal convergence in the second spatial dimension has not been included in these experiments.

The model simulation results are consistent with the observed landfalling monsoon cloud cluster. The effect of surface heat fluxes on the inland propagation and development of the monsoon cloud cluster is apparent in the model simulation. Webster (1983) suggested that the surface hydrological effects can aid the poleward movement of the monsoon through the evaporative cooling of the precipitation moistened ground. The modeled results show that the supply of sensible and latent heat from the ground to the air destabilizes the atmosphere before the cloud cluster moves inland. The development of mesoscale convective systems over the land then promotes further increase of the cloud cluster when it moves inland. There are some differences between the modelled results and the observational data with respects to magnitude of precipitation. These differences may be caused by the following reasons: (1) this is a two-dimensional model simulation. The lack of variations in the north-south direction makes the modelled system lose a portion of the vortex effect. This vortex effect influences the intensity and evolution of the depression system. (2) The two-dimensional simulation also loses a portion of the moisture convergence. This will make the modelled magnitude of the precipitation less than reality. (3) The topographic forcing effect is not included in the model simulations. There is only

flat land in the model. It is known from the results of Sanders (1984) that topographic forcing can influence the low-level easterly flow of the monsoon disturbance.

However, the modelled simulation results are still valuable in describing the following major features: (1) the evolution of the simulated cloud cluster; (2) the corresponding rainfall process and the location of the precipitation when the cloud cluster moves over the ocean and the land; (3) the interaction process between the local mesoscale convective system and the landfalling cloud cluster; and (4) the typical inner structure of the cloud cluster associated with the summer monsoon.

In the following chapters the sensitivity of the simulated cloud cluster to surface characteristics will be presented and discussed.

# Chapter 4

## SENSITIVITY EXPERIMENTS

In Chapter 3, the evolution of a simulated landfalling monsoon cloud cluster which formed over the ocean was discussed. This simulated cloud cluster, although differing in some details, is consistent with the major features of a mesoscale convective complex associated with the monsoon depression observed over the Bay of Bengal on July 7-8, 1979. The observed cloud cluster (Houze and Churchill, 1987) has the typical characteristics of the tropical cloud cluster as suggested by Houze and Hobbs (1982). The modelled cloud cluster also has a large anvil canopy near the tropopause. The cloud cluster tends to travel by a combination of translation and discrete propagation, wherein areas of cloud systematically form at the leading edge of the system. The influence of land surface evaporation on an intensification of the cloud cluster is significant.

There are two major geographic factors which influence the evolution of the mesoscale convective system: the water and the land surface. Shukla and Misra's (1977) study indicated that heavy rainfall on the Indian continent was related to a positive sea surface temperature (SST) anomaly of the Arabian Sea. As discussed in Section 1.4 and 1.5, the effect of landscape on the mesoscale weather system as well as the summer monsoon, is significant. Mooley and Shukla (1987) suggested that soil moisture influenced the ground heating which in turn determined the sensible heat flux and affected the generation and dissipation of heat lows. The soil moisture effects could, therefore, be as important as SST anomaly effects on the summer monsoon.

In this chapter, several experiments are designed to study influence of land and ocean surface characteristics on the variation of the mesoscale convective system associated with the monsoon depression.

## 4.1 Soil Moisture Sensitivity

It is virtually certain that alterations of the ground surface have caused major changes in the weather over widespread regions. The size of a land mass can result in a variation of mesoscale circulation intensity (Xian and Pielke, 1991). One of the major mechanisms that increases mesoscale rainfall is the modification of the environment through an increase of low-level moist static energy to a state more conducive to the formation of deep moist convection.

In an attempt to isolate the effects of soil moisture on the mesoscale convective system, the simulation in Chapter 3 is repeated with a variation of the soil moisture from 0.8 (relative wet land surface) to 0.3 (relative dry land surface). Everything else is identical to the control run.

Here, the evolution and propagation of the simulated cloud cluster over ground surfaces with different soil moisture will be tracked. At 1200 LST, the vertical motion field in the two experiments is very similar in the two runs with the center of upward motion located at about the same place. Two hours later at 1400 LST (Fig. 4.1a-b), the SLM run which represents the dry land surface situation, has shifted the center of the simulation's upward motion toward the west. The maximum upward motion in both the SHM simulation, which represents the wet land surface situation, and in the control run, is located along the vertical axis at the leading edge of the cloud cluster.

Before landfalling, in the SHM run, the latent heat fluxes are about 3 to 4 times larger than in the SLM run. In the wet land surface run, the deep cloud develops at 1100 LST over the ocean near the coastline first. Then the clouds form over both the land and ocean adjacent to the coastline. However, in the SLM case, the deep cloud first appears only over the land near the coastline at 1100 LST. It then moves inland (Fig. 4.2a-b). The total ice mixing ratios in the cloud cluster also exhibit relatively large values in the SHM experiment (Fig. 4.3a-b). The maximum ice mixing ratio is 0.46 g $kg^{-1}$ in the SHM run and 0.38 g $kg^{-1}$ in the SLM run at 1400 LST. The cloud cluster in the SHM run has a relative moist core when it moves over the wet ground surface.

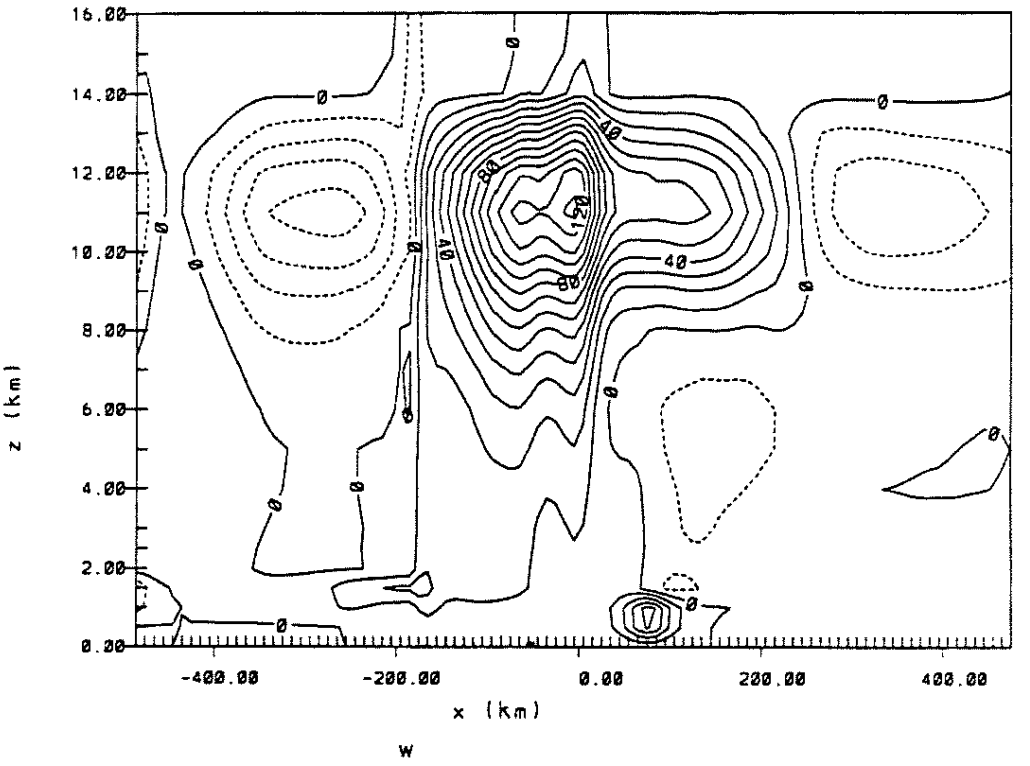


Figure 4.1: (a) Simulation of $W$ field for SHM (wetter soil) at 1400 LST.

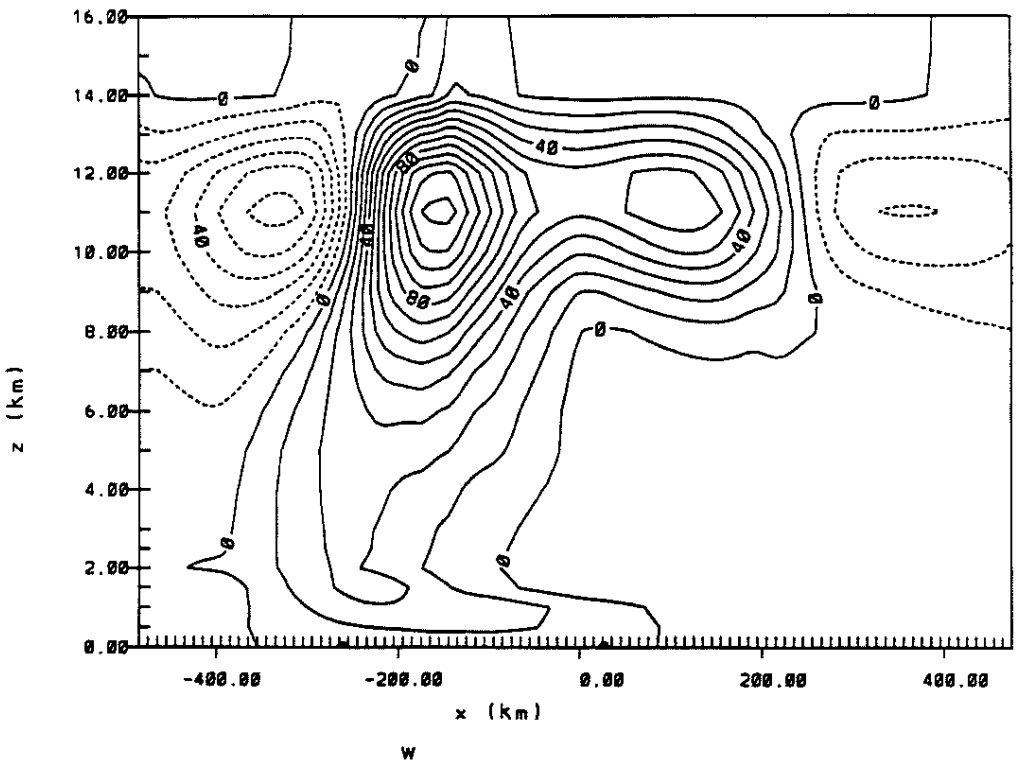


Figure 4.1: (b) Simulation of $W$ field for SLM (dry soil) at 1400 LST.

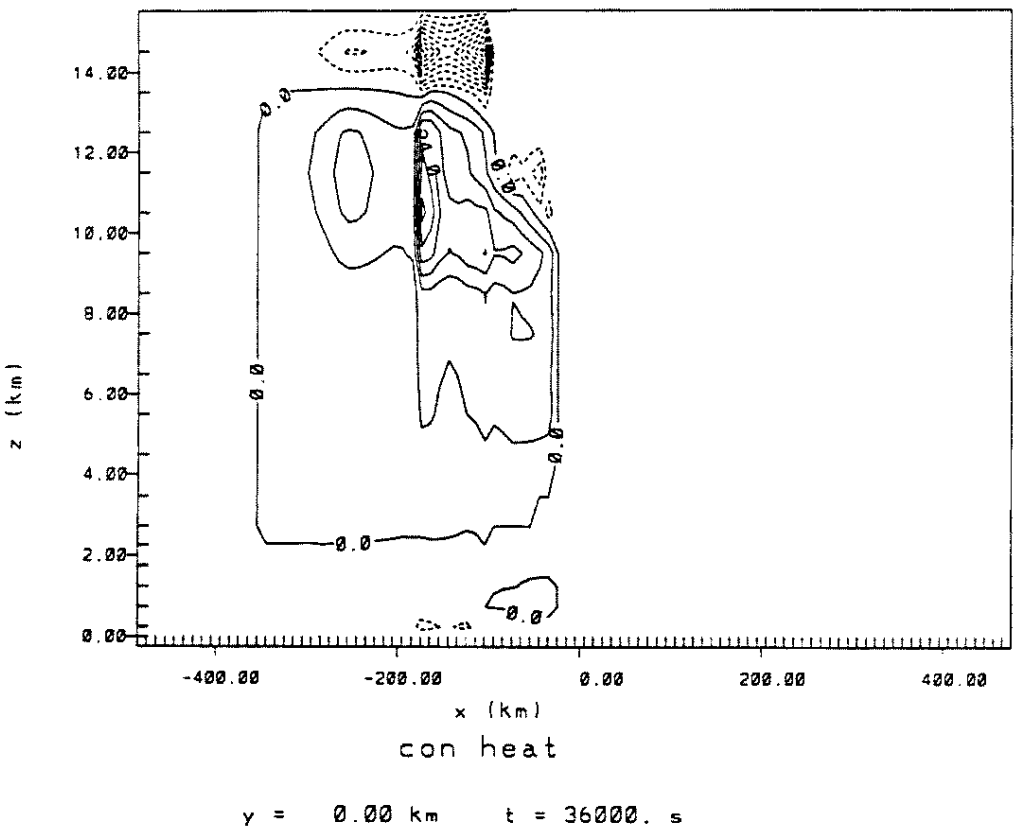


Figure 4.2: (a) Convective heating rate at 1400 LST for SHM run.

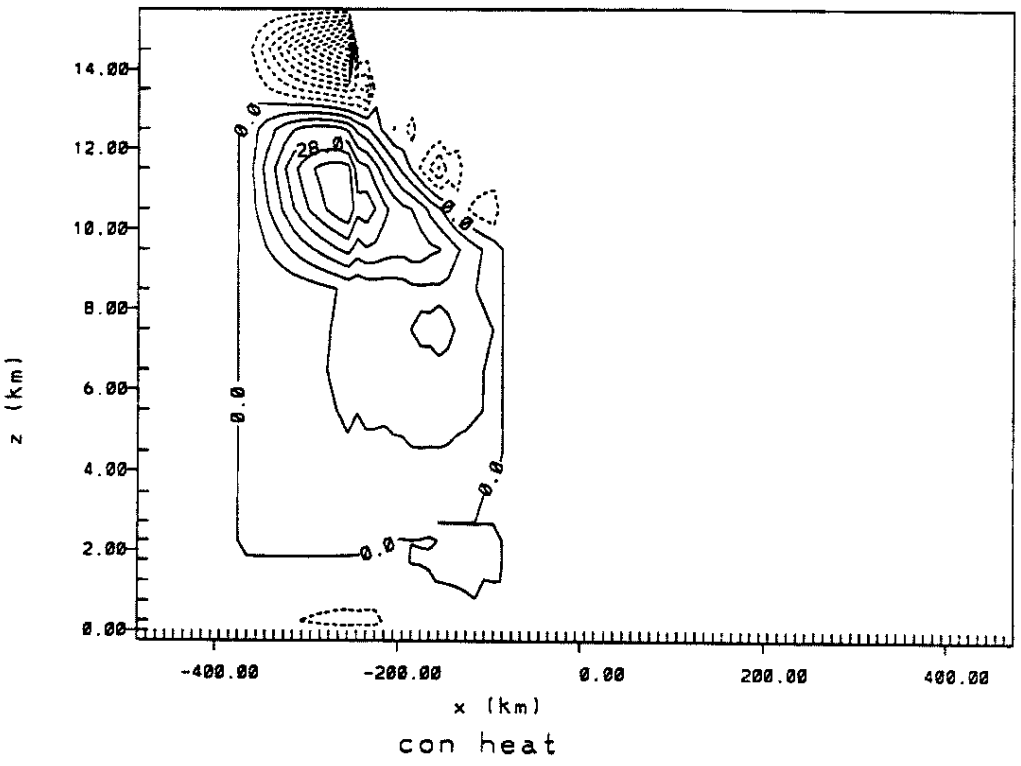


Figure 4.2: (b) Convective heating rate at 1400 LST for SLM run.

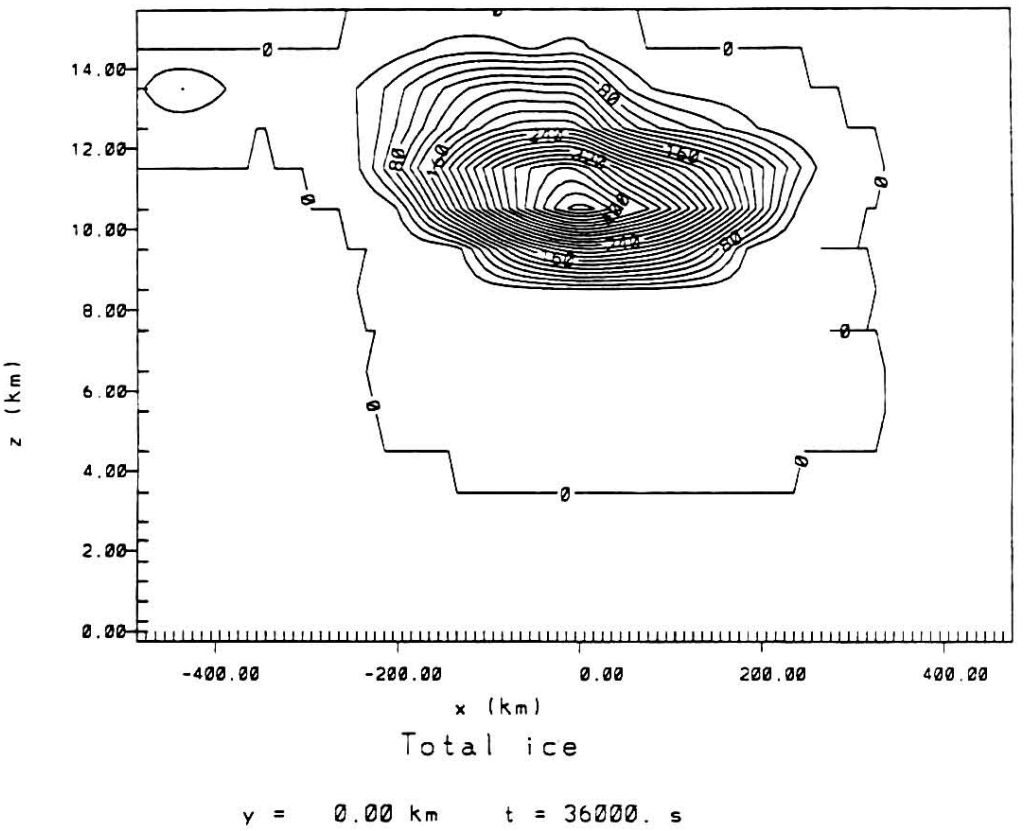


Figure 4.3: (a) Total ice at 1400 LST for SHM case.

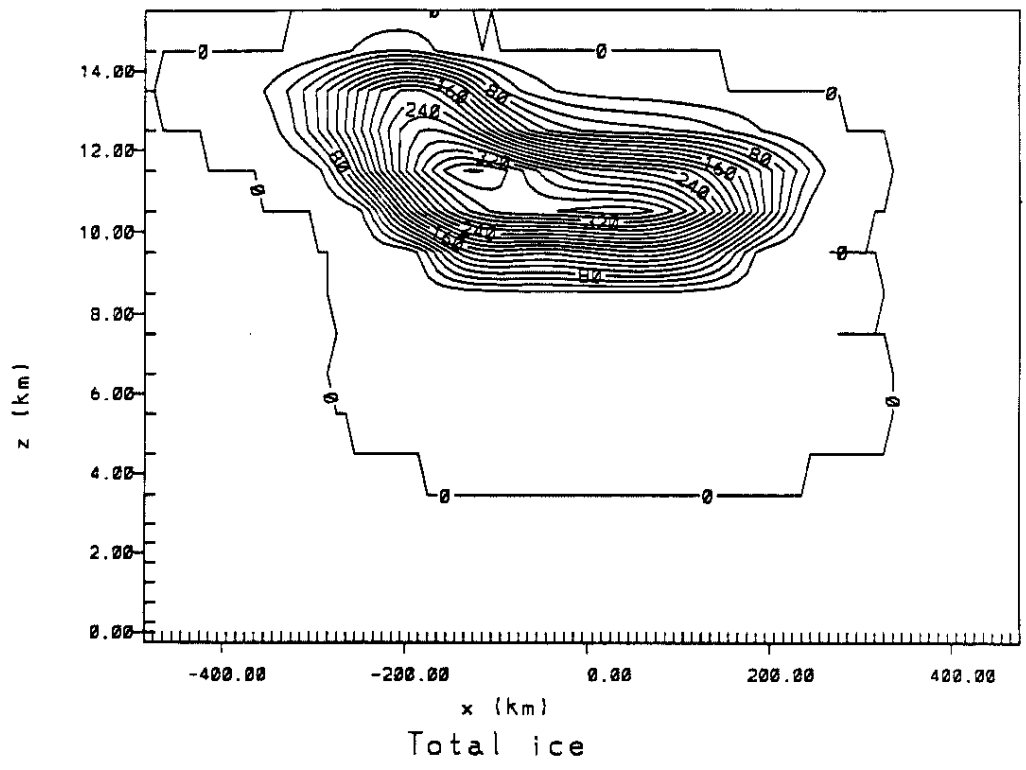


Figure 4.3: (b) Total ice at 1400 LST for SLM case.

Precipitation begins at 1300 LST in the SHM simulation. Rainfall from the stratiform cloud in the landfalling monsoon cloud cluster and the cloud cluster in front occurs first in the inland region, then in the coastline area. Minor precipitation well inland at this time indicates that the upper-level easterly flow spreads the anvil inland. However, there is no precipitation until 1600 LST in the SLM run. Rainfall in the SLM run is concentrated in a narrow inland range when it starts. The region near the coastline never gets any precipitation. It seems that most of the rainfall is from the local convective system which propagates westerly over the dry land. The cloud cluster itself, however, does not bring much precipitation at least when it initially moves over the dry land.

Figure 4.4a-c give the comparison of the total precipitation at different times in the SLM, SHM, and control runs, respectively. The figures show that the simulated cloud cluster obtains more moist static energy from the wetter land surface. Therefore, local convection can more easily develop and the greater locally forced deep convection within the wetter monsoon cloud cluster in turn results in a large amount of rainfall over the land.

Furthermore, the dynamics of the convective systems are different in the two wet ground simulations. The system in the dry soil run does not become as focused as it is in the wetter soil case. The cloud cluster in the dry soil situation exhibits a more inland upward motion center at 1600 LST. The maximum upward motion at 1600 LST in the dry soil run at 11 km is 17 cm $s^{-1}$ while it is 13.1 cm $s^{-1}$ in the moist soil run. The convective activity lasts until 2100 LST in the wet land simulation. However, the upward motion center disappears after 1800 LST in the SLM run. This comparison indicates that the high low-level moist static energy over land associated with relatively moist soil greatly promotes the mesoscale convection not only of the landfalling monsoon cloud cluster but also the concurrent local convection.

## 4.2 The Influence of Surface Roughness

Previous discussions (Section 4.1) suggest that the low-level thermal and moisture supply over land is an important factor in influencing the variation of cloud cluster structure and its precipitation pattern. Another possible factor influencing the intensity of the

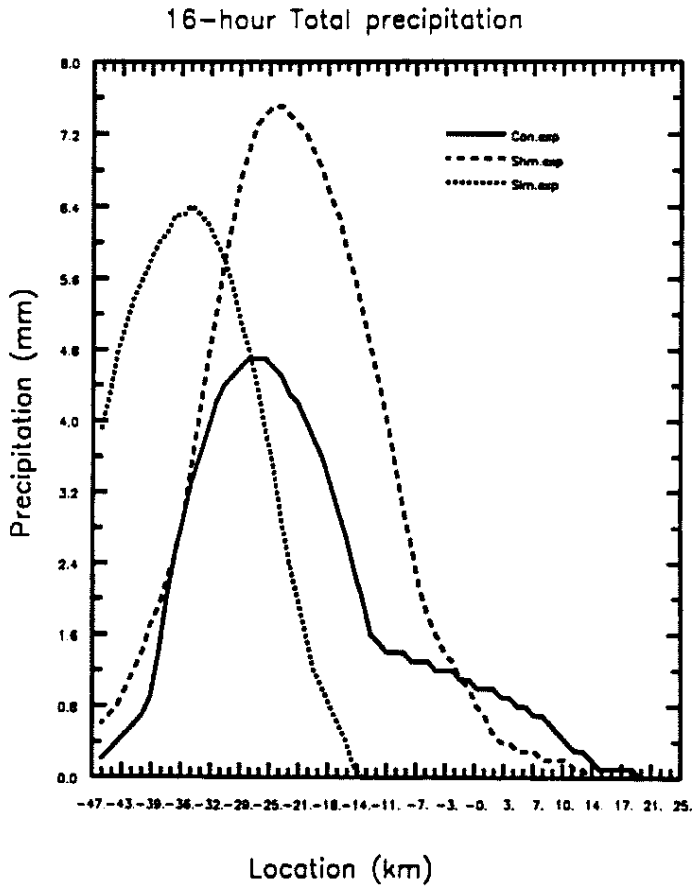


**Figure 4.4: (a) Total precipitation for SHM, SLM, and control simulations at 2000 LST.**

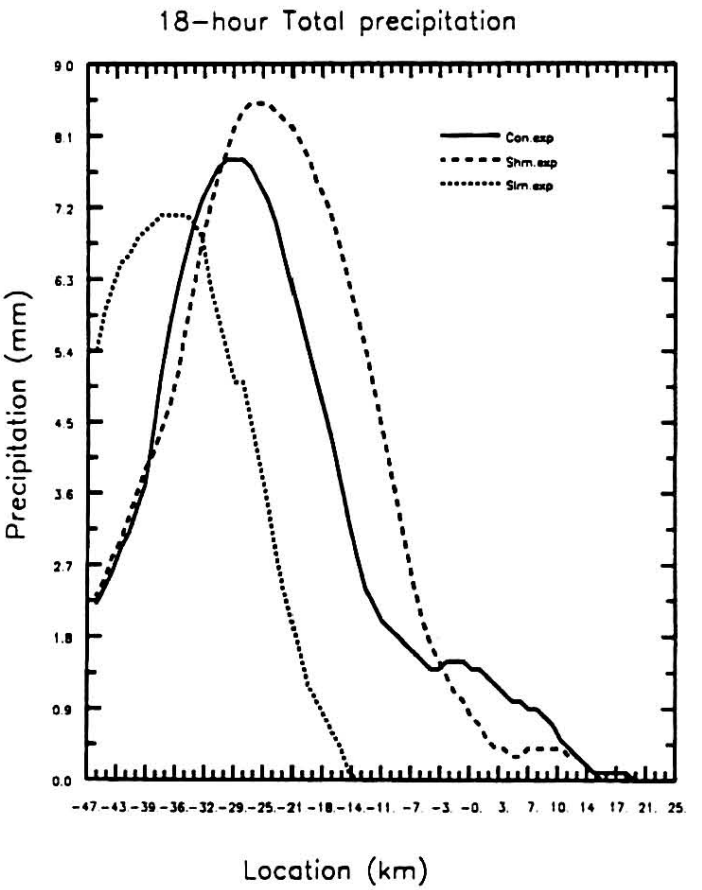


Figure 4.4: (b) Total precipitation for SHM, SLM, and control simulations at 2200 LST.

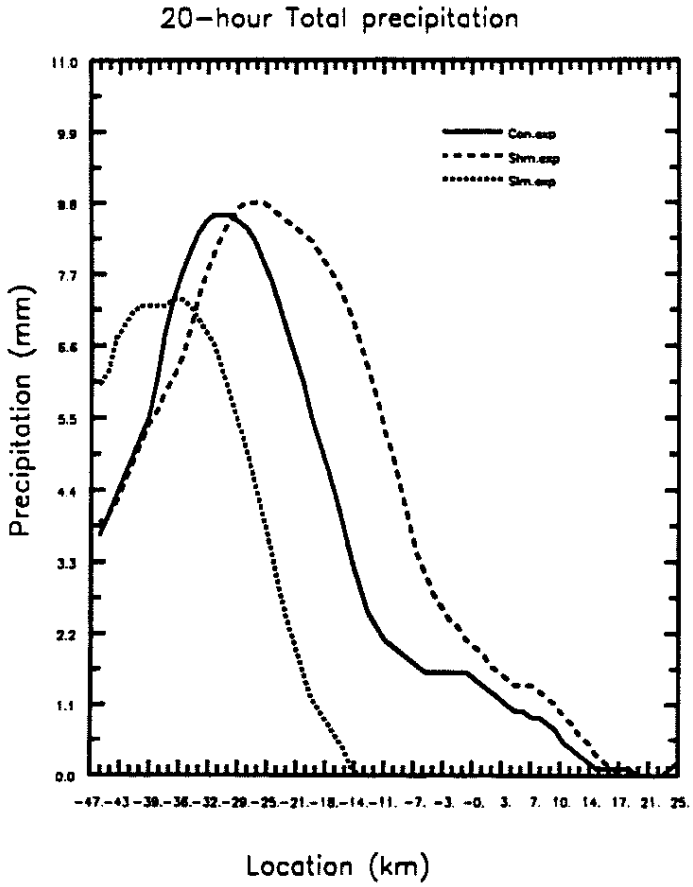


Figure 4.4: (c) Total precipitation for SHM, SLM, and control simulations at 0000 LST.

landfalling cloud cluster is low-level wind convergence flow. The intensity of this low-level convergence is related to horizontal variations in the turbulent transfer of the heat and momentum within the boundary layer.

The surface layer vertical momentum flux may be expressed as

$$\tau_v = -\overline{\rho}\overline{V'w'} = \overline{\rho}u_*^2 \tag{4.1}$$

From similarity theory (Stull, 1988),

$$\overline{V}(z) = \frac{u_*}{\kappa} ln \frac{z}{z_o} \tag{4.2}$$

where $z_o$ is referred to as the aerodynamic roughness. The value of $z_o$ is a function of surface characteristics. For instance, $z_o$ of soil is 0.1 cm, of agriculture crops, 4-20 cm, etc. (Pielke, 1984, Table 7-3). The magnitude of $z_o$ influences the vertical distribution of the wind in the surface layer and thus affects the intensity of the turbulent transfer in the convective boundary layer. Horizontal variations of $z_o$ can produce variations in wind velocity producing areas of low-level convergence or divergence. Local areas of low-level convergence would enhance convection since they would be associated with lifting of moist air.

The eastern coast of the Indian subcontinent consists of irrigated land and smooth terrain. The irrigated land usually has a larger surface roughness than non-irrigated land. In the following experiments, two different roughness values, 0.1 m for the agriculture corps land and 0.01 m for the bare surface, are chosen in the model in order to reveal the relationship between the variation of the cloud cluster formed over the ocean and the land surface roughness characteristics. The other model simulation conditions are the same as in the control experiment.

Before the simulated cloud cluster approaches the coastline, the only apparent difference between the smooth land surface ($z_o$) = 0.01 m and the rough land surface ($z_o$) = 0.1 m is the intensity of the low-level east-west wind over the land. As stated in Chapter 3, an offshore westerly flow between 1 to 4 km heights over the land had existed since the early morning. The wind speed varies approximately logarithmically with height in

the surface layer (nearly 120 m above the ground). The rough land surface produces a larger shearing stress that slows the westerly flow within the surface layer. However, the shearing stress within the surface layer is relatively weaker over the smooth land surface than over the rough land surface before the cloud cluster moves inland. Figure 4.5 gives the variation of the east-west wind in the surface layer over the different land surfaces at a position 100 km west of the coastline. The speed of the easterly flow over the rough land surface is larger than that over the smooth land surface before 1200 LST.

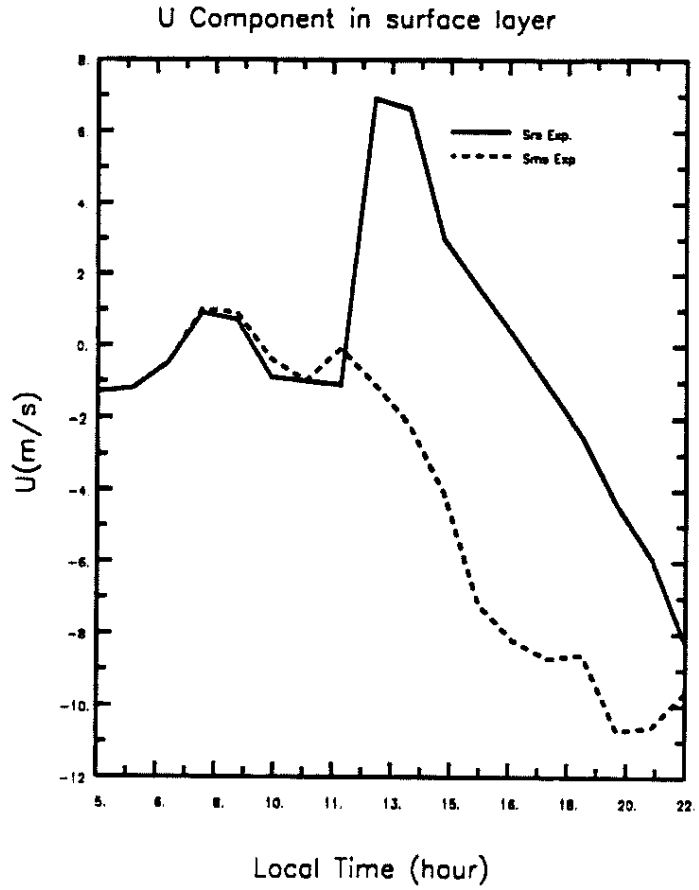


Figure 4.5: Variation of low level west-east wind $u$ of SRS (rough soil surface) and SMS (smooth soil surface).

By about noon, moist mesoscale systems develop both over the heated land and over the ocean in the two simulations. There are two apparent areas of deep convection over the rough land surface but only one over the smooth land surface at this time. Figure

4.6a-b represents the convective heating rate for both land surface situations at 1200 LST. The rough land surface is more convectively unstable due to the greater boundary layer turbulent transfer process. The higher low-level buoyant energy promotes greater deep convection over inland. Figure 4.7 gives the distribution of the east-west wind below 4500 m at 1400 LST. The wind within the planetary boundary layer is nearly uniform with height in the rougher surface run. In contrast, the wind in the smooth surface situation increases with height with a gradient.

The exchange processes between the land and atmosphere can also be described from the variation of land surface latent heat fluxes. Figure 4.8 shows the variation with time of land averaged surface latent heat fluxes in the two experiments. The reduced latent heat flux from the smooth land surface is due to lower evaporation and boundary turbulence transfer. The early inland appearance of mesoscale convective systems over the rough land increases the cloud shading effect and greatly reduces the incoming solar radiation reaching the earth. The model results show that the land surface temperature over the smooth land surface is about two degrees higher than over the rough land surface during most of the daytime. The soil moisture over the smooth land surface is about 10% higher than that over the rough land surface in the afternoon. Figure 4.9a-b depicts the variation of soil moisture and soil temperature against time at a location 100 km west of the coastline. The rough land surface has lower soil moisture due to the larger turbulent transfer and evaporation process over the rough land surface before the simulated cloud cluster moves inland and a higher one due to the larger rainfall after the cloud cluster lands. However, the early inland cloud and relative low surface temperature decreases the boundary layer buoyancy effect over the rough land when the cloud cluster moves over the land.

Figure 4.10a-b depicts vertical velocity fields at 1600 LST for the two cases. The simulated monsoon cloud cluster has partially moved onto the continent by this time. The vertical velocity over the smooth land surface exhibits two regions of deep convection. One is over the land formed by the locally generated area of deep convection merging into the upward motion in the landfalling monsoon cloud cluster. The second is a part of the upward motion associated with the upper levels of the cloud cluster over the ocean.

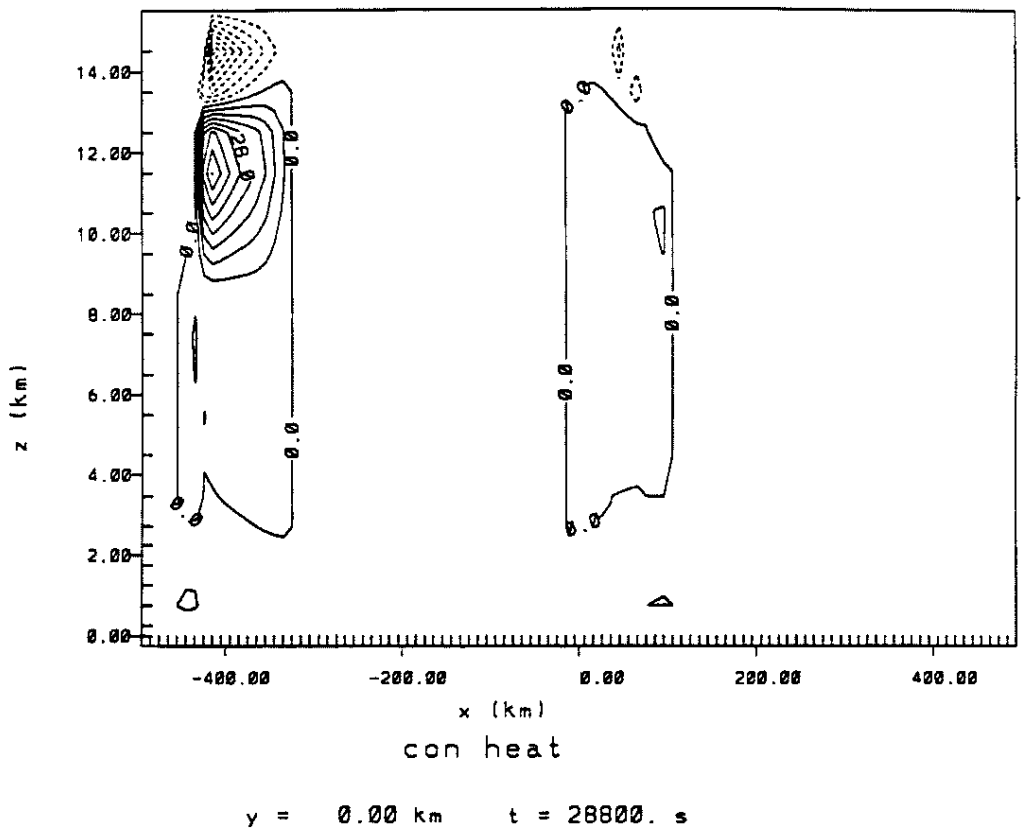


Figure 4.6: (a) Convective heating rate at 1200 LST for SRS run.

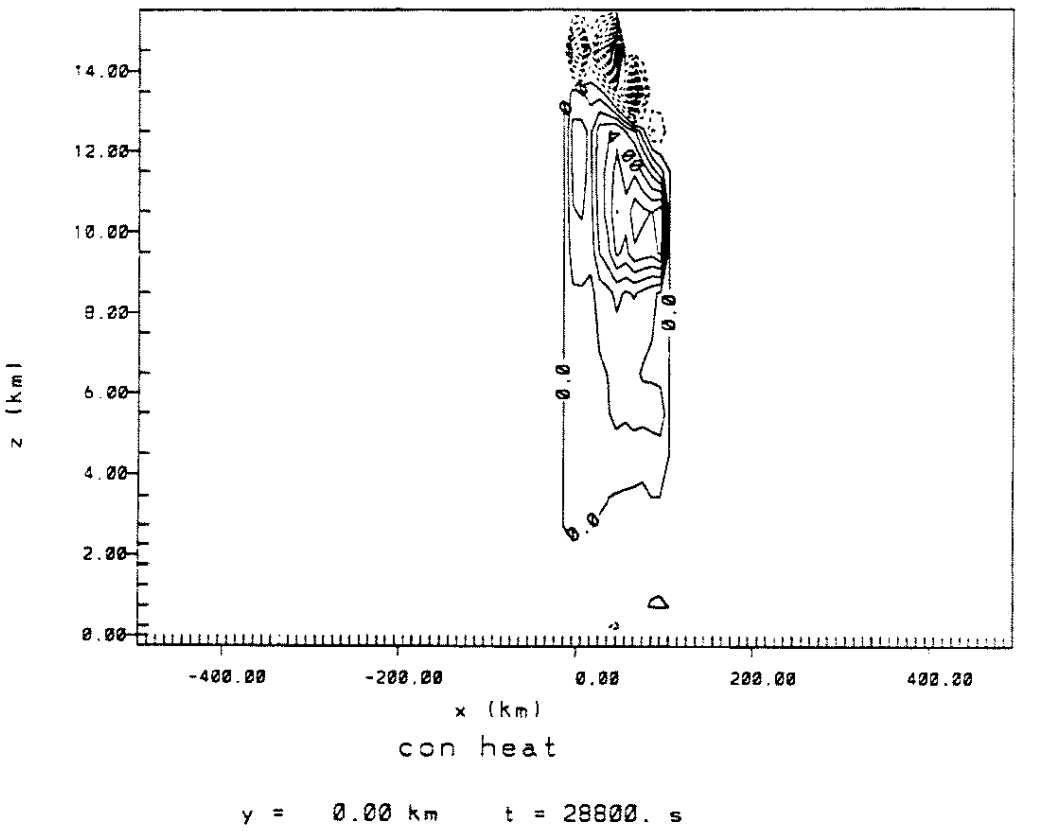


Figure 4.6: (b) Convective heating rate at 1200 LST for SMS run.

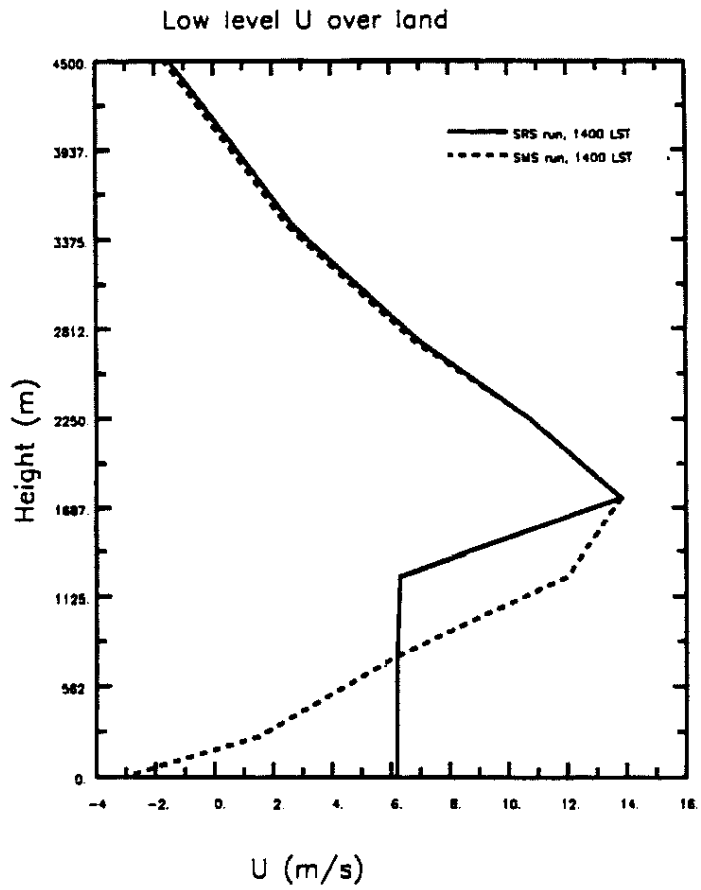


Figure 4.7: The lower level (0-4500 m) east-west wind of the SRS and SMS run at 1400 LST.

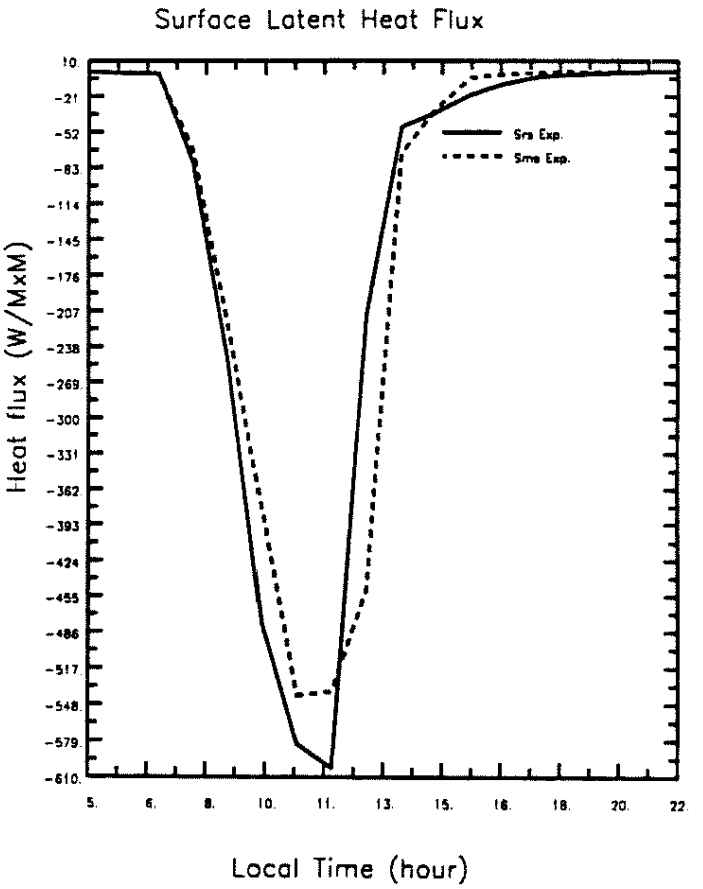


Figure 4.8: Variation of averaged land surface latent heat flux of SRS and SMS case with time.

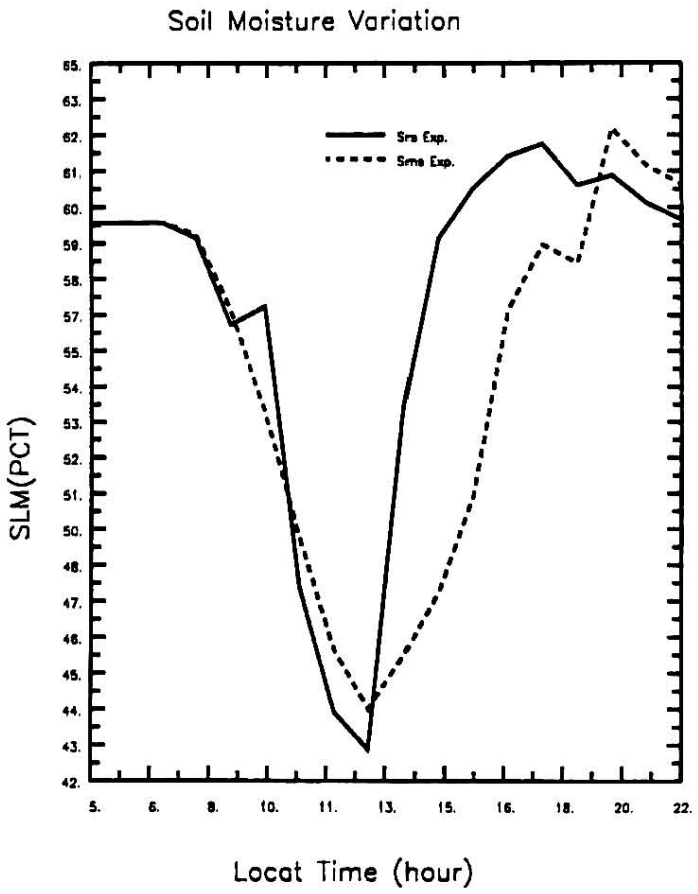


Figure 4.9: (a) Variation of soil moisture of SRS and SMS run with time.

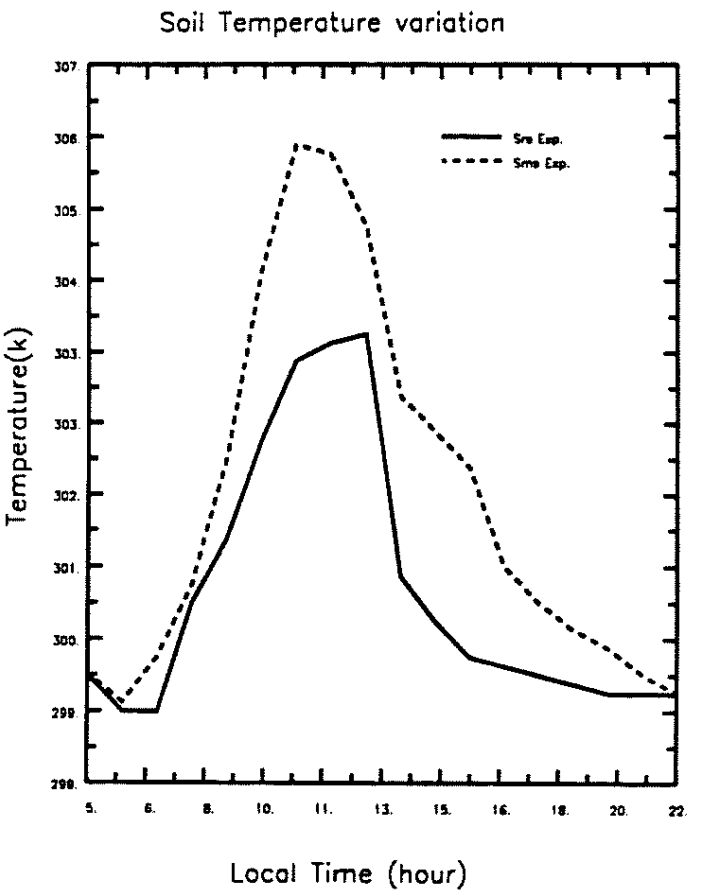


Figure 4.9: (b) Variation of surface temperature of SRS and SMS run with time.

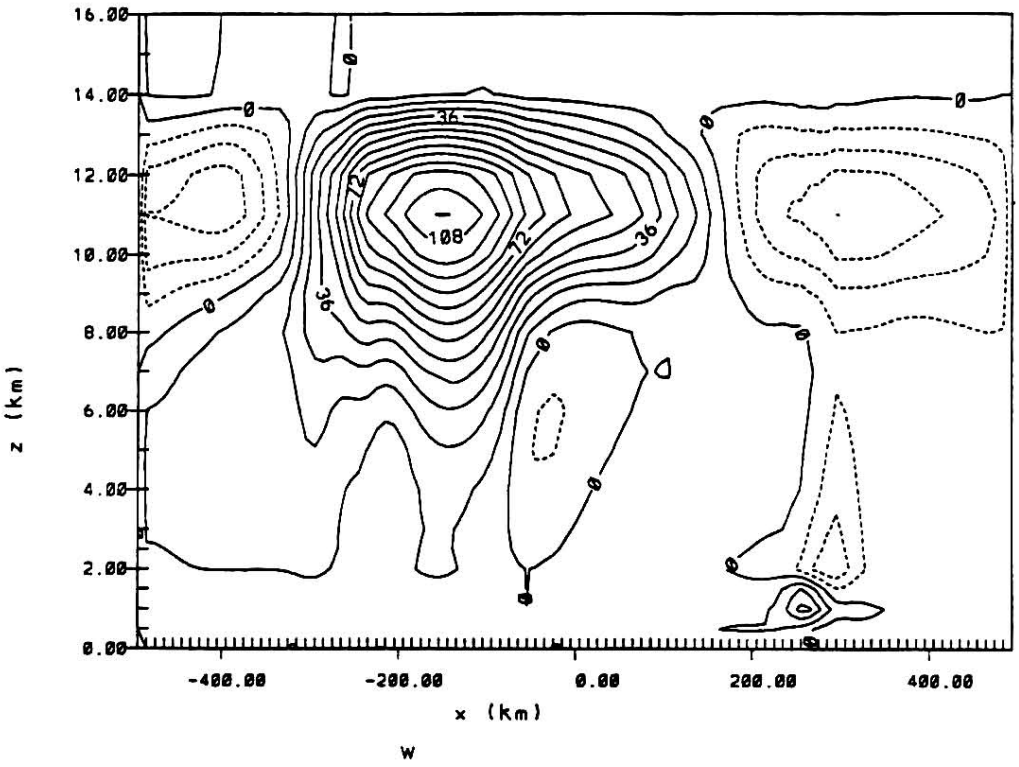


Figure 4.10: (a) $W$ field at 1600 LST of SRS run.

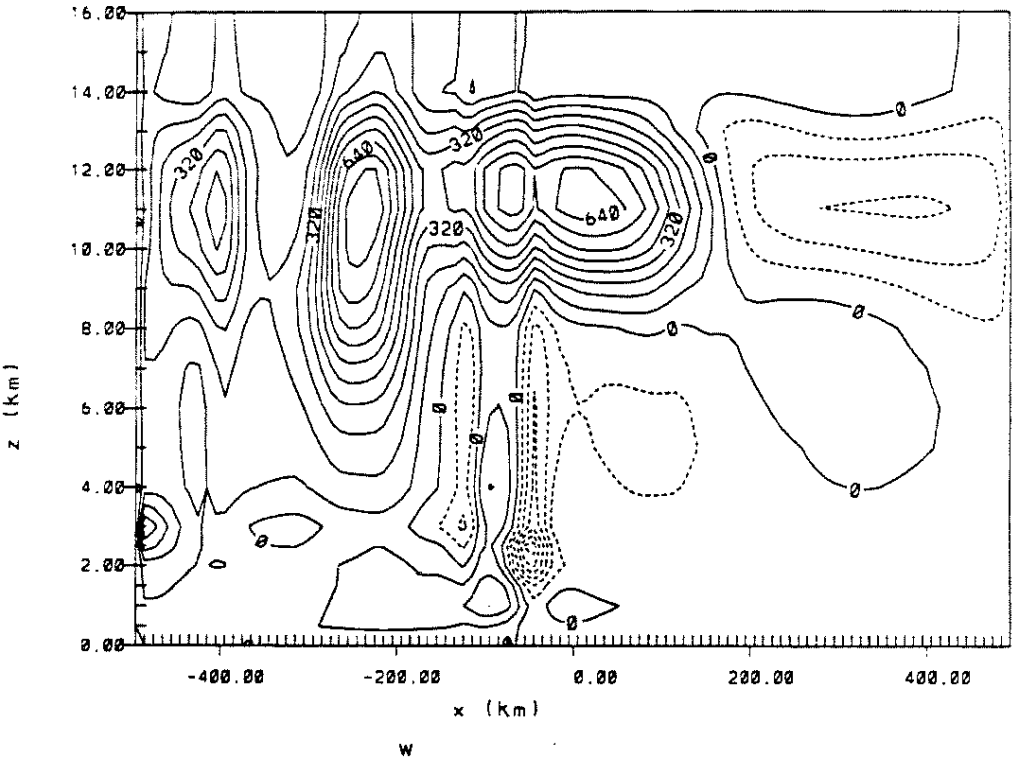


Figure 4.10: (b) $W$ field at 1600 LST of SMS run.

However, there is only one area of deep convection over both the land and the ocean in the rough land surface situation. The convection is shallow over the rough land surface (Fig. 4.11). The wind within the surface layer above the rough land surface sharply increases to a westerly flow before the cloud cluster lands and then becomes a strong easterly flow after the cloud cluster moves inland (Fig. 4.5). The local area of convection and the landfalling cloud cluster then form as a unified strong upward motion core over the land and the ocean. The low-level easterly flow over the smooth land surface is stronger after the cloud cluster moves onshore. It is also seen in Fig. 4.11 that the westward movement of the cloud cluster over the smooth land surface is faster than over the rougher surface.

Figure 4.12 gives the distribution of precipitation amounts at 2200 LST over both the land and the ocean. These precipitation results indicate that most of the rainfall concentrates inland for the smooth land surface case. However, for the rough land surface simulation, the precipitation is distributed more widely. The maximum eighteen hour precipitation amount over the smooth land surface is only 73% of the one in the control experiment. These phenomena are caused by the reduced intensity of the turbulence in the boundary layer resulting in less input of moist static energy. The cloud cluster in the smooth land surface case does not result in much development after it moves onshore. Most of the rainfall comes from the anvil that is advected westerly by the high-level easterly flow and the inland local convective region in front of the monsoon cloud cluster.

The rough land surface, however, does not result in more precipitation than the control experiment which has a land surface roughness of 0.05 m and the intensity of the upward motion is also weaker than in the control experiment.

## 4.3 Sea Surface Temperature Variation

The ocean is an important source of moisture and heat to the atmospheric circulation. The mean heat loss from the ocean to the atmosphere due to evaporation and turbulent sensible heat transfer is proportional to the vertical temperature and moisture differences between the ocean surface and the air temperature in the lower atmosphere boundary

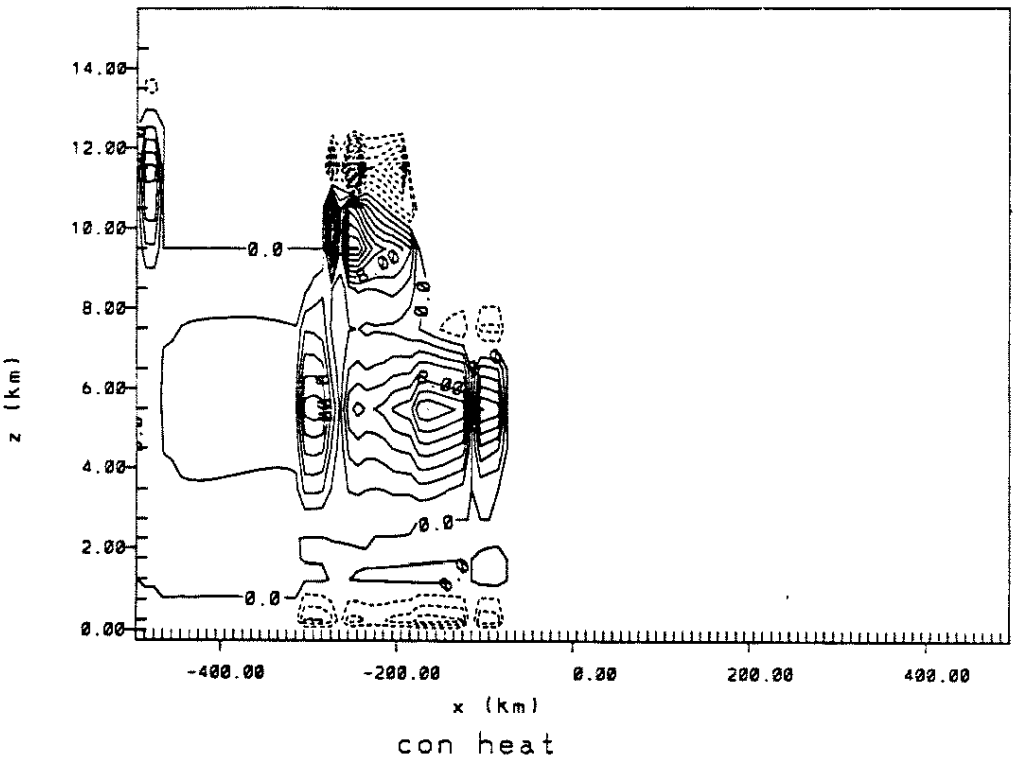


Figure 4.11: (a) Convective heating rate at 1600 LST of SRS run.

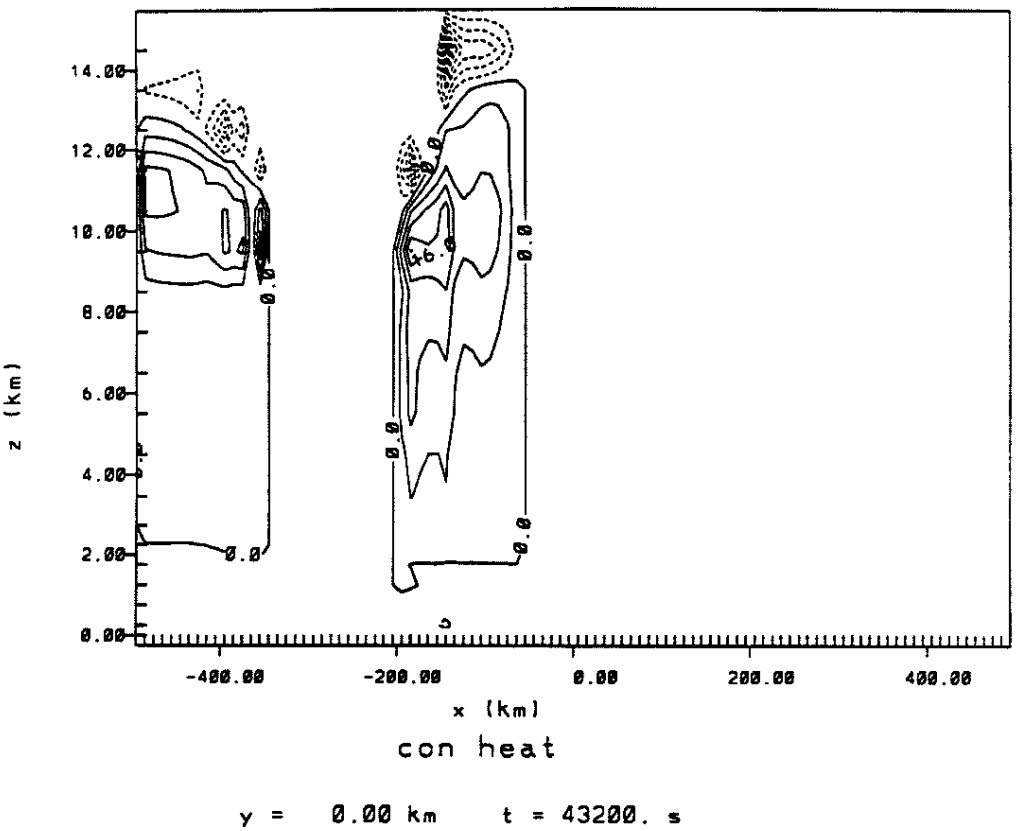


Figure 4.11: (b) Convective heating ratio at 1600 LST of SMS run.

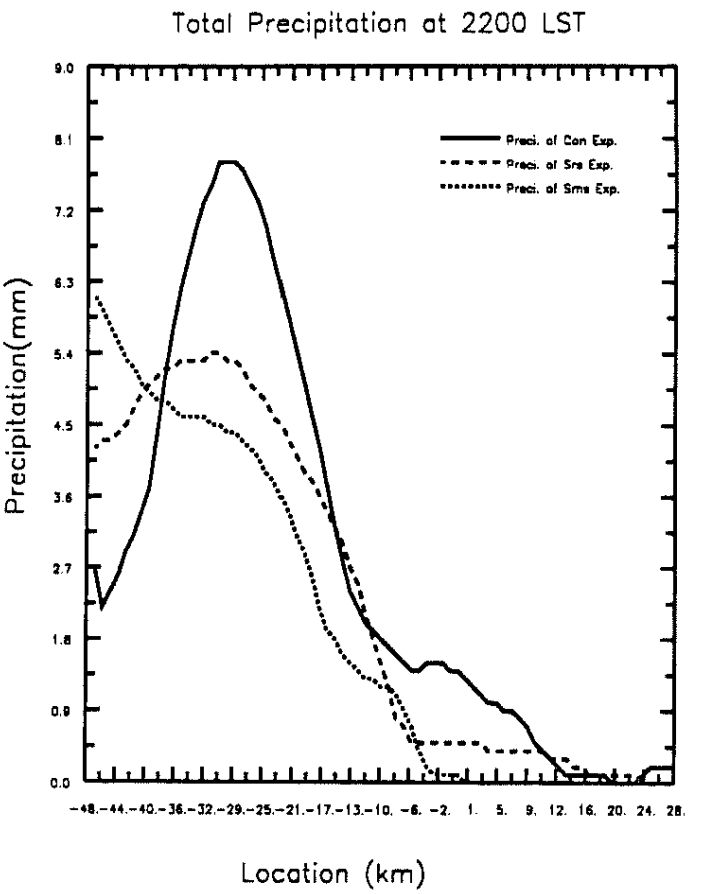


Figure 4.12: Total precipitation of control, SRS, and SMS run at 2200 LST.

layer (Bortkovskii, 1987). Shukla and Misra (1977) studied the relationship between SST over the central Arabian Sea and monsoon rainfall over India. Their results suggested that there are some positive and significant correlations between SST during July and rainfall over central and western India during August. In the Shukla (1975) numerical modeling results, the colder SST anomalies over the western Arabian Sea tend to reduce monsoon rainfall over India.

Sea surface temperature is also an important factor which affects the variation of the mesoscale convective system which forms over the ocean and moves onshore. Different SSTs will lead to different strengths of the air-sea interaction through the boundary layer mixing process. A high SST usually enhances the air-sea mixing process and leads to more transfer of the moist static energy into the atmosphere from the boundary layer. Gray (1968) suggested that SST = 28.5°C seems to be a threshold for organized deep convection. The relationship between the simulated cloud cluster formed over the ocean and the SST will be discussed here. The SSTs are assumed as 304 K (31°C) in the simulation SHT, which represents a favorable water condition for the formation of deep convection, and 300 K (27°C) in the simulation SLT, which is below the critical SST mentioned by Gray (1968). All other aspects of the model physics are the same as the control simulation.

The most significant characteristics in these simulations are the variations of the strength of the simulated cloud cluster over the ocean within the first few hours of the model simulations. By about 1200 LST, a cloud cluster occurs over the ocean in both cases. However, the convective heating rates exhibited in Fig. 4.13a-b show a maximum heating and cooling rate of 8.0 K day$^{-1}$ and $-30$ K day$^{-1}$, respectively, and a cloud cluster width of 160 km over the relatively warm ocean surface (304 K) near the coast. Over the cold ocean surface (300 K), a maximum heating rate of 7.0°K day$^{-1}$ and cooling rate of $-10.0$ K day$^{-1}$ occurs which extends about 50 km over the ocean and 50 km over the land near the coast. Although the cloud cluster extends to a height of 14 km and the maximum upward motion is located near 12 km in both experiments, the convection as well as the upward motion is stronger over the warm ocean surface than over the cold ocean surface. The high SST promotes more convection within the cloud cluster. Therefore, the

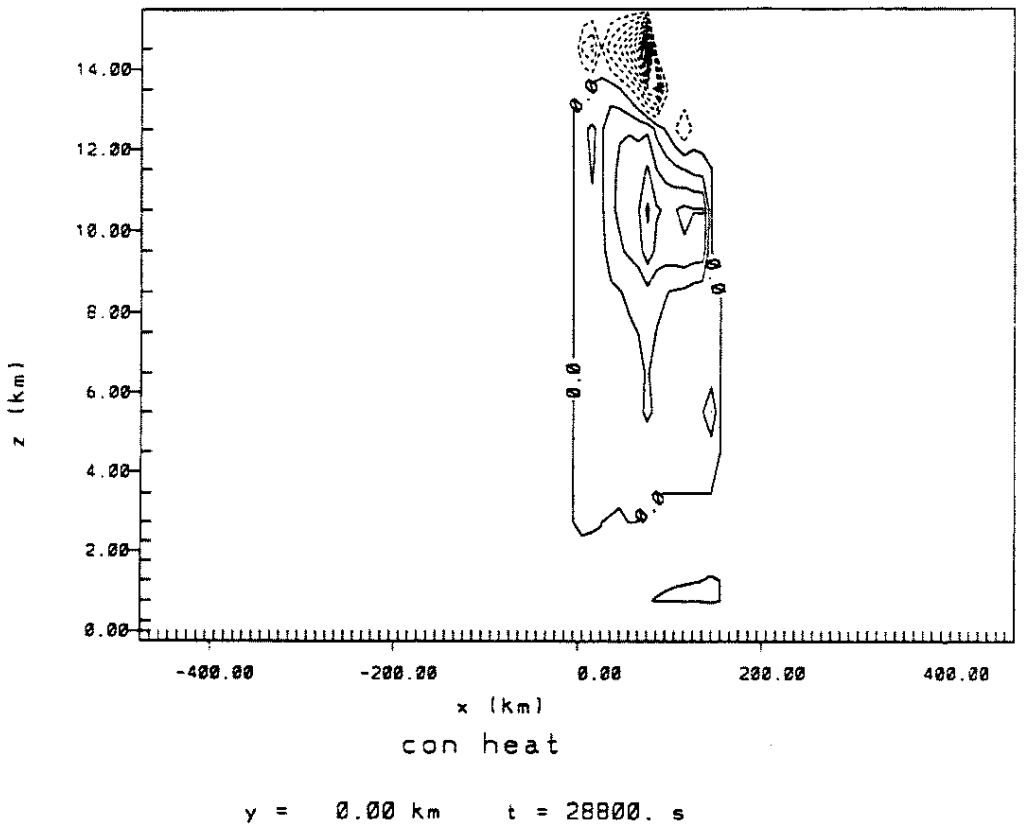


Figure 4.13: (a) Convective heating rate at 1200 LST of SHT (higher sea surface temperature) simulation.

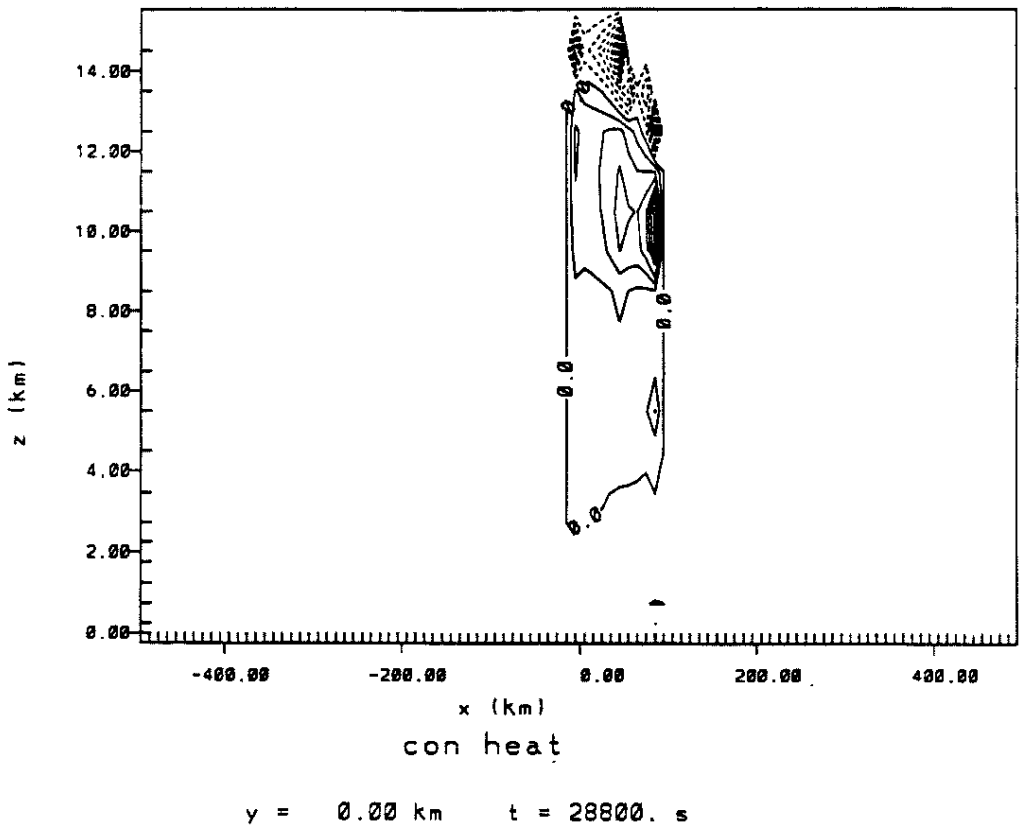


**Figure 4.13: (b) Convective heating rate at 1200 LST of SLT (low sea surface temperature) simulation.**

simulated cloud cluster over the warm ocean surface has a relatively warm and moist core when it moves onshore.

Figure 4.14a-b depicts the vertical velocity field at 1400 LST for both warm and cold ocean surface simulations. When the cloud cluster over the warm water surface approaches the coast, low-level convergence due to more intense downdrafts because of higher evaporation at the leading edge of the cloud cluster promotes convection over the land. The strength of the low-level convergence is stronger in the warm ocean surface run than in the cold surface case. The upward motion over the land near the coast then merges with the updraft in the oceanic cloud cluster and forms two upward motion centers. The upward motion field in the cold ocean situation, however, is much weaker over both the land and the ocean.

By about 1500 LST, precipitation occurs in both situations. However, the rain falls only inland about 200 km west of the coastline in the cold ocean surface run. The precipitation spreads out both over the ocean and the land around the coastline when it commences in the warm ocean surface simulation. One hour later (1600 LST), the rain falls over the land near the coastline in the SLT case. At this time, new areas of clouds appear over the land. The maximum upward motion cores are located at about 11 km for both runs. The vertical motion in the SHT case is much stronger and more focused (Fig. 4.15a-b). The downward motion area in the rear of the strongest upward motion in both runs indicate that most of the precipitation occurs over that range. The rain spreads out in a larger area, including both the land and ocean in the SLT case, but concentrates in a narrow zone over the land between the coastline and 100 km west of it in the SHT run.

Figure 4.16 gives the total precipitation amounts at 1800 LST for both ocean surface and control run cases. The apparent difference in the rainfall values and distribution is that there is more precipitation in the warm ocean case and the maximum rainfall is located 180 km west of the coast. The cloud cluster which formed over the warm ocean surface behaves as a well developed system. The warm ocean surface not only supplies more moisture and heat to the cloud cluster but also helps focus the area of deep convection.

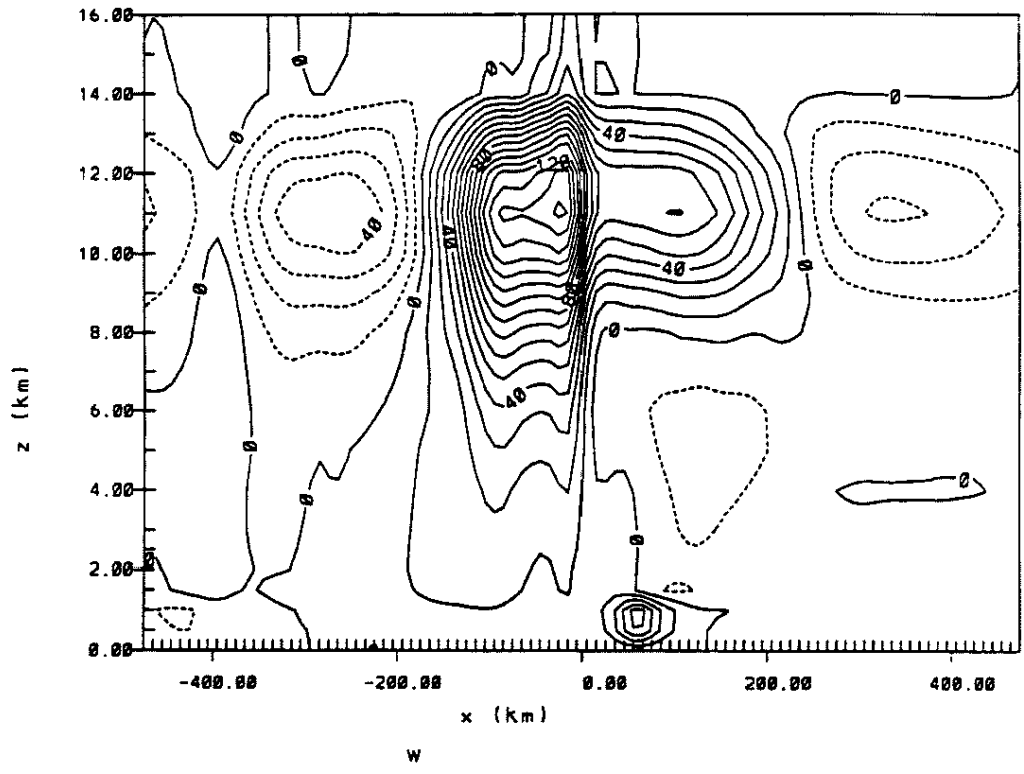


Figure 4.14: (a) $W$ field at 1400 LST for SHT run.

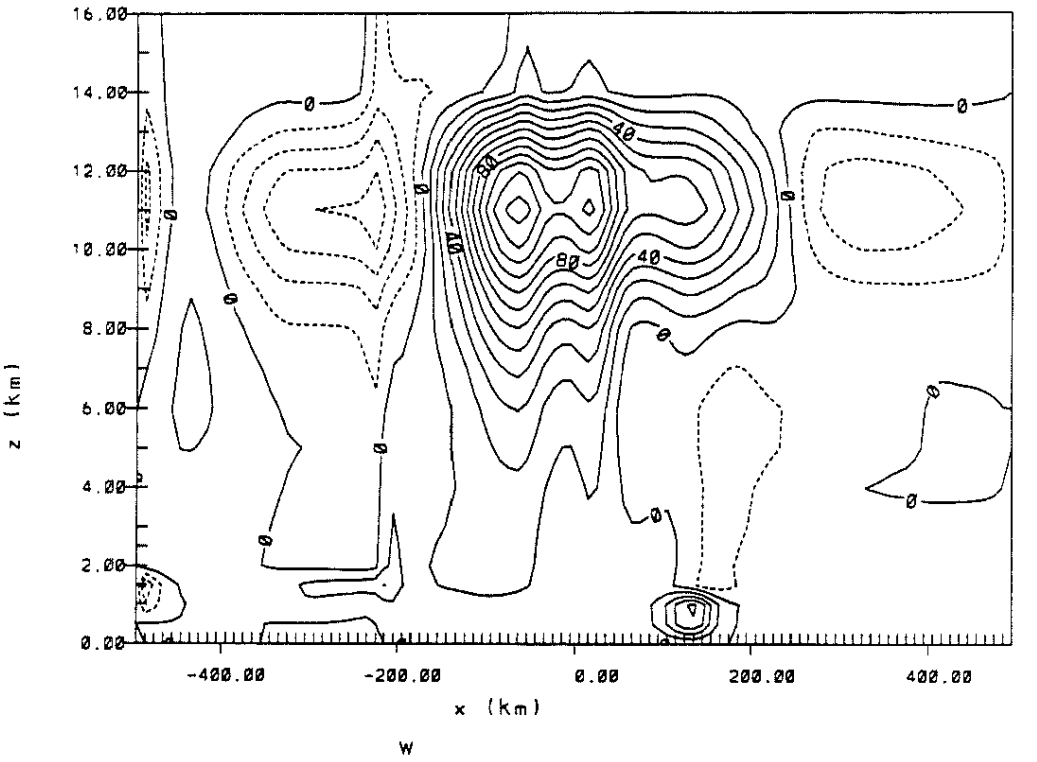


Figure 4.14: (b) $W$ field at 1400 LST for SLT run.

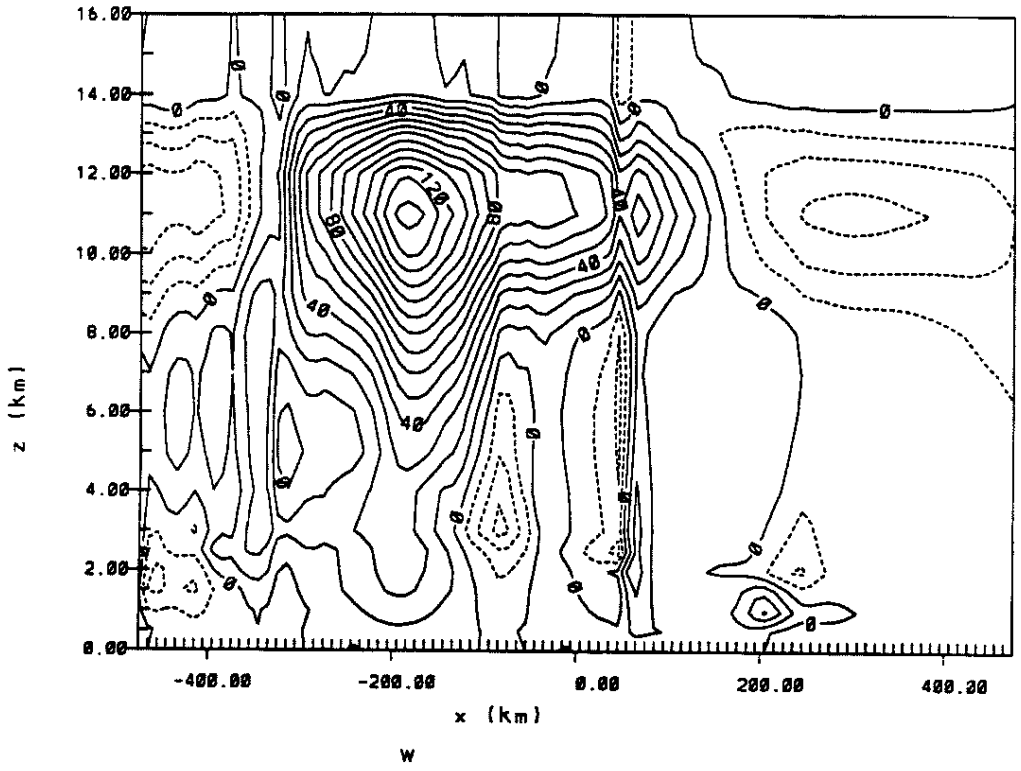


Figure 4.15: (a) $W$ field at 1600 LST for SHT run.

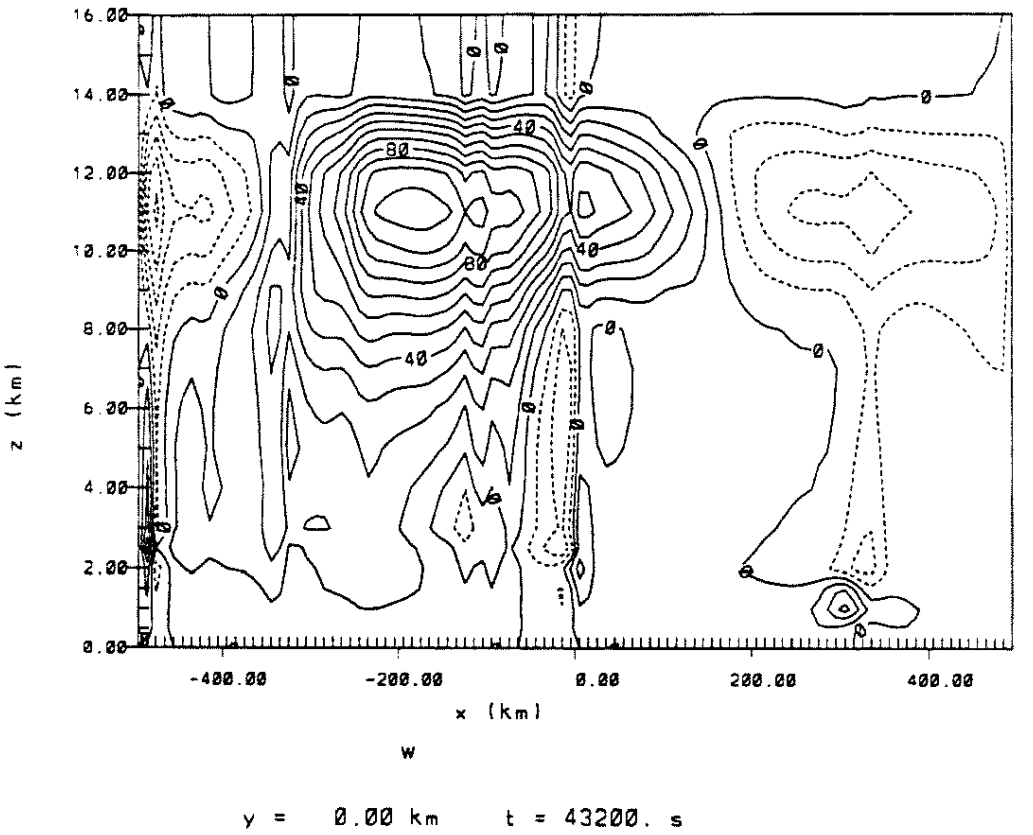


Figure 4.15: (b) $W$ field at 1600 LST for SLT run.

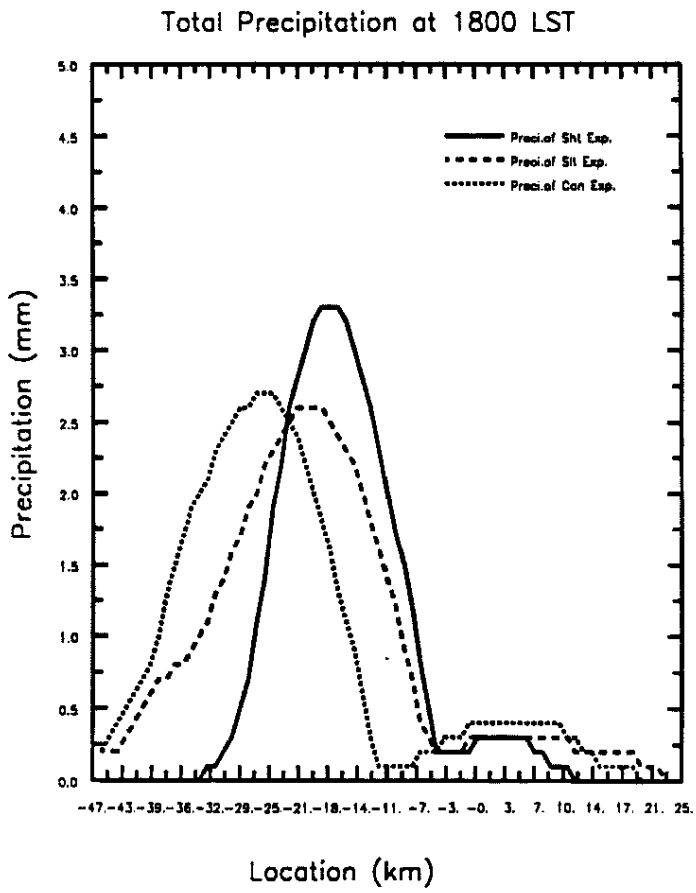


Figure 4.16: Total precipitation of SHT and SLT run at 2200 LST.

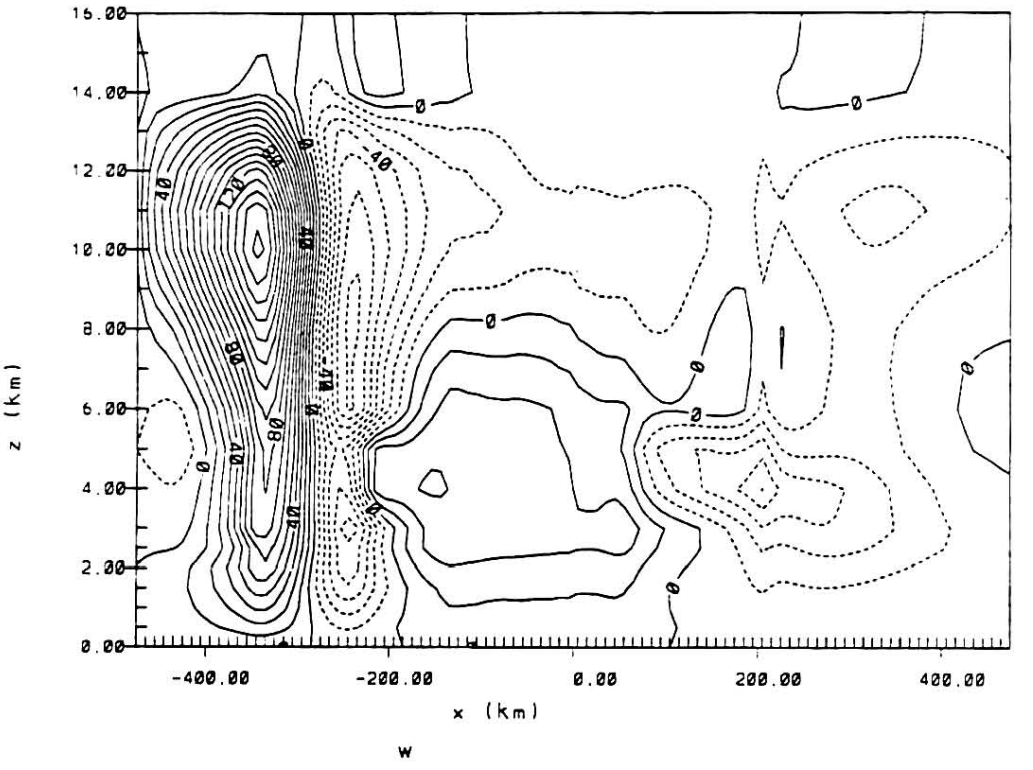


Figure 4.17: (a) $W$ field at 2200 LST for SHT run.

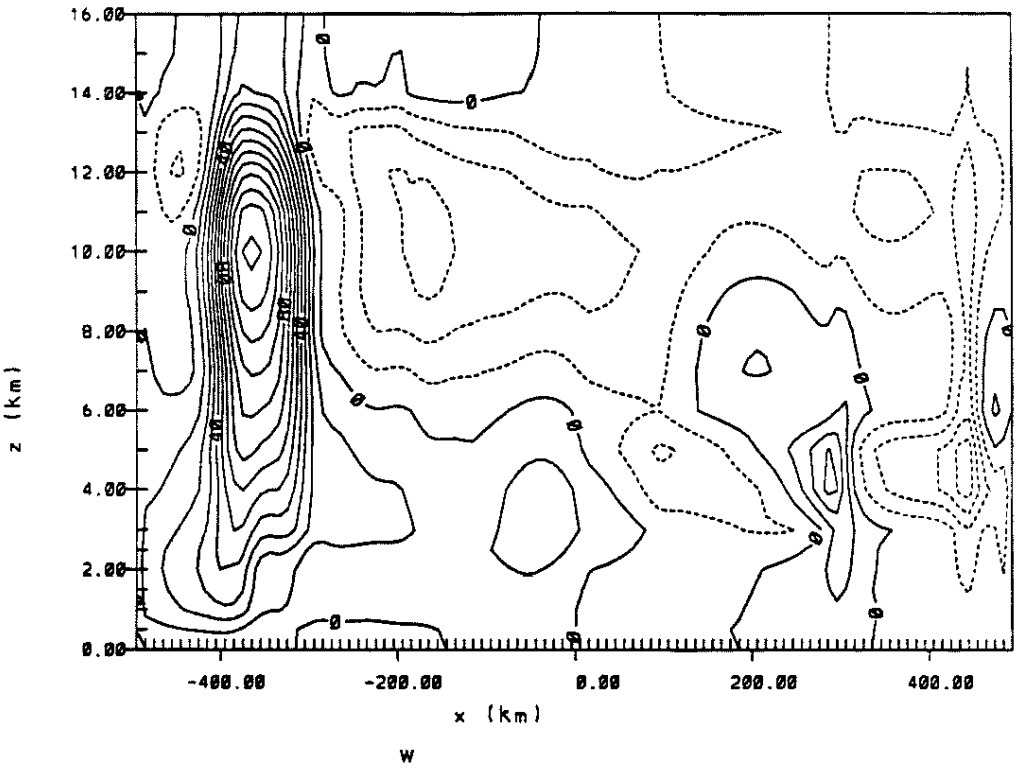


Figure 4.17: (b) $W$ field at 2200 LST for SLT run.

Figure 4.17a-b gives the vertical velocity fields of both SSTs at 2200 LST. The upward motion strengthens again when the mesoscale cloud cluster has moved inland about 200 km west of the coastline. The strength of the upward motion in the warm ocean case, however, is stronger than the one in the SLT case by about 31%. It is presumed that the cloud cluster formed over the warm ocean obtains more moist static energy. This makes the convection system more focused and not as easily dissipated. When the cloud cluster moves inland, the focused upward motion and upper-level divergence resulting from the release of the convective heating, lowers the pressure and promotes new mesoscale convection. Therefore, large amounts of rainfall is concentrated in a narrow range which propagates westward with the landfalling cloud cluster. The inland region which is located between the coastline and 300 km west of it almost does not get rainfall until the main cloud cluster moves there by about 2300 LST. In addition, the low-level (1750 to 2250 m) westerly flow over the land 200 km west of the coastline increases by about 23% in three hours during the late evening.

The increase of low-level convergence then promotes the local area of deep convection. Rain is associated with the decay of the inland cloud cluster. The maximum one hour precipitation on one grid point appears at 0000 LST with a value of 2.6 mm $h^{-1}$ in the SHT situation. In the SLT case, the value is 2.3 mm $h^{-1}$ and appears earlier at 2100 LST. The value mentioned here is the rainfall from the stratiform because in the model, total precipitation does not include convective rainfall. If the convective precipitation is added, the values will be 3.4 mm $h^{-1}$ for the SHT case and 2.5 mm $h^{-1}$ for the SLT case, respectively. The amount of precipitation also indicates that the cloud cluster formed over the warm ocean surface brings more rainfall to the continent. Figure 4.18 gives the distribution of twenty-two hour simulated precipitation over both land and ocean in the two ocean surface and control run cases. It can be concluded that the ocean surface temperature not only influences the intensity of the cloud cluster but also affects the amount and distribution of the precipitation associated with the landfalling cloud cluster. The Bay of Bengal has a SST greater than 300 K which is favorable to mesoscale convective activity and rainfall over the Indian subcontinent.

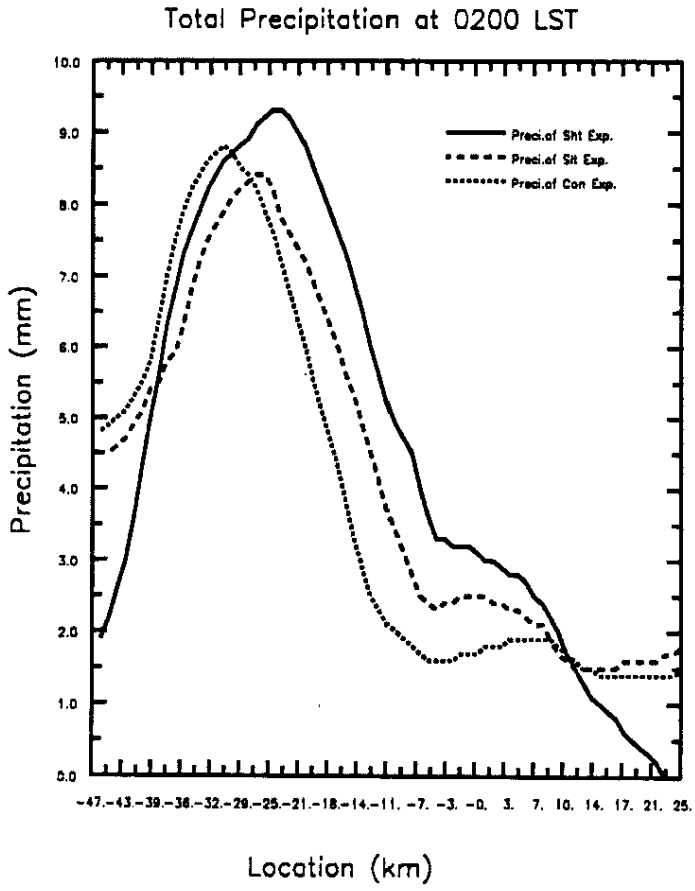


Figure 4.18: Eighteen hour simulated precipitation of SHT and SLT run at 0200 LST.

## 4.4 Low SST and Dry Land Surface

In this experiment, the SST is kept as 300 K and the soil moisture is assumed to be 0.3 which represents a relatively dry land surface. Other model conditions are the same as in the control simulation. The environmental conditions in the simulation represent the early Indian summer monsoon season.

For the first 6 hours (1000 LST) the simulated cloud cluster does not have any apparent difference from the control run. After that time, there are two major differences elsewhere in the simulation that should be mentioned. One is that the latent heat flux from the land and the ocean surface is apparently small due to the low SST and dry land surface. The percentage of the latent heat fluxes of both the ground and water surface in this case are about 23% and 10% of those in the control experiment before the simulated cloud cluster moves inland. Consistent with low soil moisture, the sensible heat flux from the land is large. The second difference is that the westward spread of the anvil has a significant effect on reducing the solar radiation reaching the ground in the morning. The cloud cluster is more diffuse because the simulated cloud cluster gets less moist static energy from the water than in the control run as it moves across the relatively cold ocean. By about 1100 LST, moist mesoscale convection occurs over the land. The intensity of the convection over the land is not strong although the sensible heat fluxes of the land surface are large. This is consistent with the fact that latent heating is the major energy source for the storm. Figure 4.19a-b represents the convective heating rate, and total ice content at 1400 LST, respectively. The convective heating effect over the land is weak although the land surface temperature is high. The ice mixing ratio indicates that the water content in the cloud cluster is very low.

When the cloud cluster moves inland, the low-level convergence in front of it is not strong. There is no obvious enhanced low-level easterly flow from the cloud cluster when it approaches the coastline. Although the upward motion in the area of moist mesoscale convection over the land merges to the ascending motion in the monsoon cloud cluster, the mesoscale convective systems do not develop significantly (Fig. 4.20). By about 1900 LST there is no obvious upward motion in the domain. This quick decay process further

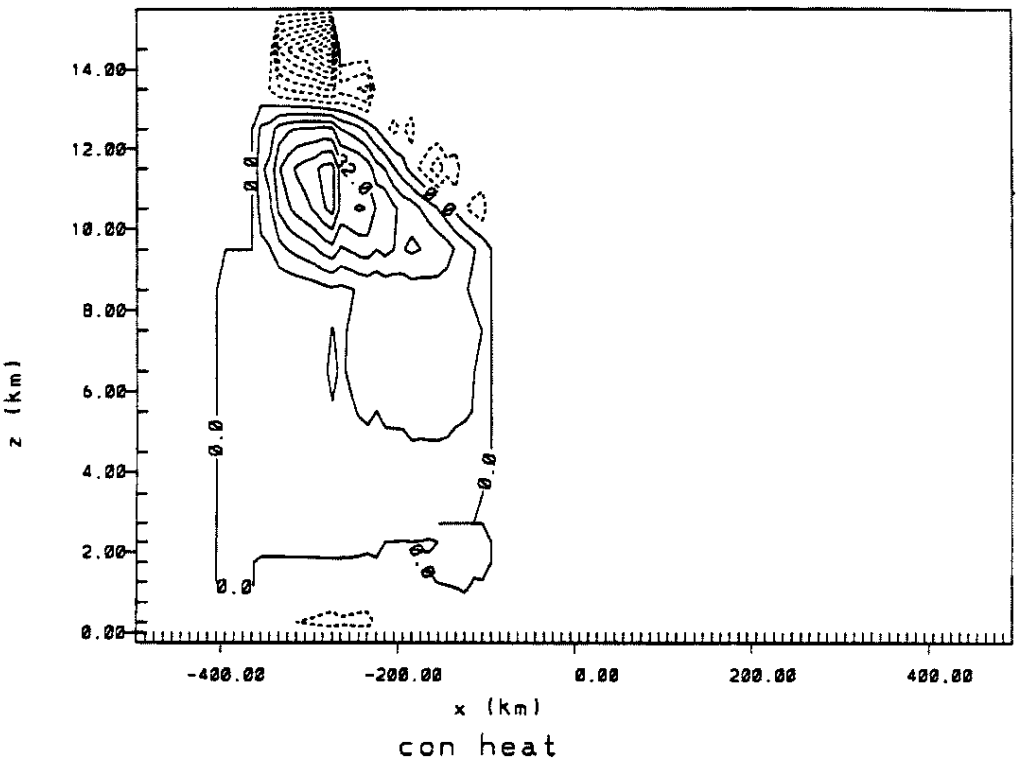


Figure 4.19: (a) Convective heating rate of SLM run at 1400 LST.

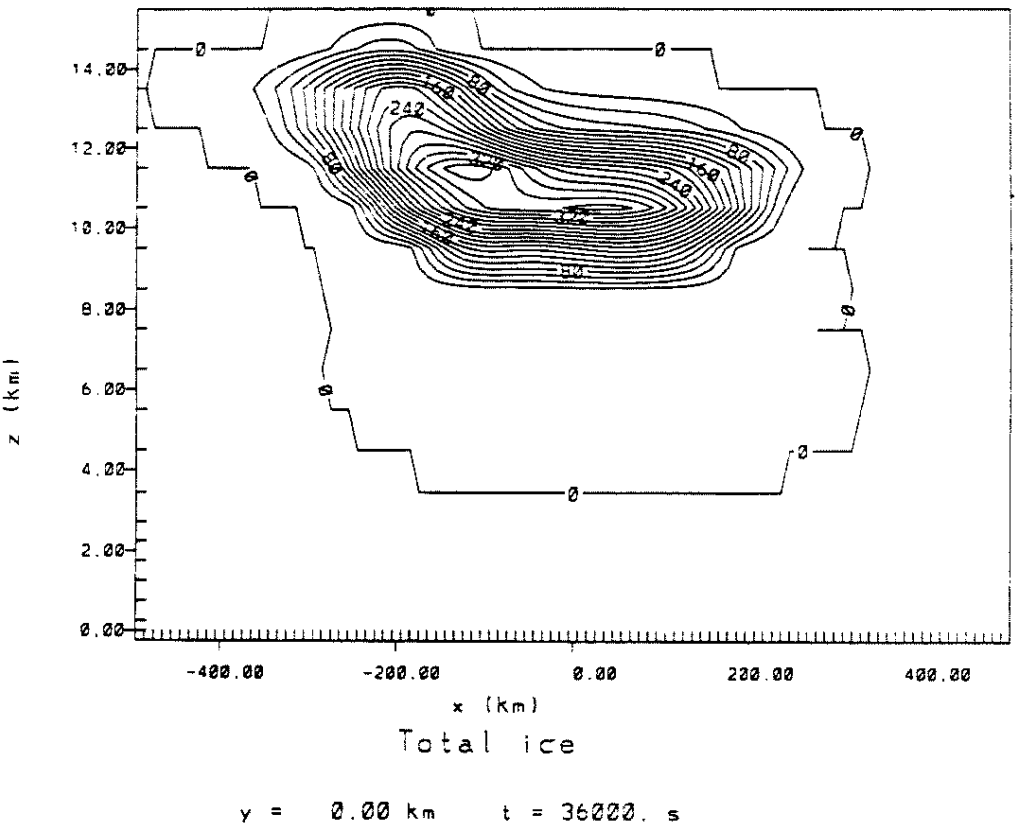


Figure 4.19: (b) Ice mixing ratio of SLM run at 1400 LST.

indicates that the moist static energy supply from the land surface is very important in maintaining the landfalling monsoon cloud cluster and the locally convective system.

The distribution of the precipitation shows that most of the rainfall occurs inland about 150 km west of the coastline (Fig. 4.21). The precipitation is mainly from the inland mesoscale convective system and the convection at the leading edge of the landfalling cloud cluster. Unfortunately, this weak intensity cloud cluster does not bring more precipitation to the continent. There is only a small amount of rainfall in a narrow region over the land. Recall the SLT simulation where the soil moisture is 0.6, and the ocean is relatively cool. The local convection was more active and lasted longer and the simulated rainfall was more widespread. The SLT simulation results suggest that the low-level moist static energy supply to the mesoscale convective system from evaporation over land is very important in the evolution of these systems.

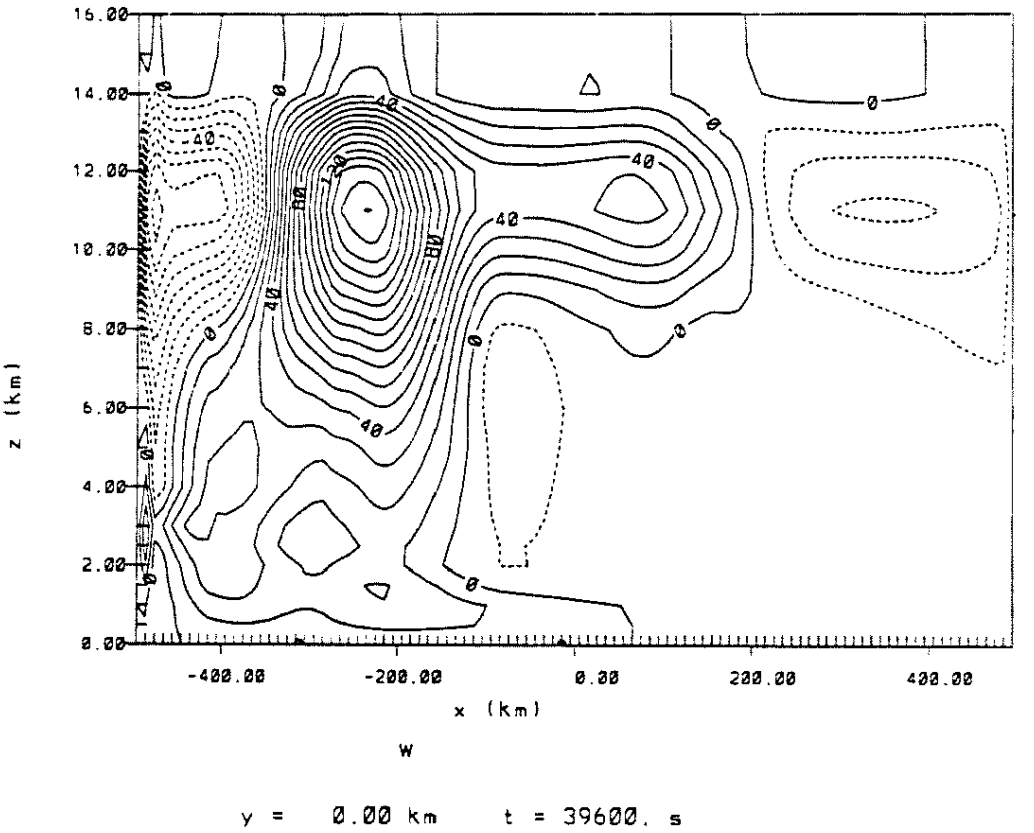


Figure 4.20: $W$ field of SML (dry soil and low sea surface temperature) simulation at 1500 LST.

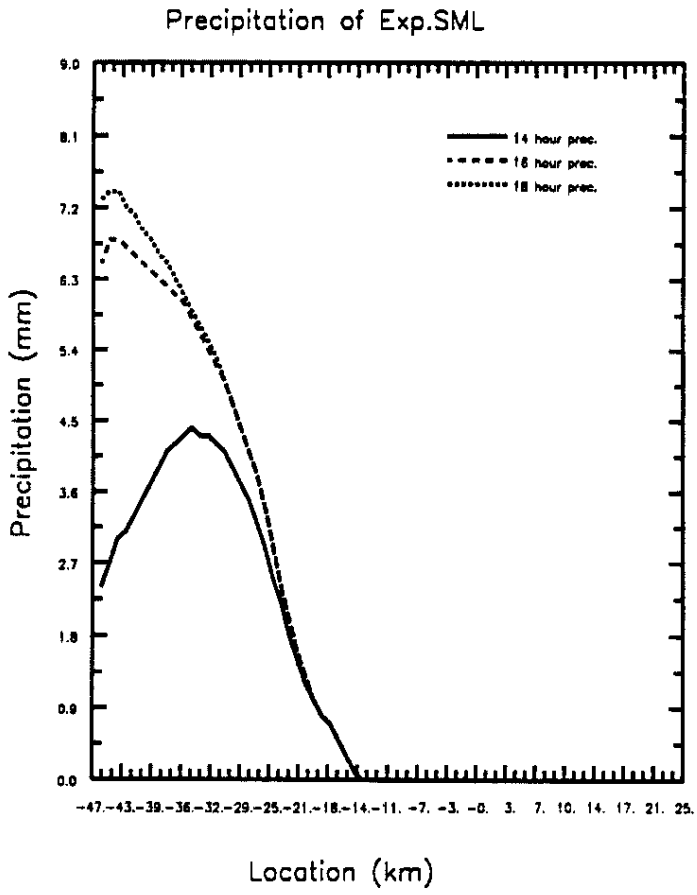


Figure 4.21: Distribution of the precipitation of 14, 16, and 18 hour simulation of SLM run.

# Chapter 5

# SUMMARY AND CONCLUSIONS

This study used a two-dimensional numerical model to investigate the importance of land surface characteristics, particularly soil moisture content, on the evolution of the mesoscale convection moving over the land from the Bay of Bengal during the summer monsoon season. A summary of the research and the major conclusions will be detailed in the following sections.

## 5.1 Summary of the Modeling Results

A two-dimensional hydrostatic version of the CSU RAMS was used. To simulate a cloud cluster with the features of a mesoscale convective system formed in the monsoon depression, two baroclinic initial disturbances were tested in the simulations. A positive temperature anomaly of 4°C at the low levels and negative temperature anomaly of −2°C at the higher levels over a horizontal distance of 250 km is proved to be reasonable.

A control run with typical environmental conditions during the summer monsoon season simulates a cloud cluster over the ocean and is consistent with general features of observed monsoon cloud clusters. The simulated cloud cluster contains both convective and stratiform clouds. The cloud cluster traveled across the ocean and onto the land. When it moves inland, a local convective system is initiated. The stratiform and cumulus precipitation has fallen over both the ocean and onshore.

Two simulations testing the effects of the soil moisture are presented. The soil wetness of the two simulations are 0.3 (relatively dry soil) and 0.8 (relatively wet soil), respectively. The wet soil run produces a wetter cloud cluster over the land. The magnitude of the maximum precipitation per grid point is larger than in the control run. The dry land run, however, obtains deep convection with a stronger intensity but with less precipitation.

Two simulations are made to examine the influence of land surface roughness. A rough land surface with $z_0$=0.10 m produced more local convection before the simulated monsoon cloud cluster moves inland. The smooth land surface with the surface roughness of 0.01 m, however, does not. The inland propagation speed of the simulated cloud cluster over the smooth ground is faster than the movement of the control one. Furthermore, the simulated cloud cluster dissipates quickly after it moves onshore in the smooth land surface simulation.

Sensitivity to a high ocean surface temperature (304 K) and a low ocean surface temperature (300 K) were also investigated. The simulated cloud cluster over the warm ocean surface exhibits strong upward motion and more active convection over both the ocean and the land. The cloud cluster brings significant amounts of precipitation to the continent. The cold ocean surface, however, does not generate a strong cloud cluster.

Finally, a simulation with a low ocean surface temperature and a dry soil was performed. The upward motion in this case seems less strong when the simulated cloud cluster lands. The low rainfall on the land near the coast indicates that the cloud cluster is not well developed by the time it approaches the coastline. Most of the rainfall came from the locally forced area of mesoscale convection in front of the landfalling cloud cluster. Furthermore, the mesoscale convection completely decays a few hours after landfall.

## 5.2 Conclusions

The current modeling simulation results investigate the influence of surface characteristics on the evolution of landfalling mesoscale convective systems associated with a summer monsoon depression in the Bay of Bengal. The simulated cloud cluster exhibits significant differences between different land surfaces when it approaches and crosses the coastline.

A favorable surface (for instance, warm ocean surface, wet land surface) can offer more moist static energy to the cloud cluster. A well developed cloud cluster will induce more mesoscale convection through enhanced low-level convergence of the higher moist static energy air. This cloud cluster usually produces anvil rainfall inland before the

main cloud cluster moves to that region. The wetter soil then is more conducive for the genesis of successive cloud clusters. The simulated widespread rainfall indicates that the precipitation is from both stratiform and cumulus clouds associated with the cloud cluster.

The dry land or cold ocean surface, however, has the identical effect on the simulated cloud cluster. Less rainfall on the ground near the coastline shows that the cloud cluster for this case does not produce much rainfall as it landfalls. Most of the precipitation is generated by the locally generated convective system and concentrates in a narrow region between 100 to 400 kilometers west of the coastline.

The roughness of the land surface plays an important role in initiating local mesoscale convection over land. The rough land surface can promote more mesoscale convection over the land. The maximum upward motion in the cloud cluster exhibits a proportional increase with the roughness of the land surface. However, the magnitude of the rainfall does not have this proportional increase.

The current two-dimensional numerical model simulations are consistent with the major features of the cloud cluster that occurred in the summer monsoon depression over the Bay of Bengal on 7-8 July 1979. The model results also correspond with the observational results indicating that the Indian monsoon is dominated by the local effects (WMO/Bulletin, 1990). However, there are a few aspects that seem incomplete. The evolution of the simulated cloud cluster over the ocean is not expressed sufficiently. The convection only occurs in the initial formation stage of cloud cluster. This may influence the intensity of the cloud cluster and its evolution process. The magnitude of the rainfall is smaller (the magnitude is only 11.8 mm within 24 hours) than the observational data due to lack of the vortex effect and north-south convergence. It is presumed that a three-dimensional simulation should be introduced to properly solve these problems. As discussed previously, the influence of the surface forcing on the evolution of the mesoscale convection system is significant. The rough surface promotes stronger upward motion when the monsoon cloud cluster moves inland. However, the bare soil surface in the model does not represent the surface condition properly. A more realistic surface condition which includes a vegetation parameterization should be included in the simulations. In

addition, the current simulations use both convection and microphysics parameterization with 10 km horizontal resolution. This horizontal scale is large for the microphysics process but small for the convection parameterization. The simulated upward motion in the mesoscale convective system is nearly tenth centimeter per-second that cannot represent the observed mesoscale convective system and its associated cumulus which has the vertical velocity of some meters per-second. A nested grid is needed in the model to represent the microphysical process that is important in evolution of the mesoscale convective system in detail.

## REFERENCES


Anthes, R.A., 1984: Enhancement of convective precipitation by mesoscale variations in vegetation covering in semiarid regions. *J. Climate Appl. Meteor.*, **23**, 541-554.

Bortkovskii, R.S., 1987: *Air-Sea Exchange of Heat and Moisture During Storms.* (Academic Press), 192 pp.

Chen, C. and W.R. Cotton, 1982: A one-dimensional simulation of the stratocumulus capped mixed layer. *Bound.-Layer Meteor.*, **25**, 289-321.

Cram, J.M., 1990: Numerical simulation and analysis of the prefrontal squall line. Department of Atmospheric Science, Colorado State University, Paper No. 471.

Dudhia, J., 1989: Numerical study of convection observed during the winter monsoon experiment using a mesoscale two-dimensional model. *J. Atmos. Sci.*, **46**, 3077-3107.

Fein, J.S. and J.P. Knettner, 1980: Report on the summer MONEX field phase. *Bull. Amer. Meteor. Soc.*, **61**, 461-474.

Flatau, P.J., G.J. Tripoli, J. Verlinde, and W.R. Cotton, 1989: The CSU-RAMS cloud microphysics model: general theory and code documentation. Department of Atmospheric Science, Colorado State University, Atmospheric Science Paper No. 451, 88 pp.

Gamache, J.F., 1990: Microphysical observations in summer MONEX convective and stratiform clouds. *Mon. Wea. Rev.*, **118**, 1238-1249.

Gamache, J.F. and R.A. Jr., Houze, 1982: Mesoscale air motion associated with a tropical squall line. *Mon. Wea. Rev.*, **110**, 118-135.

Garrett, A.L., 1982: A parameter study of interaction between convective clouds, the convective boundary layer, and a forested surface. *Mon. Wea. Rev.*, **110**, 1041-1059.

Godbole, R.V., 1977: The composite structure of the monsoon depression. *Tellus*, **29**, 25-40.

Gray, W.M., 1968: Global view of the origin of tropical cyclones. *Mon. Wea. Rev.*, **96**, 669-700.

Grossman, R.L. and D.R. Durran, 1984: Interaction of low-level flow with the western Ghat mountains and offshore convection in the summer monsoon. *Mon. Wea. Rev.*, **112**, 652-672.

Houze, R.A. Jr., 1982: Cloud clusters and large-scale vertical motion in the tropic. *J. Meteor. Soc. Japan*, **60**, 396-410.

Houze, R.A. Jr. and P.V. Hobbs, 1982: Organization and structure of precipitation cloud systems. *Adv. Geophys.*, **24**, 225-315.

Houze, R. Jr., 1989: Observed structure of mesoscale convective systems and implications for large-scale heating. *Quart. J. Roy. Meteor. Soc.*, **115**, 425-461.

Houze, R. Jr. and D.D. Churchill, 1987: Mesoscale organization and cloud microphysics in a Bay of Bengal depression. *J. Atmos. Sci.*, **44**, 1845-1867.

ICSU/WMO, 1976: The monsoon experiment. GARP publications series, No.18, World Meteorology Organization, Geneva, Switzerland, 123 pp.

Jacobson, R.W. Jr. and W.R. Gray, 1976: Diurnal variation of oceanic deep cumulus convection. Department of Atmospheric Science, Colorado State University, Paper No. 243.

Johnson, R.H. and G.S. Young, 1983: Heat and moisture budgets of tropical mesoscale anvil clouds. *J. Atmos. Sci.*, **40**, 2138-2147.

Johnson, R.H. and R.A. Houze, 1987: Precipitating cloud systems of the Asian monsoon. *Reviews in Monsoon Meteorology*, C.-P. Chang and T.N. Krishnamurti, Eds.

Keshavamurty, R.N., 1971: On the maintenance of the mean monsoon circulation and structure and energetics of monsoon disturbances. Ph.D. Thesis, Mysore University.

Klemp, J.B. and R.B Wilhelmson, 1978a: The simulation of three-dimensional convective storm dynamic. *J. Atmos. Sci.*, **35**, 1070-1096.

Klemp, J.B. and D.R. Durran, 1983: An upper boundary condition permitting internal gravity wave radiation in numerical mesoscale models. *Mon. Wea. Rev.*, **111**, 430-444.

Koteswaram, P. and C.A. George, 1958: On the formation of monsoon depression in the Bay of Bengal. *Ind. J. Meteor. Geophys.*, **9**, 9-22.

Krishnamurti, T.N., M. Kanamitsu, R. Godbole, C.B. Chang, F. Carr, and J.H. Chow, 1975: Study of a monsoon depression. I: Synoptic structure. *J. Meteor. Soc. Japan*, **53**, 227-240.

Krishnamurti, T.N., M. Kanamitsu, R. Godbole, C.B. Chang, F. Carr, and J.H. Chow, 1976: Study of a monsoon depression. II: Dynamical structure. *J. Meteor. Soc. Japan*, **54**, 208-225.

Krishnamurti, T.N., S. Cocke, R. Pasch, and S. Low-Nam, 1983: Precipitation estimates from rain gauge and satellite observations, summer MONEX. FSU Report 83-7, Department of Meteorology, Florida State University, Tallahasee.

Kuo, H.L., 1974: Further studies of the parameterization of the influence of cumulus convection on the large-scale flow. *J. Atmos. Sci.*, **31**, 1232-1240.

Lanicci, J.M., T.N. Carlson, and T.T. Warner, 1987: Sensitivity of the great plains severe-storm environment to soil-moisture distribution. *Mon. Wea. Rev.*, **115**, 2660-2673.

Leary, C.A. and R.A. Houze, 1980: The contribution of mesoscale motions to the mass and heat fluxes of an intense tropical convection system. *J. Atmos. Sci.*, **37**, 784-796.

Lee, C.S. and W.M. Gray, 1986: An observational study of tropical cloud cluster evolution and cyclogenesis in the western north Pacific. Department of Atmospheric Science, Colorado State University, Paper No. 403.

Lohar, D., B. Pal, and B. Chakravarty, 1990: Sea breeze activity at Kharagpur. Department of Physics and Meteorology, Indian Institute of Technology. (unpublished).

Louis, J.F., 1979: A parametric model of vertical eddy fluxes in the atmosphere. *Boundary-Layer Meteor.*, **17**, 187-202.

Mahfouf, J.F., E. Richard, and P. Mascart, 1987: The influence of soil and vegetation on the development of mesoscale circulation. *J. Climate Appl. Meteor.*, **26**, 1483-1495.

McCumber, M.C. and R.A. Pielke, 1981: Simulation of the effects of surface fluxes of heat and moisture in a mesoscale numerical model. I: Soil layer. *J. Geophys. Res.*, **86**, 9929-9938.

Mesinger, F. and A. Arakawa, 1976: *Numerical Methods used in Atmospheric Models.* GARP Publication Series, No.14, WMO/ICSU Joint Organizing Committee, 69 pp.

Molinari, J. and T. Corsetti, 1985: Incorporation of cloud scale and mesoscale down-drafts into a cumulus parameterization: Results of one and three-dimensional integrations. *Mon. Wea. Rev.*, **13**, 485-501.

Mooley, D.A. and J. Shukla, 1987: Variability and forecasting of the summer monsoon rainfall over India. *Monsoon Meteorology*, C.-P. Chang and T.N. Krishnamurti, Eds., Clerendon Press, 544 pp.

Nicholls, M.E., R.A. Pielke, and W.R. Cotton, 1991: A two dimensional numerical investigation of the interaction between sea-breezes and deep convection over the Florida Peninsula. *Mon. Wea. Rev.*, **23**, 298-323.

Nitta, T. and K. Masuda, 1981: Observational study of a monsoon depression developed over the Bay of Bengal during summer monex. *J. Meteor. Soc. Japan*, **59**, 672-682.

Nitta, T., 1980: Preliminary budget computations over the Bay of Bengal during summer monex. *FGGE Operations Report*, **9**, 145-150.

Ookouchi, Y., M. Segal, R.C. Kessler, and R.A. Pielke, 1984: Evaluation of soil moisture effect on generation and modification of mesoscale circulations. *Mon. Wea. Rev.*, **11**, 2281-2292.

Physick, W.L., 1980: Numerical experiments on the inland penetration of the sea breeze. *Quart. J. Roy. Meteor. Soc.*, **106**, 735-746.

Pielke, R.A., 1984: *Mesoscale Meteorological Modeling.* Academic Press, New York, 612 pp.

Pielke, R.A. and X. Zeng, 1989: Influence on severe storm development of irrigated land. *Nat. Wea. Dig.*, **14**, 16-17.

Ramanadham, R., S.V.S. Somanadham, and R.R. Rao, 1981: Heat budget of the north India oceanic surface during Monsoon-77. *Monsoon Dynamics*, S.J. Lighthill and R.P. Pearce, Eds., 735 pp.

Sanders, F., 1984: Quasi-Geostrophic diagnosis of the monsoon depression of 5-8 July 1979. *J. Atmos. Sci.*, **41**, 538-552.

Segal, M., R.A. Pielke, and Y. Mahrer, 1984: Evaluation of surface sensible heat flux effects on the generation and modification of mesoscale circulation. *Second International Symposium on Nowcasting,* European Space Agency, Norrkoping, Sweden, 263-269.

Shukla, J., 1975: Effect of Arabian Sea surface temperature anomaly on Indian summer monsoon – a numerical experiment with GFDL model. *J. Atmos. Sci.*, **32**, 503-511.

Shukla, J. and B.M. Misra, 1977: Relationship between sea temperature and wind speed over the central Arabian Sea and monsoon rainfall over India. *Mon. Wea. Rev.*, **105**, 998-1002.

Stull, R.B., 1988: *An Introduction to Boundary Layer Meteorology.* Kluwer Academic Publishers, Netherlands, 666.

Tremback, C.J., 1990: Numerical simulation of a mesoscale convective complex: Model development and numerical results. Department of Atmospheric Science, Colorado State University, Paper No. 465.

Tremback, C.J., G.J. Tripoli, and W.R. Cotton, 1985: A regional scale atmospheric numerical model including explicit moist physics and a hydrostatic time-split scheme. *Preprints, 7th Conference on Numerical Weather Prediction.*, Montreal, Quebec, American Meteorological Society.

Tremback, C.J., J. Powell, W.R. Cotton, and R.A. Pielke, 1987: The forward in time upstream advection scheme: Extension to higher orders. *Mon. Wea. Rev.*, **115**, 540-555.

Tripoli, G.J. and W.R. Cotton, 1982: The Colorado State University three-dimensional cloud/mesoscale model-1982. Part I: General theoretic framework and sensitivity experiments. *J. de. Rech. Atmos.*, **16**, 185-220.

Tuleya, R.E., M.A. Bender, and Y. Kurihara, 1984: A simulation study of the landfall of tropical cyclones using a movable nested-mesh model. *Mon. Wea. Rev.*, **112**, 124-136.

Walker, J. and Rowntree, P.R., 1977: The effect of soil moisture on circulation and rainfall in a tropical model. *Quart. J. Roy. Meteor. Soc.*, **103**, 29-46.

Warner, C., 1984: Core structure of a Bay of Bengal monsoon depression. *Mon. Wea. Rev.*, **112**, 137-152.

Warner, C. and R.H. Grumm, 1984: Cloud distributions in a Bay of Bengal monsoon depression. *Mon. Wea. Rev.*, **112**, 153-172.

Webster, P.J., 1983: Large-scale structure of the tropical atmosphere. *Large scale dynamical processes in the atmosphere*, B.J. Hoskins and R.P. Pearce, Eds., 235-275.

Webster, P.J., 1983: Mechanisms of monsoon low-frequency variability: Surface hydrological effects. *J. Atmos. Sci.*, **40**, 2110-2124.

Webster, P.J., 1987: The variable and interactive monsoon. J.S. Fein and P.L. Stephens, Eds., *Monsoons*, John Wiley & Sons, New York, 269-330.

WMO, 1990: Recent research on monsoons based on observational analyses. *Bulletin*, **39**, No. 3, 169-173.

Xian, Z. and R.A. Pielke, 1991: The effects of land masses on the development of sea breezes. *J. Appl. Meteor.* (accepted).

Yan, H. and R.A. Anthes, 1988: The effect of variation in surface moisture on mesoscale circulation. *Mon. Wea. Rev.*, **116**, 192-208.

## APPENDIX

$u$ – east-west wind component

$v$ – north-south wind component

$w$ – vertical wind component

$f$ – Coriolis parameter

$K_m$ – eddy viscosity coefficient for momentum

$K_h$ – eddy viscosity coefficient for heat and moisture

$\theta_{il}$ – ice-liquid water potential temperature

$r_n$ – water mixing ratio species of total water (n=1), rain (n=2), pristine crystals (n=3)

$\rho$ – density of air

$con$ – subscript denoting tendance of convection parameterization

$rad$ – subscript of tendance of radiation parameterization

$res$ – subscript of tendance of microphysical parameterization

$g$ – gravity acceleration

$r_t$ – total water mixing ratio

$r_v$ – water vapor mixing ratio

$\pi$ – total Exner function

$\pi'$ – perturbation Exner function

$\theta_v$ – virtual potential temperature

$p$ – pressure